

Investigating follicle development using *in vitro* technologies

Belinda Kwok Man Lo

Worcester College

University of Oxford

A thesis submitted for the degree of

Doctor of Philosophy

Extended Trinity Term

2017

Acknowledgements

First and foremost, I am grateful to my supervisor Dr. Suzannah Williams for offering me the opportunity to undertake this DPhil. I would not have managed without her constant guidance, understanding and support, particularly during trying times. I could not have wished for a better advisor and mentor.

I would also like to thank my co-supervisor, Prof. Dagan Wells, for his support throughout my DPhil.

My DPhil would have certainly been dull without the Williams Group members, both past and present (Dr. Heidy Kaune, Dr. Panayiota Ploutarchou, Sairah Sheikh, Arwa Alageel, Charlotte Walker, Xi Wei, Eleni Papadopoulou), and the students in the End Office. Sairah – your constant advice and help has made this DPhil an unforgettable experience. I would also like to thank my two dear friends Eszter Dombi and Helena Rodriguez Caro for making my life in Oxford a lot more fun.

Finally, I want to thank my family for all their love and encouragement. Mum and dad – I would not have reached this point without your love and support, as well as the sacrifices you both have had to make. Alvin, my brother, best friend and personal cheerleader – you have been a constant source of inspiration and support. I love you all.

Abstract

Patients with dysfunctional ovaries, such as those with premature ovarian insufficiency and granulosa cell tumours, do not have normal follicle development and may not respond to traditional assisted reproductive techniques. Using the reaggregated ovary (RO) technique, these patients' oocytes may be reaggregated with functional supporting cells and cultured *in vitro* to develop fertilisable eggs. However, current research using ROs have only used murine ovaries as a somatic cell source. In this thesis, with the aim of moving towards a clinical treatment, we assessed follicle development in ROs *in vitro* and progressed to using the technique with human tissues. To assess whether an older murine somatic cell source resulted in advanced follicle development, and how follicle development differed between transplanted and cultured ROs, ROs were generated using postnatal day 2 (P2) and P6 mouse ovaries. To investigate theca cell development in follicles from cultured tissue, mouse ovaries were cultured with mouse serum or encapsulated in hyaluronan hydrogels. Prior to generating and culturing chimeric human-mouse ROs (HuMoROs), competent handling and digestion of bovine cortical tissue was required. Broadly, ROs generated from both P2 and P6 exhibited similar follicle development *in vitro* after 14 d of culture, and follicles from cultured ROs were more developed than those from transplanted ROs. Theca cell development observed in follicles from cultured ovaries was still poorer than those from *in vivo* ovaries, even when ovaries were cultured in mouse serum or encapsulated in a hyaluronan hydrogel. Finally, some follicles containing potential human oocytes developed within the generated HuMoROs after 7 d of culture. These results have highlighted the potential of the RO technique as a method to generate fertilisable eggs and identified further aspects which need to be targeted in order to improve the success of the technique.

Abbreviations

AGCT	adult granulosa cell tumour
AMH	anti-Müllerian hormone
AR	androgen receptor
ART	assisted reproductive techniques
BL	basal lamina
BMP	bone morphogenetic protein
BSA	bovine serum albumin
CL	corpus luteum
COC	cumulus oocyte complex
CPA	cryoprotectant media
D/C	Dispase II/Collagenase I
DHEA	dehydroepiandrosterone
DM	double mutant
ECM	extracellular matrix
EDTA	ethylenediaminetetraacetic acid
EG	ethylene glycol
EGF	epidermal growth factor
ER	oestrogen receptor
ESC	embryonic stem cell
FA-IPN	fibrin alginate interpenetrating network
FBS	foetal bovine serum
FGF	fibroblast growth factor
FSH	follicle stimulating hormone
GC	granulosa cell
GDF	growth and differentiation factor
GnRH	gonadotrophin releasing hormone
HA	hyaluronan
hCG	human chorionic gonadotrophin
HPG axis	hypothalamic-pituitary-gonadal axis

HuMoRO	human-mouse reaggregated ovary
IGF	insulin-like growth factor
iPSC	induced pluripotent stem cell
ITS	insulin transferrin selenium
IVF	*in vitro* fertilisation
JGCT	juvenile granulosa cell tumour
KL	Kit ligand
LH	luteinising hormone
LPM	litres per minute
MII	meiosis II
MoRO	mouse reaggregated ovary
MSC	mesenchymal stem cell
Oc	ovary culture
OCTB	Oxford Cryopreservation Tissue Bank
PEG	polyethylene glycol
PGC	primordial germ cell
POI	premature ovarian insufficiency
PR	progesterone receptor
RBC	red blood cell
RGD	arginylglycylaspartic acid (Arg-Gly-Asp)
RO	reaggregated ovary
ROc	reaggregated ovary culture
ROt	reaggregated ovary transplanted
SD	standard deviation
TC	theca cell
T/E	Trypsin/EDTA
TGFβ	transforming growth factor ß
VEGF	vascular endothelial growth factor
X-gal	5-bromo-4-chloro-3-indolyl-β-D-galactopyranoside
ZP	zona pellucida

Table of Contents

Abstract **3**

Abbreviations **5**

Chapter 1: Introduction **12**

1.1 Ovarian function **13**

1.1.1 Oogenesis 13

1.1.2 Follicle development 14

1.1.3 Factors involved in follicle development 19

1.2 Follicle development in different species **27**

1.2.1 Menstrual cycle versus oestrous cycle 28

1.3 Follicle development *in vitro* **30**

1.3.1 Ovarian tissue culture 30

1.3.2 Follicle culture 34

1.4 Artificial ovaries **35**

1.4.1 Hydrogels 39

1.4.2 Decellularised extracellular matrix 43

1.4.3 3D printed scaffold 44

1.4.4 Reaggregated ovaries 46

1.5 Aims **49**

Chapter 2: Materials and Methods **50**

2.1 Mouse colonies **51**

2.1.1 Ethical approval 51

2.1.2 ROSA*LacZ* mice 51

2.1.3 Mouse colony management system 51

2.1.4 Mouse breeding regime 52

2.1.5 Timed matings 52

2.1.6 Tail tipping, ear clipping and weaning 53

2.2 Genotyping **54**

2.3 Reaggregated ovaries **55**

2.4 Ovary culture **59**

2.5 Transplantation of reaggregated ovaries **60**

2.6 Histological processing **61**

2.6.1 Fixation 61

2.6.2 Embedding 62

2.6.3 Sectioning 63

2.6.4 Haematoxylin-eosin staining 64

2.6.5 Assessment of follicle development 65

Chapter 3: Follicle development in cultured reaggregated mouse ovaries **67**

3.1 Introduction **68**

3.2 Aims **69**

3.3 Materials and Methods **70**

3.3.1 Mice 70

3.3.2 Ovaries and reaggregated ovaries 70

3.3.3 Tissue collection and assessment of follicle development 70

3.3.4 Statistical analysis 72

3.4 Results **72**

3.4.1 Validation of cell isolation 72

3.4.2 Number of germ and somatic cells from digested neonatal ovaries 74

3.4.3 Follicle development in neonatal ovaries 74

3.4.4 Age-related differences in follicle development in transplanted ROs 76

3.4.5 Follicle development in cultured ovaries, cultured ROs, transplanted ROs and *in vivo* Control ovaries after 14 d 77

3.4.6 Follicle development in ovaries and ROs after 21 days of culture 83

3.5 Discussion **84**

Chapter 4: Morphological analysis of follicle development in cultured reaggregated mouse ovaries **90**

4.1 Introduction **91**

4.2 Aim **92**

4.3 Materials and Methods **92**

4.3.1 Analysis of cultured ROs, cultured ovaries, transplanted ROs and age-matched *in vivo* ovaries 92

4.4 Results **93**

4.4.1 Cultured ovaries and ROs are associated with fewer theca and granulosa cells 93

4.4.2 Oocyte and follicle area in ovaries and ROs 97

4.4.3 Granulosa cell area and granulosa cell density in ovaries and ROs 101

4.4.4 Correlations between follicle area, granulosa area and granulosa cells 105

4.5 Discussion **107**

Chapter 5: Exploration of theca cell development in different culture conditions **110**

5.1 Introduction **111**

5.1.1 Theca cell development 111

5.1.2 Differences between transplantation and culture 114

5.2 Aims **120**

5.3 Materials and Methods **121**

5.3.1 Mice 121

5.3.2 Mouse serum collection 121

5.3.3 Ovary culture with mouse serum 122

5.3.4 Ovary culture using hyaluronic acid hydrogel 123

5.3.5 Tissue collection and processing 126
5.3.6 Statistical analysis 126
5.4 Results 128
5.4.1 Follicle development in ovaries cultured in collected mouse serum ...128
5.4.2 Follicle development in ovaries cultured in commercial mouse serum 132
5.4.3 Follicle development in ovaries cultured in hyaluronan hydrogel 135
5.5 Discussion 138
Chapter 6: Dissection and digestion of bovine cortical tissue 142
6.1 Introduction 143
6.2 Aims 145
6.3 Materials and Methods 145
6.3.1 Collection of bovine ovaries 145
6.3.2 Dissection of bovine cortical strips 146
6.3.3 Cryopreservation and thawing of bovine cortical strips 149
6.3.4 Digestion of bovine cortical strips 150
6.3.5 Statistical analysis 152
6.4 Results 152
6.4.1 Dissection and cryopreservation of bovine cortical strips 152
6.4.2 Enzymatic digestion of bovine cortical strips 152
6.5 Discussion 155
Chapter 7: Investigating the potential of human ovarian germ cells to function in a reaggregated ovary 159
7.1 Introduction 160
7.1.1 Issues in human follicle development 160
7.2 Aims 164
7.3 Materials and Methods 164

7.3.1 Human ovarian tissue.....164
7.3.2 Human ovary collection, dissection and cryopreservation 166
7.3.3 Human cortical strip thawing 167
7.3.4 Cortical strip culture.....168
7.3.5 Chimeric reaggregated ovaries using human and murine ovarian tissue 168
7.3.6 Statistical analysis 171
7.4 Results 171
7.4.1 Generation of human-mouse chimeric reaggregated ovaries using fresh ovarian medulla 171
7.4.2 Haemolytic removal of red blood cells from the medulla cell suspension 174
7.4.3 Number of germ and somatic cells from digested cortical strips.....175
7.4.4 Follicle development in chimeric human-mouse reaggregated ovaries (HuMoROs) generated from cortical strips 178
7.5 Discussion.....182
Chapter 8: Conclusions 186
References 192

Chapter 1: Introduction

1.1 Ovarian function

The ovary is central to female reproduction, and is responsible for developing and maturing fertilisable eggs. The ovary is also an important endocrine gland, and produces steroid hormones to support puberty, follicle development and any subsequent pregnancies (1,2). To develop a fertilisable egg, the egg (known as an oocyte prior to ovulation) is encapsulated within a follicle, the functional unit of an ovary. The process of follicle formation and development is to ensure oocyte survival by providing somatic cell support. The generation of oocytes and formation of primordial follicles in the ovary is referred to as oogenesis, while the subsequent activation and maturation of these primordial follicles is known as follicle development.

1.1.1 Oogenesis

Oocytes develop from primordial germ cells (PGCs), which migrate from the allantois towards the genital ridges at approximately 7 weeks of gestation in humans (3) and embryonic day 10.5 to 12.5 (E10.5-12.5) in mice (4). After sex determination, PGCs within the developing ovaries are referred to as oogonia, and proliferate via mitosis.

Oogonial entry into meiosis begins at approximately at 11-12 weeks of gestation in humans (5) and E13.5 in mice (6-8). Upon entry into meiosis, oogonia are referred to as oocytes (9), and they progress through prophase I, before arresting at the diplotene stage (also known as dictyate) (10).

The oocytes are also connected by residual cytoplasmic bridges (11), forming groups of oocytes known as germ cell nests. These connections allow the transfer of organelles, cytoplasm and signalling molecules (12). Around the period of diplotene arrest, germ cell cysts begin to break down (around 16 weeks of gestation in humans (13) and around the time of birth in mice (14)), resulting in apoptosis and the loss of two-thirds of all germ cells (14). It is hypothesised that the initiation germ cell nest breakdown occurs once mouse pups are born, due to the drop in exposure to circulating maternal oestrogens and progesterone (15).

During nest breakdown, somatic cells also invade the nests, and surround the oocytes, eventually forming primordial follicles. The resultant primordial follicles consist of a single oocyte, surrounded by a layer of squamous pregranulosa cells and a layer of basal lamina (BL) which separates it from the surrounding stroma. The primordial follicle pool is established *in utero* in humans at approximately 20 weeks of gestation (2,16) and within the first few days after birth in mice (12,14,17).

1.1.2 Follicle development

Primordial follicles can remain arrested in a meiotically quiescent state for many years particularly in humans before recruitment for follicle development. However, some primordial follicles are immediately activated after formation and grow, though the exact factors involved in follicle activation remain unclear. Once activated, primordial follicles develop through the primary, secondary, preantral and preovulatory stages, resulting in the ovulation of a mature egg (2) (Figure 1.1). Follicle development requires complex bidirectional communication between the

oocyte and its somatic cells, the granulosa cells (GCs) and theca cells (TCs), involving the exchange of signalling growth factors and nutrients (discussed in Section 1.1.3).

Clusters of quiescent primordial follicles are found concentrated in the cortical area of the ovary, a dense, collagen-rich area (4,18). The first follicles to grow are those situated at the cortico-medullary region of ovary, while non-growing primordial follicles remain in the edges of the cortex, below the ovarian surface (19). During follicle development, the growing follicles potentially migrate from the cortex towards the medulla, which is less dense, with less extracellular matrix (ECM), and complete their development before ovulation (20). The activation of primordial follicles and development to the primary follicle stage is marked by the growth of the oocyte (21,22) and the differentiation of squamous pregranulosa cells into cuboidal GCs (2,4,23-25). The primary follicle stage is typified by one complete layer of cuboidal GCs surrounding the oocyte (Figure 1.1).

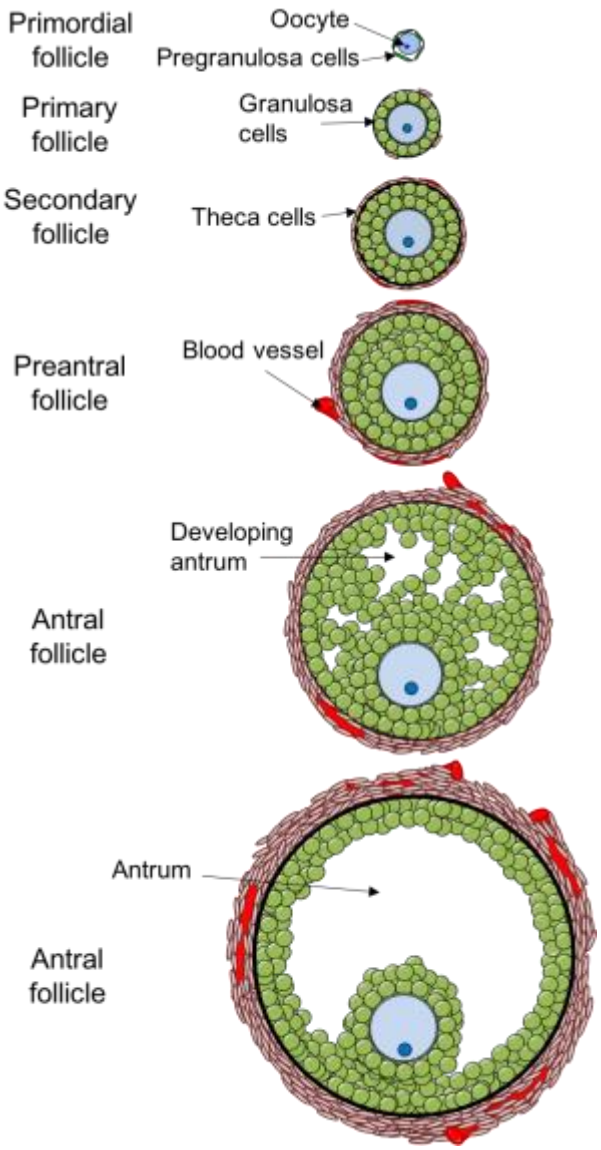


Figure 1.1 Follicle development from the primordial stage to the antral stage.

Follicle growth is associated with the growth of the oocyte and the proliferation of its accompanying granulosa cells and theca cells. The follicle stage is classified by the number of complete granulosa cell layers it has: primary (one complete layer), secondary (two complete layers) and preantral (three or more complete layers). Once an antrum appears, the follicle is classified as an antral follicle.

At the primary follicle stage, theca precursor cells are recruited from the stroma to form the TC layer (26) and the oocyte begins to secrete zona pellucida (ZP) glycoproteins (27). Proliferation of both the GCs and TCs results in the formation of secondary follicles (two complete layers of GCs) and preantral follicles (three or more complete layers of GCs), and is accompanied by the vascularisation of the TC layer (Figure 1.1). Follicle development prior to antrum formation is gonadotrophin responsive (2,28-30). Antrum formation is dependent on gonadotrophins (28,31), as demonstrated by female mice lacking follicle-stimulating hormone ß (FSHß) (28) or FSH receptor (FSHR) (29) which only develop follicles up to the preantral follicle stage.

FSH is released from the anterior pituitary gland upon stimulation with gonadotrophin releasing hormone (GnRH, expanded upon in Section 1.1.3.1), and promotes GC proliferation and the formation of small fluid-filled antral cavities in preantral follicles. The follicular fluid in these antral spaces contain growth factors and low molecular weight serum proteins vital for follicle development. These constituents are thought to be derived from GCs and the circulation, via the capillaries within the TC layer (32-34). The presence of antral spaces, another hallmark of follicle development, denotes the follicle as having reached the antral follicle stage. Increased FSH during the follicular phase of the menstrual cycle (or oestrus cycle; see Section 1.2.1) leads to the recruitment of a cohort of follicles for further development and ovulation (35).

The small antral spaces coalesce to form a single antral cavity, which functionally separates the GCs into two populations – the mural GCs, which line the wall of the follicle, and the cumulus GCs (cumulus cells), which surround the oocyte (4).

The luteinising hormone (LH) surge from the pituitary induces cumulus expansion, resumption of meiosis, germinal vesicle breakdown and extrusion of the first polar body (36,37). After ovulation, the cumulus oocyte complex (COC) is collected by the fimbrae of the Fallopian tubes, allowing the transport of the COC to the site of implantation (38,39). The LH surge also induces BL breakdown and GC and TC luteinisation, resulting in the formation of a corpus luteum (CL). This highly vascularised endocrine gland synthesises progesterone to support any subsequent pregnancy. However, if no pregnancy follows, the CL undergoes luteolysis, a functional and structural regression of the gland, whereby progesterone production ceases and the cells within the CL undergo cell death (e.g. apoptosis, necrosis) (40,41).

Many of the primordial follicles which undergo activation and growth do not reach the preovulatory stage and ovulate, but undergo atresia at various stages of follicle development (10,21,42,43). The majority of the activated follicles undergo atresia at the antral follicle stage, which suggests that the final stages of follicle development are most vulnerable to atresia (1,44). Programmed cell death (apoptosis) within the follicles is thought to be caused by the reduction in anti-apoptotic factors (e.g. oestrogen, gonadotrophins) or the increase of pro-apoptotic

factors (e.g. androgens), death ligand-receptor systems and members of the B-cell lymphoma 2 protein family (Bcl-2) (reviewed by Hsueh et al. 1994 (43).

1.1.3 Factors involved in follicle development

Follicle development is coordinated at an endocrine level by the hypothalamic-pituitary-gonadal (HPG) axis (2,31,45,46) and at the autocrine and paracrine level by intra-ovarian factors (47-51).

1.1.3.1 Hormonal regulation of follicle development

The HPG axis is regulated by GnRH, which is released in a pulsatile fashion by hypothalamic neurones in the arcuate nucleus, into the hypophysial portal circulation (52,53). The binding of GnRH to the GnRH receptor within the anterior pituitary leads to the pulsatile release of the gonadotrophins LH and FSH into the circulation (54-58). Circulating levels of FSH and LH are regulated via positive and negative feedback mechanisms by other hormones such as oestrogen, progesterone, activins, inhibins and Anti-Müllerian hormone (AMH) (discussed in Sections 1.1.3.2 and 1.1.3.3).

The gonadotrophins FSH and LH share a common α subunit, but differing ß subunits, the latter of which confers receptor specificity (59). The receptors for FSH (FSHR) and LH (LHR) are found on GCs and TCs, respectively, and are central to the two-cell two-gonadotrophin model (Figure 1.2) (46,60-66).

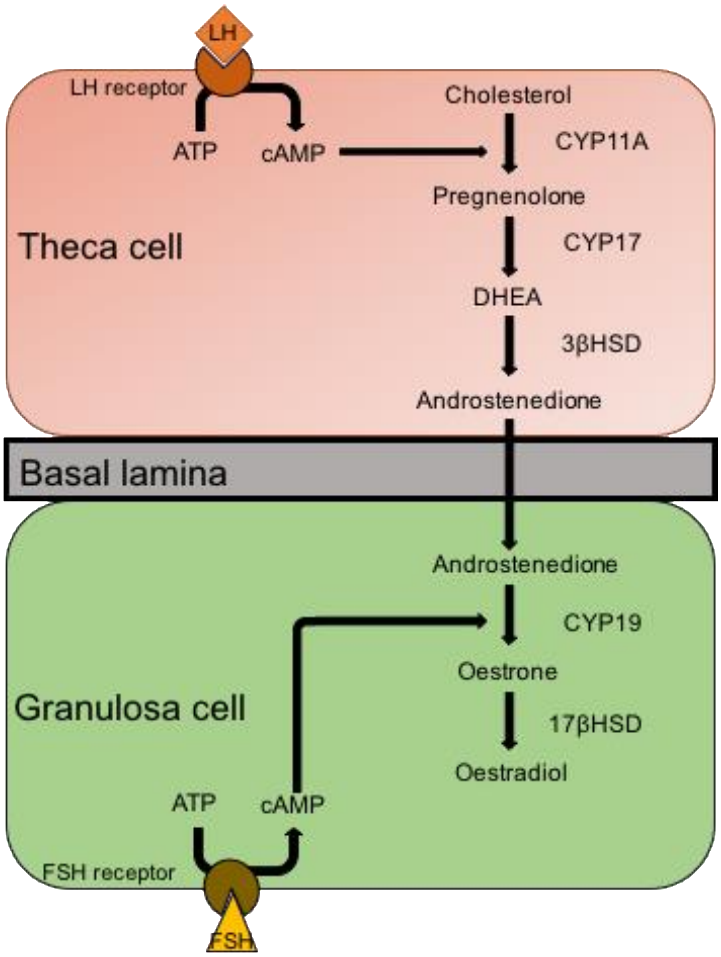


Figure 1.2 Two-cell two-gonadotrophin model.

Adapted from Erickson et al. 1985 (67). Luteinising hormone (LH) binds to LH receptors, stimulating the adenylyl cyclase pathway (cAMP pathway), leading to the production of androstenedione from cholesterol, via the sequential production of pregnenolone and dehydroepiandrosterone (DHEA). Androstenedione can diffuse through the basal lamina, into the granulosa cells (GCs). Upon follicle stimulating hormone (FSH) binding to the FSH receptor, the cAMP pathway is activated and stimulates GC production of aromatase (CYP19), which aromatises androstenedione into oestrone. Oestrone can then be converted into oestradiol by 17ß-Hydroxysteroid dehydrogenase (17ßHSD).

1.1.3.2 Ovarian steroids

Produced in the ovary from cholesterol, the ovarian steroids (oestrogens, progestins and androgens) play important roles in growth and differentiation of reproductive tissues, as well as follicle development (46).

1.1.3.2.1 Oestrogens

The production of oestrogens has been described in Figure 1.2, as part of the two-cell two-gonadotrophin model. The capacity of follicles to make oestrogen is first apparent in the secondary stage, when they possess all the components of the two-cell two-gonadotrophin model. The highest intrafollicular levels of oestradiol, the principal oestrogen (68), are at the preovulatory follicle stage, as these follicles have the largest number of GCs present and can aromatise androgens readily (65). Oestrogen also has mitogenic effects on GCs (69), and acts through a positive feedback mechanism to promote follicle responsiveness to FSH and LH action, stimulating further oestrogen production (70-72).

Oestrogens signal via oestrogen receptors (ERs), which have two main forms (ERα and ERß) (73-77). The ERß form is the predominant form within the ovary in rats (78,79). However, both forms of ER are vital for fertility, as demonstrated by knockout mice, since ERα knockout (ERKO) mice are infertile due to follicle development arrest at the antral stage, while ERß knockout (BERKO) mice are subfertile due to abnormal ovulation (80-82). Using selective ER agonists have also revealed that ERα and ERß perform different roles; ERα inhibited ovulation,

likely through the HPG axis, while ERß promoted follicle growth, decreased atresia and enhanced the number of oocytes ovulated in rats (83).

The role of oestrogen in ovarian function has also been revealed using aromatase knockout (ArKO) mice, which lack functional aromatase, and are unable to produce oestrogen (84-86). Without oestrogen present, follicle development was arrested at the antral stage in the ovaries of ArKO mice, and were unable to be ovulated, rendering the mice infertile (87). Over time, the primordial follicle pool was depleted (85,87,88), which may be due to the decreased oestrogen or AMH present due to fewer follicles.

1.1.3.2.2 Progesterone

Once ovulation occurs, the GCs and TCs luteinise to form a CL, which secretes progesterone. Progesterone has key roles in ovulation, implantation and the maintenance of pregnancy (89) by binding to the progesterone receptor (PR).

The two isoforms of PR (PR-A and PR-B) arise from a single gene (90,91), but have functionally different roles (92,93). *In vitro* data using human endometrial HeLa cells suggest that PR-A is a dominant repressor of PR-B action, and that the balance of PR-A to PR-B determines cellular responsiveness to progesterone (94,95). In addition, selective knockouts of PR-A in mice (PRAKO) were infertile, and histological analyses of their ovaries revealed several mature anovulatory

follicles (96), while PR-B knockout (PRBKO) mice had unaffected ovulation (97). This indicates that progesterone mainly acts through PR-A for ovulation.

1.1.3.2.3 Androgens

Androgens, in particular androstenedione and testosterone, are produced in TCs upon stimulation by LH, and are central to the production of oestradiol in the GCs (Figure 1.2). Acting via the androgen receptor (AR), androgens play a vital role in regulating follicle development by enhancing GC apoptosis (69) and inhibiting FSH-stimulated LHR expression in GCs (98), required for ovulation. Androgens have been shown to impede follicle development – a single injection of dihydrotestosterone, a non-aromatisable androgen, resulted in cycling mice becoming subfertile (99). The role of androgens in ovarian function were also demonstrated with AR knockout (ARKO) mice, which were subfertile, with abnormal follicle development and fewer CLs (100).

1.1.3.3 Transforming Growth Factor ß superfamily

Several growth factors which influence follicle development and growth belong to the transforming growth factor ß (TGFß superfamily), including activins, inhibins, AMH, growth and differentiation factors (GDFs) and bone morphogenetic proteins (BMPs) (49-51).

1.1.3.3.1 Activins and inhibins

Activins and inhibins are dimeric protein members of the TGFß superfamily, and are named respectively for stimulating and inhibiting FSH secretion from the pituitary (101). Activin subunits (ßA and ßB), activin receptors (type-I and type-II) and follistatin (activin-binding protein) have been detected in early stage follicles, indicating that both have a role local autocrine/paracrine activities in early follicle development. Expression of activin ßA and ßB subunits and follistatin localised predominantly in GCs, while the activin receptors (type-I and type-II) are expressed on TCs, GCs and the oocyte (102-105).

Although there are three types of activins present (A, AB and B), most research has focused on the actions of activin A, which consists of two ßA subunits. Supplementation of activin A to preantral follicle culture enhanced follicle growth and also promoted GC proliferation, all of which could be reversed by supplementation with follistatin (106-109). However, activin A only affects larger follicles, as it has no effect on early follicle progression when supplemented into bovine ovarian cortex culture (110). The highest levels of activin B (ßB dimer) have been found in the follicular fluid of small antral follicles, but levels decrease as follicle size increases. Along with activin A, activin B also suppresses androgen production (111).

Inhibins, unlike activins, are composed of a common α subunit and either one of the two ß subunits (ßA or ßB) (101). To inhibit the action of activin, inhibins competitively bind to activin receptors (reviewed by (112)). The major ovarian

source of inhibin A are GCs. Inhibin inhibits oocyte meiosis (113), increase the number of ovarian follicles (114) and stimulate TC steroidogenesis *in vitro* (115). In comparison, follistatin, while structurally unrelated to inhibins, also neutralises activin activity (116) by binding to activin with a similar affinity to activin with its receptors (117).

1.1.3.3.2 Anti-Müllerian Hormone

Originally named due to its role in Müllerian duct regression during male foetal sex differentiation (118), AMH also plays a role in primordial follicle activation. Unlike the stimulatory actions of most other members of the TGFß superfamily generated in the ovary, AMH is thought to inhibit the recruitment and progression of early stages of follicle development (119). AMH is first detected in GCs of primary follicles (120,121), and reaches its highest expression levels in preantral and small antral follicles (121,122). The role of AMH in the ovary was revealed by studies using AMH-deficient (AMHKO) mice; in the absence of AMH, the primordial follicle pool was depleted earlier than the Control counterparts. This rapid decrease was caused by increased recruitment of primordial follicles in the AMHKO mice, indicating that AMH inhibited follicle activation (119). AMH has also been shown to suppress FSH-induced follicle growth by reducing follicle sensitivity of FSH (123).

1.1.3.3.3 Oocyte-secreted factors GDF-9 and BMP-15

Growth differentiation factor-9 (GDF-9) and bone morphongenetic protein-15 (BMP-15) are both glycoproteins essential for fertility, and are produced by oocytes from the primary follicle stage onwards (124-126). Homodimeric GDF-9 binds to

BMPR2 and ALK5 to signal via the SMAD2/3 signalling pathway (127,128), while homodimeric BMP-15 binds to BMPR2 and ALK6 to signal via the SMAD1/5/8 signalling pathway (129). However, GDF-9 and BMP-15 also bind as heterodimers, acting as a ligand to BMPR2, ALK4 and ALK6, and have greater bioactivity than their homodimeric equivalents (130).

In vitro supplementation of GDF-9 to murine ovarian tissue culture promotes progression beyond the primary follicle stage (131,132), while the addition of BMP-15 stimulated the proliferation of undifferentiated GCs (133). The use of BMP-15 (*Bmp15*$^{-/-}$) and GDF-9 (*Gdf9*$^{-/-}$) null mice have been useful in further elucidating the role of these oocyte-secreted factors in follicle development. *Bmp15*$^{-/-}$ mice present as subfertile (134), while initial studies using *Gdf9*$^{-/-}$ mice revealed that follicle development did not progress beyond the primary follicle stage (125). However subsequent studies have demonstrated that the primary follicle arrest in *Gdf9*$^{-/-}$ mice is due to increased GC production of inhibin A (135), and that mice lacking both inhibin A and GDF-9 (*Inha*$^{-/-}$*Gdf9*$^{-/-}$) were able to develop follicles until the late preantral stage (136).

1.1.3.3.4 Other signalling factors

Although the oocyte can be considered the ‘master organiser’ of follicle assembly and growth (137), other factors which are also vital for follicle activation and development need to be considered, including Kit ligand (KL) and c-Kit, leukaemia inhibitory factor (LIF) and insulin-like growth factors (IGFs) (reviewed in (4,26,138-142)).

1.2 Follicle development in different species

Although mice are routinely used for research into the mechanisms behind follicle development (as evidenced in Section 1.1.3), it is important to note that the mechanisms elucidated may not be transferrable to humans, particularly given the differences between mice and humans in reproductive characteristics (Table 1.1).

Table 1.1 Reproductive characteristics of mice, cattle and women

Based on Campbell et al. 2003 (143), with additional data added with appropriate references.

Characteristic	Mice	Cattle	Women
Eggs per cycle	~10	1	1
Duration of folliculogenesis	21 days (Peters 1969 (21))	6 months	6 months
Diameter of ovulatory follicle (mm)	0.55 (Brambell, 1928 (144))	16-22	19-25
Diameter of oocyte from preovulatory follicle (µm)	72.3 (Griffin et al. 2006 (145))	110 (Hyttel et al., 1997 (146))	120 (Griffin et al. 2006 (145))
Ovulatory cycle (days)	Oestrus cycle: 4-6 (Allen 1922 (147))	19-24	26-29
Follicular phase	Pro-oestrus, oestrus: 2-3 days (Caligioni 2009 (148))	Pro-oestrus, oestrus: 2-3 days	14 days
Luteal phase	Metoestrus, dioestrus: 2-4 days (Caligioni 2009 (148))	Metoestrus, dioestrus: 16-19 days	14 days
Duration of gestation (days)	19-21	280	280

Mice are particularly useful for research as they are relatively easy to manipulate and use for research at specific ages, due to their high parity and relatively short gestational time compared to humans. However, they offer relatively few advantages for transferable reproductive research. Mice are polytocous, and have a significantly shorter ovarian cycle compared to humans (see Table 1.1), and only undergo a luteal phase if the female mouse has mated and been impregnated (149). In comparison, large animal species such as cows are monovular and polycyclic, and have similar ovarian pathologies as humans, such as follicular cysts, luteinised anovulatory follicles and suppression of follicle development or ovulation due to lactation or stress (150,151).

1.2.1 Menstrual cycle versus oestrous cycle

The reference point for beginning of the ovarian cycle differs between humans and other animal species; menstruation is considered the beginning of the human menstrual cycle, while for mice and cows, oestrus is the beginning of the oestrous cycle. However, both of these points refer to different physiological stages during the ovarian cycle (152).

The menstrual cycle in women spans an average of 28 days, with 14 days of follicular phase and 14 days of luteal phase. The menses usually span the first five days of the follicular phase, and oestradiol from the preovulatory follicle stimulates endometrial lining growth during the follicular phase (153). Once ovulation occurs, the developed CL provides progesterone, which supports the endometrium. If conception occurs, circulating hCG prevents luteolysis; however, in the absence of

conception, luteolysis and regression of the CL occurs. Regression of the CL decreases the circulating levels of progesterone, thus allowing the endometrium to be shed during menstruation (154).

Unlike women, the endometrial lining in both mice and cows do not undergo periodic shedding (152). The oestrous cycle is divided into the following phases (Table 1.2).

Table 1.2 Phases of the oestrous cycle in mice and cattle

Adapted from Peter et al. (2009) (155) and Adams et al. 2012 (152).

Oestrous phases	
1. Pro-oestrus	Development of the ovulatory follicle
2. Oestrus	Period of “sexual receptivity” Final follicular maturation and ovulation
3. Metoestrus	Period of corpora lutea formation
4. Dioestrus	Period when corpora lutea are mature and produce progesterone

Although the follicular phase in cows is significantly shorter than that of humans (2-3 days versus 14 days), the growing period between the emergence of the recruited cohort of follicles to the ovulation of the dominant follicle is comparable between cows and humans. In humans, this growing phase of the dominant ovulatory follicle takes approximately 14 days of the 28 day cycle (156), while in cows, it occupies approximately 11 days of the 21 day oestrous cycle (157). Most bovine oestrus cycles have two or three waves of follicle development (i.e. the

synchronous group of follicles recruited by a FSH surge) (157,158), which is also found in most menstrual cycles as well (156). In comparison with both cows and humans, the mouse oestrous cycle spans 4-6 days (147), and multiple follicles become dominant during each oestrus cycle, resulting in the ovulation of multiple eggs (2).

1.3 Follicle development *in vitro*

Techniques for *in vitro* culture of ovarian tissue or individual follicles have been established to further understand the physiological regulation of follicular development, as well as to develop mature oocytes for assisted reproductive technologies (ART). These *in vitro* techniques have been used to study follicle development in a variety of species, including mice, rats, cattle, sheep, pigs, primates and humans (159-162).

1.3.1 Ovarian tissue culture

The acquisition of tissue for ovary culture is relatively straightforward, with the collection of tissue and removal of extraneous tissue prior to culture. Ovarian culture systems have used varying physical supports when culturing them in wells, dishes or watch glasses. To ensure tissue survival, the ovarian tissues have been minimally submerged in media, with a source of media adjacent to the physical support (163).

1.3.1.1 Mouse ovarian tissue culture

Mouse foetal ovarian fragments (E16) have been successfully cultured for up to 50 days. However, during those 50 days of culture, large numbers of oocytes disappear from culture due to degeneration (164). Embryonic ovary culture is often used for reproductive toxicology studies, as they contain pre-meiotic germ cells, prior to follicle formation, which makes them particularly vulnerable to chemicals (reviewed in (165)).

Since primordial follicle assembly occurs after birth in mice, neonatal mouse ovary culture is an appropriate culture system to study primordial follicle assembly and the primordial to primary follicle transition. Generally, static ovary culture is performed to assess the production of factors in culture (166,167) and the effect of different culture conditions on follicle development and subsequent offspring (15,168-173). A dynamic ovary culture system has also been developed to allow to continuous replacement of culture media, to mimic circulation (174).

Using neonatal ovary culture as an initial step, fertilisable oocytes have been developed entirely *in vitro*, resulting in the first birth of a mouse (159). Neonatal ovaries were first cultured for 8 day (8 d) to promote primordial follicle growth to the secondary follicle stage. However, for further follicle development, these secondary follicles were isolated and cultured as oocyte-GC complexes for 14 d. This combination of ovary culture and follicle culture is referred to as two-step culture. After follicle culture, the oocytes were matured for 15-18 h, fertilised, and the resultant 2-cell embryos transferred to pseudopregnant females. However, the

efficiency of this technique was poor, as less than 2% of the 2-cell embryos reached blastocyst stage, and only two foetuses were produced after the transfer of 190 2-cell embryos (159). This two-step technique was subsequently improved, resulting in the birth of multiple, normal offspring (160). Later work by other groups have also demonstrated the ability develop live offspring from oocytes cultured from foetal ovaries using a similar two-step technique (175,176).

1.3.1.2 Bovine and human ovarian tissue culture

Ovaries from larger species contain more ECM and cannot be cultured whole; only ovarian fragments of approximately 1 mm^3 can be cultured (177). Since primordial follicles are enriched in the cortical area (110), dissection and culture of cortical strips ensures that a large number of primordial follicles can be initiated to grow. The culture of these thinner cortical strips also minimises the chance of necrosis by maximising the surface area for nutrient and gaseous exchange, and still provides an ovary-like support system, where the follicles within the cortex are still intact and in contact with stromal cells (178).

Cortical strip cultures have been performed using bovine tissue (179-186), and also using human tissue (161,177,187-195). However, the addition of foetal bovine serum (FBS) (189) and ECM (177,187,188,191), the latter of which has shown been to modulate follicle survival (177,196) may not be appropriate for human cortical strip culture in an ART setting. Serum is often added to culture media, as a source of albumin, which acts as a scavenger, and as a source of precursors for steroidogenesis (197). Long-term culture containing serum has also

been linked to epigenetic modifications and foetal overgrowth syndromes in cattle (198,199). To avoid the use of serum, human cortical strips have been effectively cultured in serum-free media containing either bovine serum albumin (BSA) (161,190) or human serum albumin (177,191-195).

The ECM commonly used in ovarian culture is Matrigel, which is derived from Engelbreth-Holm-Swarm mouse sarcoma cells (200). Matrigel contains a variety of growth factors, including TGFßs, fibroblast growth factor (FGF), epidermal growth factor (EGF) and insulin-like growth factor (IGF) (201,202), all of which are involved in follicle development (reviewed in Matzuk and Lamb (2008) (138)). Although a reduced growth factor version of Matrigel is available, the exposure of human cortical strips to unknown levels of growth factors may be unsuitable for the development of fertilisable oocytes for the clinical treatment of infertility.

Using a serum-free two-step culture, follicles were grown in bovine (184) and human (161) cortical strips to the preantral stage. These preantral follicles were then isolated for individual follicle culture. Bovine cortical strips containing follicles with a diameter of less than 40 µm were cultured for 6 days before preantral follicles with a mean diameter of 111 µm were manually dissected out for 15 d follicle culture. The follicles cultured with activin A grew to 200 µm in diameter, while those cultured with activin A and FSH reached 247 µm in diameter (184). The human cortical strips were cultured similarly for 6 d, and preantral follicles with a mean diameter of 100 µm were dissected out and cultured in the presence or absence of activin A for 4 d. Follicles cultured without activin A increased in size to 111 µm in diameter, while

those cultured with activin A grew to 143 µm in diameter (161). This demonstrates that follicle development is accelerated *in vitro*, as the *in vivo* development of a primordial to the preantral stage takes over 300 days (203).

1.3.2 Follicle culture

Once follicle growth reaches the preantral stage the ovary or cortical strip environment is inhibitory for further growth. The two-step system (mentioned previously in Sections 1.3.1.1 and 1.3.1.2) is therefore required to enable follicle development to continue. For follicle culture, the preantral follicles developed within the cultured ovaries or cortical strips are isolated mechanically or enzymatically (178,204).

Follicle culture systems can be generally classified as two-dimensional (2D), which require follicle adhesion, resulting in the loss of follicle integrity (205,206), or three-dimensional (3D). Three-dimensional follicle culture has been achieved through culturing in V-bottomed dishes (161,184,207-210), in hydrophobic membranes that prevent attachment (211), or encapsulation by hydrogels (reviewed by Vanacker and Amorim 2017 (162)). Other techniques, such as the hanging droplet, which is often used for organoid culture, has been used for follicle culture, but is a not commonly used technique (212).

Although follicle culture using primordial and primary follicles have been attempted in both mice (187,188,207,213-218) and humans (193,219,220), there

have been difficulties in optimisation. Current research efforts have now focused on culturing secondary or preantral follicles with the aim to develop mature, fertilisable oocytes (reviewed by Smitz et al. (2010) (204), Telfer and McLaughlin (2012) (221) and Guzel and Oktem (2017) (222)).

Meiotically competent meiosis II (MII) stage human oocytes were first successfully cultured from multilaminar secondary follicles encapsulated in 0.5% alginate gel (223). The rigidity of the alginate gel encapsulating provides inert mechanical support without cell adhesion (224) (see Section 1.4.1). Isolated human follicles (mean diameter 165 µm) were encapsulated individually and cultured for 10-15 days, until they reached a diameter of 400-500 µm with an antrum present. A portion of these follicles were then released from the alginate and further cultured in low-attachment plates for 30-40 days. Of the follicles further cultured outside of the alginate hydrogels, 4 out of 20 of follicles produced meiotically competent MII stage oocytes (223).

1.4 Artificial ovaries

Since the follicle is a three-dimensional structure, and contact between the oocyte and its GCs is vital for development (137,159,206,225), the use of an artificial ovary can potentially improve *in vitro* follicle development by providing physical support for follicles to retain their 3D structure within a group culture setting. The scaffold can even be a source of factors, either impregnated within the ovary scaffold or from additional supporting cells included in the structure. The definition of an artificial ovary is varied, and can be defined as multiple intact follicles seeded

into a scaffold or encapsulated together, or ‘organoids’ consisting of dissociated germ or somatic cells. The former are considered an extension of follicle culture, as the follicles remain intact and in group culture, while the latter are more aligned to organ culture. To promote follicle development, these can be transplanted into a host, or cultured *in vitro*.

Currently, there are four major types of scaffolding approaches used in the generation of artificial ovaries: hydrogels, self-assembled 3D microtissues, decellularised ovaries and 3D printed scaffolds. This, however, excludes reaggregated ovaries (ROs), another type of artificial ovary, which does not have any scaffold material exogenously added (Table 1.3).

Table 1.3 Scaffolds used in artificial ovaries.

Scaffold type	Scaffold material	Type of artificial ovary	Pros	Cons	References
No scaffold	N/A	Reaggregated ovary	Can separate out germ and somatic cells	Follicle development has only been demonstrated using mouse somatic cells	(226-232)
External scaffold	Alginate hydrogel	Multiple follicle encapsulation within hydrogel (human, mouse) Hydrogel-encapsulated reaggregated ovary	Ease of crosslinking polymers Permeable to proteins No cell adhesion	Rigid; growing follicles are exposed to increasing pressure Exposure to divalent cations (e.g. Ca^{2+}) for crosslinking	(214-218,223,233-247)
	Fibrin hydrogels	Multiple follicle encapsulation within hydrogel (mouse)	Can be impregnated with factors Hydrogel combination with alginate may maintain hydrogel structure for longer	Pure fibrin hydrogels only provide support for a limited period Hydrogel contains other factors involved with follicle development	(238,241,248-254)
	Hyaluronan hydrogels	Multiple follicle encapsulation within hydrogel (mouse)	Naturally occurring in ovaries Optical transparency Ease of use	Fewer MII oocytes developed compared to Control (no encapsulation)	(255)
	PEG hydrogels	Multiple follicle encapsulation within hydrogel (mouse)	Can be modified to allow cell-matrix interactions Degrade in response to follicle-secreted proteases, allowing follicle expansion	Requires additional steps for modifications	(256,257)

Internal scaffold	3D printed agarose scaffold	Intact mouse follicles and somatic cells seeded onto scaffold and cultured	MII oocytes produced	Requires 3D printer No further reports using this method	(258)
	3D printed gelatin scaffold	Intact mouse preantral follicles seeded onto scaffold and transplanted	Supported terminal differentiation of follicles	Requires 3D printer	(259)
	Decellularised extracellular matrix	Intact mouse follicles seeded onto decellularised bovine extracellular matrix and transplanted	Host mice regained ovarian endocrine function Follicle development observed	Requires tissue to decellularise to have extracellular matrix	(260)

The choice of scaffold for the artificial ovary must be able to physically support the follicles within. However, the material must not be too rigid, as this can restrict growth and expansion of the follicles (261). In addition, the scaffold must also be permeable to nutrients within the culture media and allow the diffusion of proteins and hormones into the cells (262). Depending on the size and the setup of the artificial ovary, the size of the cultured tissue may still be restricted to approximately 1 mm^3 to maintain permeability of gases and nutrients and reducing necrosis within the centre of the tissue. However, larger artificial ovaries may be cultured if a perfusion or bioreactor method can be used to improve nutrient and gas exchange (174,190,263,264).

If the artificial ovary is to be grafted into a patient, it is important that the scaffold is biodegradable, since this encourages vascularisation and supports follicle growth (265). Depending on the design of these grafts and the subsequent

treatment regimes, these transplanted artificial ovaries have the potential to restore reproductive and endocrine function for premature ovarian insufficiency (POI) patients (261).

1.4.1 Hydrogels

Hydrogels, such as those used for follicle culture, have been implemented in artificial ovary design. These artificial ovaries normally involve the encapsulation of multiple follicles within a single droplet; essentially a group follicle culture. Hydrogels are formed by the cross-linking of water-soluble polymers. Naturally derived polymers have been used in follicle culture (collagen (266), alginate, fibrin, hyaluronan (HA)), as well as synthetic polymers (polyethylene glycol (PEG)). The hydrogels can also be impregnated with factors to provide localised action; such as vascular endothelial growth factor (VEGF) (252,267).

1.4.1.1 Alginate hydrogels

Alginate is a collective term for polysaccharides produced by brown algae or bacteria, which consist of β-D-mannuronic acid and α-L-guluronic acid chains in an alternating structure (268). To form a hydrogel, the alginate, containing the follicles, is exposed to concentrations of calcium or other divalent cations, leading to the crosslinking of the polymers (269). The mesh-like structure of the alginate hydrogel is permeable enough to allow the diffusion of proteins such as FSH (233) and also provide mechanical support for the follicles without cell adhesion (224).

Encapsulation of multiple late primary and secondary murine follicles within a single alginate bead (0.5% alginate) showed improved follicle survival and growth after 13 days of culture compared to individually encapsulated and culture (216). Follicles encapsulated and cultured together in groups of tens were able to reach MII stage, indicating that group culture may improve outcomes due to paracrine signalling between follicles (216).

Follicles isolated from human medulla, ranging from the primordial to the secondary follicle stage, have also been encapsulated in groups of 2-10 follicles with and without interstitial tissue (270). However, significant atresia of primordial and primary follicles and few secondary follicles reaching antral stage was observed after 7 d of culture. This indicates that further optimisation of culture media and conditions, as well as 3D support, is required to improve human follicle development in the alginate artificial ovary.

Pure alginate hydrogels may not be the best scaffold for artificial ovaries, as they do not degrade, and growing follicles are exposed to increasing pressure from the hydrogel (271). To address this problem, fibrin-alginate (FA-IPN) inter-penetrating networks have been used for follicle culture.

1.4.1.2 Fibrin hydrogels

Fibrin is generated by the polymerisation of fibrin by thrombin, both of which are isolated from the blood plasma. By incorporating fibrin with alginate to form FA-

IPN, the fibrin and alginate polymers are entangled, allowing the matrix to be degraded by follicle-secreted proteases (249,272,273). As the follicle grows, the secreted proteases will degrade the surrounding fibrin, and allow follicle expansion. So far, only individual follicles have been encapsulated in FA-IPN for culture (238,241,248,249,253).

FA-IPN-based artificial ovaries have been used in transplantation into adult mice, but showed less follicle development compared to artificial ovaries of fibrin. All mice which were transplanted with fibrin-based artificial ovaries (containing primordial and primary follicles and ovarian cells) resumed cycling, and those which were also impregnated with VEGF resulted in live births (252).

Several other groups have also developed the use of fibrin as a scaffold for artificial ovaries. Primordial, primary and secondary murine follicles were encapsulated with stromal cells in fibrin and transplanted into mice; after one week of transplantation, 223 of 713 follicles were retrieved, of which 10 were at the antral follicle stage, while 180 were at the secondary follicle stage (250). Although follicle development does occur within these artificial ovaries, a large number of follicles do not survive the isolation, encapsulation and engraftment procedure (250,251,254). Further work has demonstrated the primordial-primary follicles have lower recovery rates than secondary follicles, but both are still able to grow within the fibrin-based artificial ovaries (254).

Although fibrin hydrogels can allow follicles to expand, they can only provide a support for a limited period, as the follicle will continue to degrade the hydrogel (251). Therefore, the addition of alginate, which is not degradable, in an FA-IPN may possibly maintain the hydrogel structure for longer.

1.4.1.3 Hyaluronan hydrogels

The first application of hyaluronan (HA) hydrogels as a scaffold for the encapsulation of preantral follicles was performed by Desai et al. (2012), using a tyramine-based HA in culture. Hyaluronan, a glycosaminoglycan, is the major component of the expanded cumulus oophorous in preovulatory follicles (274), which is involved in cellular signalling, matrix organisation, wound repair and morphology in various tissues (275).

After initial testing of HA concentrations and encapsulation techniques, oocytes from both freshly isolated and cryopreserved preantral follicles were able to reach the MII stage after 12-13 days of culture within the artificial ovary. Despite this novel demonstration, HA-encapsulated follicles did not have the same percentage of MII oocytes as Control cultures (255). However, the optical transparency, ease of use and support of follicle development makes this hydrogel particularly attractive as a scaffold for artificial ovaries.

1.4.1.4 PEG hydrogels

As a synthetic hydrogel, PEG can easily be modified (276,277), and can be used to mimic the ECM. Poly(ethylene glycol) vinyl-sulfone (PEG-VS) has previously been used in follicle culture (256), and can be modified with integrin-binding peptides (such as RGD (Arg-Gly-Asp)) to allow for cell-matrix interactions (278,279).

Primordial and primary follicles, along with stromal cells were encapsulated in PEG-VS hydrogels modified with RGD to form artificial ovaries. These were then grafted into the ovarian bursae of bilaterally ovariectomised mice. After 30 days of engraftment, the artificial ovaries contained antral follicles and CL, and even after 60 days of engraftment, the FSH levels within the mice remained at physiological levels (277). The maintenance of the selective follicle recruitment, as well as the restoration of the HPG axis, also demonstrates that PEG hydrogels are also a potential candidate as a scaffold for artificial ovaries *in vitro*.

1.4.2 Decellularised extracellular matrix

Decellularisation of an organ or tissue results in the removal of its cellular material, but leaves the ECM, which provides a scaffold that resembles the native structure of a tissue. This decellularised ECM can be reseeded with cells to form a new artificial organ.

Using decellularised bovine tissue, primary mouse ovarian cells, which included GCs, TCs and potentially oocytes, were seeded onto the scaffold. After 48h of culture, the primary cells formed a confluent layer on the periphery of the scaffold, and were grafted into pre-pubertal mice which were previously ovariectomised. As a Control, mice were also grafted with sham scaffolds which did not have seeded cells. The mice which were grafted with the artificial ovary initiated puberty and had had normal oestradiol levels, indicating restoration ovarian endocrine function. One of the grafts also contained 2 antral follicles, indicating the primary ovarian cells seeded may have contained a few primordial follicles or denuded oocytes, and had a supportive niche for follicle development (260).

1.4.3 3D printed scaffold

1.4.3.1 Gelatin-based 3D scaffold

Following on from the artificial ovary generated using a decellularised bovine ECM as a scaffold, Laronda et al. (2017) used 3D printing to generate a gelatin hydrogel-based scaffold, seeded with murine preantral follicles throughout all the layers, to produce an artificial ovary.

Using varying angles in each layer to adjust the scaffold geometry, thus adjusting follicle contact points, the results revealed that struts within the scaffolds angled 30° and 60° created pores. Within these pores, the follicles were able to come into contact with the scaffold at two or more points. Interestingly, the more contact points a follicle had with the scaffold, the higher the chance of follicle survival (259).

When the artificial ovary was cultured *in vitro* for 4 d, 3-ß hydroxysteroid dehydrogenase (3ßHSD), was active in the TCs of the seeded follicles and E_2 production also increased. To test the *in vivo* actions of the artificial ovary, they were transplanted into ovariectomised mice. The cultured scaffold also supported the terminal differentiation of follicles, and ovulated mature MII oocytes. The ensuing litters were identified as having resulted from eggs ovulated from the artificial ovaries. The five pups born were also supported by milk by their lactating artificial ovary-recipient mothers, indicating that the progesterone support from the ovary was sufficient to initiate prolactin production and lactation (280). The five pups also subsequently sired or gave birth to their own litters (259).

This interesting new development in artificial ovary scaffold generation highlights the adaptability of a 3D printing system, as well as the versatility of the scaffold after transplantation. No additional manipulation was required to release the egg for ovulation, and the live birth was achieved without the addition of angiogenic growth factors, hormone transfer or embryo transfer, which highlights the ability of this type of artificial ovary to independently restore HPG function.

1.4.3.2 Agarose-based 3D scaffold

Krotz et al. (2010) first described the generation of an artificial ovary using an agarose scaffold seeded with TCs and GCs. Each of the 18 honeycomb-shaped wells within the scaffold was seeded with TCs isolated from human antral follicles and cumulus GCs stripped from the oocytes of *in vitro* fertilisation (IVF) patients. After the scaffold was populated by TCs and GCs, cumulus-oocyte-complexes from

early antral follicles were seeded into the agarose scaffold and cultured within the artificial ovary for 45 h. Although the results indicate the TCs and GCs continued to produce hormones in culture, it was not measured, and therefore it is unclear whether the oocytes matured to MII stage due to the environment within the artificial ovary, or spontaneously (258). This technique was published in 2010, but there have been no further reports using the same methods.

1.4.4 Reaggregated ovaries

Although the scaffolds mentioned previously (Sections 1.4.1 to 1.4.3) have demonstrated the ability to support follicle development, restore the HPG axis and result in live births, all the techniques are reliant on functional somatic cells (i.e. GCs, TCs, stromal cells). Therefore, for patients abnormal follicle development due to dysfunctional ovaries (e.g. premature ovarian insufficiency (POI) or granulosa cell tumours (GCTs)) (281-285), the aforementioned techniques may not support follicle development to generate fertilisable eggs.

The reaggregated ovary (RO) technique was developed by Eppig and Wigglesworth (2000) to determine whether oocytes or somatic cells orchestrated the rate of follicle development. Using differential adhesion, the somatic cells could be cleanly isolated from germ cells (i.e. oocytes), and reaggregated to form reaggregated ovaries (ROs). The ROs were transplanted into ovariectomised, immunocompromised mice to promote follicle development. Using *LacZ*-expressing mouse germ cells and rat somatic cells to generate chimeric ROs, and vice versa, xenogeneic follicles were able to form within the ROs, with oocytes reaching the MII

stage. Chimeric ROs containing mouse oocytes and rat somatic cells were able to generate fertilisable eggs from the xenogeneic follicles, and resulted in one live birth. The female mouse derived from this oocyte also continued on to have 83 normal offspring (226).

Aside from using chimeric ROs to generate xenogeneic follicles from mice and rats, ovarian cells from other species, including cats, have been reaggregated with mouse cells and developed follicles (personal correspondence between Dr. Williams and Karen Wigglesworth). Work in the Williams laboratory has also demonstrated that follicle development can occur in ROs generated from the reaggregation bovine ovarian stem cells and mouse somatic cells, and the reaggregation of adult and neonatal ovaries (unpublished data). The technique has also been used *in vivo* to assess whether oocytes are the central regulators of follicle development (228) and the role of connexins in oocyte-somatic cell interactions (229,231).

Previous work performed in the Williams lab (unpublished work) has also demonstrated that the arrested follicle development found in a mouse model of premature ovarian insufficiency (POI), known as the Double Mutant (DM) can be restored. This POI mouse model has an oocyte-specific deletion, resulting in an age-associated decline in fertility and abnormal follicle development (286). Interestingly, follicle development is restored when germ cells from infertile DM mice are reaggregated with neonatal somatic cells (unpublished data).

However, the transplantation of ROs into host mice does not allow the real-time visualisation of follicle development and would not be acceptable as a clinical treatment to develop eggs for ART. Generating an *in vitro* culture technique for ROs to enable ongoing observations of follicle development would be hugely advantageous to understanding follicle development and remove the need for xenogeneic transplantation. Although ROs have previously been cultured using neonatal or foetal mouse cells, none had produced follicles which reached the preantral stage, which would allow the follicles to be dissected out for follicle culture (227,230,234).

After this project began, Hikabe et al. (2016) published a report that demonstrated that mature mouse oocytes could develop entirely *in vitro* from ROs. The germ cell source for these ROs were either mouse embryonic stem cells (ESCs) or induced pluripotent stem cells (iPSCs) from mouse embryonic or adult fibroblasts, which were reaggregated with mouse embryonic (E12.5) ovarian somatic cells. After 3 weeks of culture, the RO formed primary follicles, and after a further 11 days of culture, *in vitro* maturation was performed to develop MII stage oocytes. The full female germline was also reconstituted by the rederivation pluripotent stem cell line from these *in vitro* generated eggs. To determine whether the eggs were functional, IVF was performed, leading to the birth of live pups (232). The publication of these results highlights the ability of the RO technique as an *in vitro* platform to understand follicle development, as well as a potential fertility treatment as an artificial ovary.

Although these results indicate that the entire germline can be recapitulated from these murine sources and that the oocytes generated from cultured ROs can result in live offspring, there is still a need to assess the follicle development in cultured ROs and to adapt the technique for use with human tissues. This thesis was therefore structured to address these overall aims.

1.5 Aims

The aims of this thesis are:

- To adapt the *in vivo* RO technique into a culture technique
- To compare follicle development in cultured ROs to that in transplanted ROs, cultured ovaries and Control *in vivo* ovaries
- To assess the effect of serum and rigidity on theca cell proliferation in cultured ovaries using mouse serum and hyaluronan hydrogels
- To assess different enzymatic mixtures for bovine cortical strip digestion
- To investigate the potential of germ cells from human ovarian tissue to generate ROs

Chapter 2: Materials and Methods

2.1 Mouse colonies

2.1.1 Ethical approval

All experiments involving mice were done with permission from the Home Office and the Local Ethical Review Panel at the University of Oxford, in accordance with the UK Animals (Scientific Procedures) Act 1986, under a project licence held by Dr. Williams (Project Licence number 30/2780 (before October 2015) and 30/3352 (as of October 2015)).

2.1.2 ROSA*LacZ* mice

The ROSA26*LacZ* colony contained mice with a C57BL/6 on a background, ubiquitiously expressing the *LacZ* gene (287). All mice had water and food *ad libitum* and were maintained on a 12:12 hour light:dark cycle.

2.1.3 Mouse colony management system

Two management systems for tracking the colony were used: excel sheets originally generated by Dr. Williams and the Sanger system used by the Home Office. Prior to the adoption of the Sanger system, Dr. Williams' excel sheets were updated biweekly to track breeding cage productivity, genotype of offspring, mice allocation and use of mice. The Sanger system, which was adopted in the animal facility used in 2016, became the official method to track the procedures performed, breeding cages, and the fate of mice. The excel sheets were continually used to plan experiments and allocate mice.

2.1.4 Mouse breeding regime

Breeding cages to generate ROSA26*LacZ* mice were set up with pairs or trios (one male paired with two females). Ideally, the male mice expressed *LacZ* (*LacZ*$^{+}$), while the females did not (*LacZ*$^{-}$); this was preferred as these males could then also be used for timed matings (see Section 2.1.5). Breeding cages were set up with 6 week old mice. Decisions regarding breeding timetables were based on mouse gestation length (19-21 days), and the production of litters every 3 weeks, since females have post-partum oestrus.

2.1.5 Timed matings

If a large number of females were required for experiments, mating cages were set up with male mice (from breeding cages, expressing ROSA*LacZ*$^{+}$; or C57BL/6 wildtype mice (University of Oxford Biomedical Services, Oxford, UK)) with CD-1 mice (Envigo, Blackthorn, UK) rotated in. Female CD-1 mice were preferred, as they have large litter sizes (>10 mice per litter) compared to C57BL/6 females.

One or two females were placed with each male, and at around 9 am the next morning, plugs were detected using a probe. If a plug was present, the female mouse was returned to a stock cage, and a replacement female was added. To ensure pup survival and utilise the postpartum oestrous, pregnant females were paired for about a week with a male prior to littering down.

2.1.6 Tail tipping, ear clipping and weaning

Neonatal mice up to 7 days old (P7) were tail tipped to collect tissue for genotyping. To numb the tail prior to tail tipping, the tail was exposed to an ethyl chloride-based cryogesic fine spray (Acorus Therapeutics Ltd., Chester, UK). Once the tail became mostly pale, local anaesthesia was considered sufficient, and a piece of tail (approximately 1-2 mm in length) was removed using a scalpel blade and collected for genotyping.

Mice that had not been tail tipped as a neonate for genotyping, once it reached P12-14, it was ear clipped for identification and genotyping purposes. To ear clip, the mice were scruffed with the non-dominant hand, and the ear biopsy taken with the dominant hand using the ear biopsy tool (Vet-tech, Congleton, UK) which was placed into a sterile microcentrifuge tube. Tools were cleaned with 70% ethanol (Sigma-Aldrich, Dorset, UK) between tissue collection from each mouse.

Mice were weaned into stock cages at 3 weeks of age. Males and females were weaned into separate cages. Females from different cages can be caged together. However, since males are territorial, males from different cages cannot be weaned into a single cage unless carried out within a short period (2-3 days). Males also cannot be caged together after separation, even if they were initially weaned together.

2.2 Genotyping

LacZ gene expression can be determined using X-gal staining, which detects the presence of the product of *LacZ*, β-galactosidase. To genotype using X-gal staining, the samples (ear clips or tail tips from neonates) were incubated at 37°C for at least 1 h in X-gal staining solution, containing 50mg/ml X-gal (Sigma-Aldrich), 250mM potassium ferricyanide, 250mM potassium ferrocyanide, 1M $MgCl_2$, 1% sodium deoxycholate, 1% NP-40 (Sigma-Aldrich), 1M Tris (pH 7.3) and 0.1M PBS (pH 7.3). Tissue from mice expressing the *LacZ* gene are stained blue after exposure to X-gal solution. Positive and negative control tissues were included in every X-gal staining procedure.

Details of the components of the solutions are detailed in Table 2.1.

Table 2.1 X-gal staining.

Step	Reagent	Volume (µl) per 1ml solution
Fixation	25% glutaraldehyde	8
	1M $MgCl_2$	2
	0.1M PBS (pH 7.3)	990
Detergent rinse	1M $MgCl_2$	2
	1% sodium deoxycholate	10
	1% NP-40	20
	0.1M PBS (pH 7.3)	968
X-gal staining	50mg/ml X-gal	20
	250mM potassium ferricyanide	20
	250mM potassium ferrocyanide	20
	1M $MgCl_2$	2
	1% sodium deoxycholate	10
	1% NP-40	20
	1M Tris (pH 7.3)	20
	0.1M PBS (pH 7.3)	888

2.3 Reaggregated ovaries

The generation of ROs was performed based on Eppig and Wigglesworth 2000 (226), with modifications. For each RO, ovaries from four P2 or P6 mice were collected in warmed Dulbecco's PBS (DPBS, Sigma, Gillingham, UK) supplemented with 1 mg/ml bovine serum albumin (BSA, Factor V Heat Shock Treated; Fisher Scientific, Loughborough, UK). After the removal of bursa and fat using fine forceps (Dumont #5; Fine Science Tools, Heidelberg, Germany) and microscissors (Fine Science Tools), the ovaries were washed twice in DPBS/BSA.

To dissociate the ovaries into a single cell suspension, the ovaries were digested in 0.05% trypsin and 0.53 mM EDTA (Gibco, ThermoFisher Scientific, Paisley, UK) supplemented with 0.02% DNase-I (Sigma) and incubated at 37°C for 30 min. Digestion was aided by frequent gentle agitation by pipetting the tissue and solution. After dissociation, the cell suspension was transferred to a 15 ml centrifuge tube containing an equal volume of M199/FBS medium: Medium 199 (M199; Gibco, ThermoFisher Scientific) supplemented with 10% foetal bovine serum (FBS; Batch #10846; Labtech, Uckfield, UK), 31.3 mM sodium DL-lactate (Sigma) and 10 mg/ml penicillin-streptomycin (P0781; Sigma). After centrifugation for 5 min at 663 x *g* to pellet the cells, the supernatant was discarded, and the cells resuspended in 3 ml M199/FBS.

The germ and somatic cell population were separated using differential cell adhesion. The cell suspension was transferred to a tissue culture dish and cultured overnight at 37°C in an atmosphere of 5% CO_2 and 95% air. After overnight culture, somatic cells adhered to the culture dish (somatic cell population). The germ cell population remained unattached, and consisted of germ cells (oocytes), non-viable somatic cells and red blood cells. Unattached cells were carefully removed without dislodging the monolayer underneath, and added to a new tissue culture treated dish and cultured with M199/FBS. The adherent somatic cell population was vigorously rinsed with PBS/BSA three times to remove any unattached and loosely attached cells. The adherent somatic cell population was removed using 2 ml of trypsin/EDTA for 5 min. The cells were then transferred to a 15 ml centrifuge tube with 2 ml of M199/FBS, and centrifuged at 663 x *g* for 5 min to create a cell pellet. The supernatant was discarded, the cells resuspended in 3 ml M199/FBS and this

cell suspension was then transferred to a new tissue culture dish. Both germ and somatic cell suspensions were cultured for a further 6 h for a second round of differential adhesion. After the 6 h of culture, both germ and somatic cell populations were collected and centrifuged as previously. The supernatant was removed and each pellet resuspended in 200 µl M199/FBS.

To determine cell numbers, a sample of 10 µl was taken from each cell suspension and mixed with 10 µl Trypan Blue (Sigma) and assessed using a Neubauer Improved haemocytometer. After 10 µl of the cell suspension/Trypan Blue mixture was loaded into the haemocytometer, cells were counted in each corner quadrant (each quadrant contains 16 squares; 4 quadrants per haemocytometer grid) and averaged. To determine the number of cells remaining in the 190 µl of cell suspension, the following formula was used:

$$\frac{Cells}{ml} = Average\ number\ of\ cells\ in\ the\ quadrants \times 10^4 (Volume\ factor\ for\ the\ haemocytometer) \times 2\ (due\ to\ 1{:}1\ dilution\ with\ Trypan\ Blue)$$

$$\frac{Cells}{190\ \mu l} = \frac{Cells}{ml} \times 0.2\ (cells\ were\ resuspended\ in\ 200\ \mu l) \times 0.95\ (10\ \mu l\ was\ taken\ for\ haemocytometer\ assessment)$$

Germ and somatic cells were combined, using 1/3 of germ cells and all somatic cells (this ratio is routinely used for neonatal ROs (226)). Phytohemagglutinin (PHA-P; Sigma) was added to create a final concentration of

35 µg/ml to promote cell cohesion. After centrifugation of the suspension at 10,000 x *g* for 1 min, the reaggregated cells, now described as an RO, were cultured overnight in Waymouth MB752/1 media (Sigma) supplemented with 10% FBS. The ROs were transferred with minimal medium onto a polycarbonate Transwell membrane (6.5 mm diameter, 0.4 µm pore; Corning, New York, USA) in a 24-well tissue culture treated plate (Corning Costar). To prepare the membrane for overnight culture, 250 µl of Waymouth/FBS medium was added above and below the membrane. Once the RO was transferred to the edge of the membrane to ensure the RO rounded up, excess media was removed (see Figure 2.1). The 24-well plates containing the ROs were cultured at 37°C with an atmosphere of 5% CO_2 and 95% air. For transplantation, ROs were transplanted beneath the kidney capsule of ovariectomised immunocompromised mice (Section 2.5).

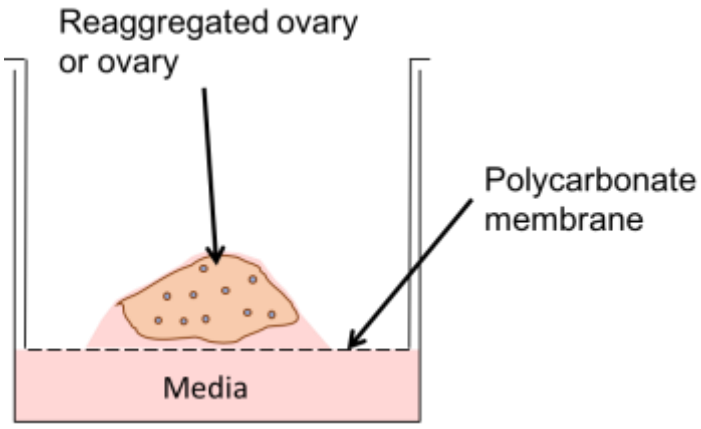


Figure 2.1 Culture setup of reaggregated ovary (RO) and ovary culture.

To encourage the 'rounding up' of reaggregated ovaries (ROs), the ROs were transferred to the edge of the polycarbonate membrane for overnight culture with minimal media covering the tissue. After overnight culture, the membrane holding the RO was transferred to a new well containing culture media and the RO moved to the centre of the membrane. This was considered 0 d of culture. Whole neonatal mouse ovaries were cultured similarly, with the ovary placed in the middle of the membrane and covered with a thin layer of media.

2.4 Ovary culture

After overnight culture, the membrane holding the RO was transferred to a new well containing 300 µl ovary culture media; this was considered 0 d of culture. Both ROs and whole ovaries were cultured for 14 and 21 d in Waymouth-based culture media: Waymouth medium supplemented with 5% FBS, 2.5 IU recombinant FSH (Gonal-F; Merck-Serono, Middlesex, UK) suspended in minimal essential medium, alpha modification (MEM Alpha; Fisher Scientific), 10 µg/ml BSA (Factor V heat shock treated; Fisher); 1% insulin-transferrin-selenium (ITS-G; Life

Technologies, UK), 100 IU/ml penicillin and 0.1mg/ml streptomycin (Sigma) and 25 µg/ml ascorbic acid (Fisher) suspended in MEM Alpha. The culture media was replaced every two days, with excess media used to gently move the RO or ovary, and prevent adherence to the membrane. This excess media was removed afterwards to leave a thin film of media covering the ROs or ovaries (see Figure 2.1). The cultures were maintained at 37°C in an incubator infused with 5% CO_2 and 95% air.

2.5 Transplantation of reaggregated ovaries

Induction of anaesthesia was performed in an induction chamber using 4% isofluorane (Isoflo; Abbott Laboratories, Abbott Park, IL, USA) and 2.5 litres per minute (LPM) of oxygen. Once fully anaesthetised, the mice were transferred to the anaesthesia mask with 2-2.5% isofluorane (Abbott Laboratories) and 1 LPM oxygen on a heated pad (37°C). The surgical site was prepared by removing the fur using clippers and cleaned aseptically using a chlorhexidine solution (HiBiScrub; Mölnlycke Health Care Ltd., Oldham, UK). Post-surgical analgesia was provided by a subcutaneous injection of 0.05-0.1 mg/kg buprenorphine (Vetergesic, Alstoe Ltd, York, UK). Depth of anaesthesia was assessed using the pedal withdrawal reflex. Once the absence of the reflex was confirmed, the surgical procedure was initiated.

Under magnification, the left kidney was exteriorised via a dorso-lateral incision, and the kidney capsule opened using fine tip forceps. A sterile fine-tipped pipette was used to place the RO under the capsule and gently push the RO away from the capsule opening. Once the kidney was placed back into the body cavity, a

bilateral ovariectomy was performed, and the body wall and skin were closed with interrupted sutures. The mice were then placed in a warm recovery chamber and assessed constantly until mobile and eating and drinking. After 3-4 h post-surgery, the mice were returned to the animal house maintenance room with easy access to food and water, and evaluated daily for 48 h using a recovery sheet. Signs of distress or infection were noted.

All surgeries were performed by Ms. Sairah Sheikh.

2.6 Histological processing

2.6.1 Fixation

If the reaggregated ovaries (ROs) *LacZ* expressing cells, the ROs were fixed in 25% glutaraldehyde (Sigma-Aldrich) in 0.1M PBS supplemented with 1M $MgCl_2$ for 2 h. The ROs were then washed 3 times for 15 mins in a detergent rinse containing 1M $MgCl_2$, 1% sodium deoxycholate, 1% NP-40, 1M Tris (pH 7.3) and 0.1M PBS (pH 7.3). The samples were then incubated overnight at 37°C in X-gal solution (see Section 2.2), and then washed 3 times in detergent rinse again. The ROs were then stored in PBS until embedding for a maximum of 3 weeks at 4°C.

Whole ovaries and ROs without *LacZ* expressing cells were fixed in 10% buffered formalin for 6 h and then transferred to 70% ethanol and stored at 4°C until embedding.

2.6.2 Embedding

Tissues were transferred into PBS prior to dehydration. If the tissues were small, they were lightly stained with 10% eosin (Sigma-Aldrich) in 50% ethanol for 30 min to aid visibility, which was useful for the embedding procedure. Tissues were then dehydrated through increasing concentrations of ethanol (50% to 100% ethanol) and three steps of xylene (Fisher Scientific, Loughborough, UK) (Table 2.2). The ethanol steps were performed in 96-well plates containing 200 µl of reagent per well. To saturate the tissues with xylene, glass embryo dishes containing 1 ml of xylene was used, as xylene dissolves plastic. Tissue was quickly transferred between wells using wide bore P200 or P1000 tips (Starlab, Milton Keynes, UK) to minimise tissue damage while handling.

Table 2.2 Reagents and timings for dehydration steps for embedding

Reagents	Time
50% Ethanol	15 min
70% Ethanol	15 min
80% Ethanol	15 min
95% Ethanol	15 min
100% Ethanol I	15 min
100% Ethanol II	15 min
100% Ethanol III	15 min
Xylene I	20 min
Xylene II	20 min
Xylene III	20 min

After saturation with xylene, the tissues were carefully transferred to plastic moulds containing melted paraffin wax (Histoplast; ThermoScientific, Waltham, MA, USA) and incubated in the wax at 62°C for 2 h. Labelled cassettes were placed on top of the moulds after incubation to secure the wax embedded tissue, and the moulds were left to cool overnight. To remove the paraffin block and cassette from the mould, the moulds were placed in the fridge for 1 h.

2.6.3 Sectioning

Paraffin blocks were removed from the moulds and the excess wax trimmed around the sample. The blocks were cut using a microtome (Leica, Nussloch, Germany) and serially sectioned at 3 or 5 µm. Wax sections were floated in a water

bath at ~45°C and collected on positively charged microscope slides (Superfrost® Plus, VWR International, Leuven, Belgium) using electrostatic adhesion. After overnight drying at room temperature, the slides were placed in an oven at 62°C for 1 h for the tissue to bind to the slides, and then stored in slide boxes at room temperature (Fisher Scientific).

2.6.4 Haematoxylin-eosin staining

Details for the staining are presented in Table 2.3. The haematoxylin staining method used is regressive. Slides were dewaxed in three steps of xylene and rehydrated in decreasing concentrations of ethanol (100% to 50%) and water. Nuclear staining was performed by immersing slides in haematoxylin (Shandon Gill 2 Haematoxylin; Fisher Scientific) for 2 min before washing them in tap water. To reduce the intensity of nuclear haematoxylin staining, the slides were dipped for 5 secs in acid alcohol (1% HCl in 70% ethanol), and washed with tap water. After exposure of the sections to 80% ethanol, cytoplasmic staining was performed using eosin (Sigma-Aldrich). Slides were dehydrated in ascending concentrations of ethanol and finally with two steps of xylene. Coverslips were attached to slides using DPX (Sigma-Aldrich) and left to dry flat overnight.

Table 2.3 Haematoxylin and eosin staining protocol

Step	Reagent	Time
Dewaxing	Xylene	3 steps: 8, 4, and 4 min
Rehydration	100% Ethanol	2 steps: 3 min each
	90% Ethanol	2 min
	70% Ethanol	2 min
	50% Ethanol	3 min
	Tap water	3 min
Staining	Haematoxylin	2 min
	Running water	5 min
	Acid alcohol	5 sec
	Running water	5 min
	80% Ethanol	1 min
	Eosin	1 sec
Dehydration	95% Ethanol	30 sec
	100% Ethanol	3 steps: 45 sec, 1 and 2 min
	Xylene	2 steps: 8 min each

2.6.5 Assessment of follicle development

To determine the location and number of follicles present in each ovary or RO, paraffin embedded tissues were serially sectioned (3 µm or 5 µm), and all 5th sections were stained with haematoxylin and eosin. Images were taken using a Leica DM 2500 microscope (Microscope Services Ltd., Woodstock, UK) and a MicroPublisher 5.0 RTV camera (Qimaging; Microscope Services Ltd.). Healthy follicles (without nuclear vacuoles or pyknotic bodies) containing an oocyte with clear nuclei were assessed. Follicles containing at least one full complete layer of cuboidal granulosa cells (GCs) were defined as primary follicles, while secondary follicles contained at least two complete layers of GCs. Preantral follicles had at

least three complete layers of GCs and no antrum, while antral follicles had at least three complete GC layers and antrum present. GC number and TC number was determined. To determine the TC number, TCs with a squamous appearance extending from the follicle basal lamina (BL) of the follicle up to the visibly different stromal cells were counted.

Chapter 3: Follicle development in cultured reaggregated mouse ovaries

3.1 Introduction

The development of follicles in the ovary requires complex bidirectional interactions between the somatic cells (GCs and TCs) and the germ cells, with certain steps requiring specific endocrine support. Furthermore, to ensure a continuous supply of mature eggs during a female's reproductive life, follicle development is highly regulated and carefully coordinated. However, in some instances, follicle development is perturbed, such as in premature ovarian insufficiency (POI 1% of women below 40 years of age (288)), or the ovaries are diseased, such as in ovarian cancer (4.22% of female cancer registrations in England in 2015 (289)). In these instances, the carefully regulated process of follicle development does not, or cannot, proceed *in vivo*. Therefore, despite the inherent complexity that exists throughout follicle development, we need to optimise techniques to enable us to generate developmentally competent mature eggs *in vitro* from ovarian tissues or isolated germ cells.

To develop oocytes for fertilisation, ovarian tissues can be cultured which provides a valuable tool for observing follicle development over time (159-161,176,238). Although in instances such as ovarian dysfunction or disease, the somatic cells present are not functionally optimal. However, ovarian germ cells from mice can be isolated and combined with an alternate source of somatic cells to generate a reaggregated ovary (RO). This RO can then be transplanted into an immunocompromised host that allows the RO to develop follicles over the following 3-4 weeks (226,229,231). Offspring have been generated from eggs developed in

an RO (226). Alternately, short-term (4 days (4 d) or 10 d) culture of ROs have been carried out using either P2 or foetal (E12.5 to E17.5) ovaries respectively (230,234).

ROs have been made using ovaries from ages ranging from E12.5 to P12 (226,228-231,234). The definition of a neonate is broad, and can be defined as mice aged P0-P7 (290), but the ovarian physiology at each age is quite different. For example, at P0-P1, primordial germ cells exist within germ cell nests and the germ cells are in a syncytium connected by cytoplasmic bridges (14,17). From P2 onwards, these germ cell nests begin to break down into individual primordial germ cells with many germ cells undergoing apoptosis, however, this process is not complete till P4-P5 (14). In addition, ROs generated with older ovaries may contain more developed follicles and therefore the resultant RO contains more differentiated somatic cells such as granulosa and theca cells.

Therefore, we aimed first to determine if follicle development in an RO was affected by the age of the neonatal ovaries and to accomplish this, we compared follicle development in ROs generated from P2 and P6 mice. Second, we aimed to determine how follicle development differed between ROs developed *in vivo* and *in vitro* comparing to whole ovaries developed *in vivo* and *in vitro*.

3.2 Aims

- To determine if follicle development in an RO is affected by the age of neonatal ovaries used (P2 compared to P6).

- To determine if follicle development differed between cultured ROs, transplanted ROs, cultured ovaries and in *vivo* Control ovaries.

3.3 Materials and Methods

3.3.1 Mice

Male ROSA*LacZ* mice were mated with female CD-1 mice to obtain hybrid F1 mice. F1 pups at postnatal day 2 (P2) and 6 (P6) were cervically dislocated and the ovaries isolated to generate ROs. Ovaries were also collected from F1 mice at P2, P6, P16 and P20 for histological analysis. Immunocompromised B6Rag1 mice were used as recipients for transplantation, and were generously donated by Professor Fiona Powrie, Nuffield Department of Medicine, University of Oxford.

3.3.2 Ovaries and reaggregated ovaries

Ovaries from four neonatal mice (P2 or P6) were used to generate ROs as (Section 2.3), and surgically transplanted in immunocompromised mice (Section 2.5). Reaggregated ovaries, along with P2 and P6 ovaries, were cultured as described in Section 2.4 for 14 or 21 d.

3.3.3 Tissue collection and assessment of follicle development

Reaggregated ovaries which required X-gal processing to differentiate *LacZ* expressing cells from wildtype cells were processed according to Section 2.6.1. The remaining tissues were collected and fixed in 10% buffered formalin (Sigma) for 6 h and stored in 70% ethanol. All tissues were dehydrated in increasing concentrations

of ethanol and xylene, and embedded in paraffin wax. All tissues were serially sectioned at 3 µm, and all 5th sections were stained with haematoxylin (Shandon Gill 2 Haematoxylin; Fisher Scientific) and eosin (Sigma) (Section 2.3). Healthy follicles (without nuclear vacuoles or pyknotic bodies) containing an oocyte with clear nuclei were counted in every 5th (cultured ROs and ovaries) or 20th section (*in vivo* ROs and ovaries). The total number of follicles at each follicle stage in ovaries and ROs was corrected using the Abercrombie correction factor (291). The formula for calculating the Abercrombie-corrected total number of follicles is:

$$Total\ number\ of\ follicles = crude\ count\ of\ follicles \times Abercrombie\ correction\ factor$$

where:

$$crude\ count\ of\ follicles = number\ of\ follicles\ counted \times sampling\ number$$

- The sampling number in this case was either 5 or 20, depending on whether the 5th or 20th section was assessed.

$$Abercrombie\ correction\ factor = \frac{Thickness\ of\ sections\ (\mu m)}{Average\ nuclear\ diameter\ (\mu m) + Thickness\ of\ sections\ (\mu m)}$$

Nuclear diameter was assessed using the ImageJ software (292).

3.3.4 Statistical analysis

Analysis was performed using GraphPad Prism version 7.00 (GraphPad Software, La Jolla, California, USA). Data was tested for normality using D'Agostino & Pearson normality test. Analysis of cell numbers was either performed using t-tests with Welch's correction (for normally distributed data) or Mann-Whitney U tests (for non-normally distributed data). Two-way ANOVAs with Sidak's multiple comparisons test were performed to compare differences in follicle numbers, at each follicle stage, between different age groups and conditions. Results are presented as mean ± SD, with $P \leq 0.05$ considered significant.

3.4 Results

3.4.1 Validation of cell isolation

Germ cells from P6 ovaries *LacZ* expressing mice (*LacZ*$^{+}$) were reaggregated with wildtype (*LacZ*$^{-}$) P6 somatic cells and cultured for 14 d and analysed to demonstrate the technique achieved complete separation between the two cell types (Figure 3.1). All oocytes were stained blue, while all somatic cells did not contain any blue precipitate, and were counterstained with eosin. Clean separation of the germ and somatic cell compartments within ROs was demonstrated at least three times.

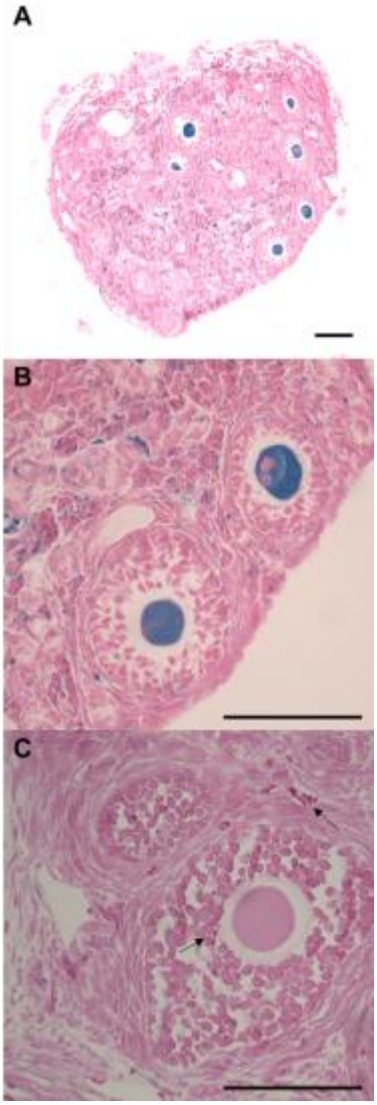


Figure 3.1 Cultured reaggregated ovary demonstrating clean separation between germ and somatic cells.

(A) A representative section of a 14 d cultured reaggregated ovary (RO) containing *LacZ*$^{+}$ germ cells (blue oocytes) and *LacZ*$^{-}$ somatic cells (pink; counterstained with eosin). (B) Higher magnification of the follicles in a 14 d cultured RO. (C) 14 d transplanted RO (counterstained with eosin) containing *LacZ*$^{-}$ cells, with arrows pointing to potential background staining from X-gal. Scale bars: 100 µm.

3.4.2 Number of germ and somatic cells from digested neonatal ovaries

ROs were generated using ovaries from four neonatal mice (P2 or P6). These were digested into a single population and separated into germ and somatic cells. The number of cells was assessed using Trypan Blue to determine if dead or alive. The number of Trypan blue positive dead germ cells was similar between P2 and P6 (mean ± SD; P2: 2682 ± 5973; P6: 2171 ± 5520; $P>0.99$). The total number of live germ cells was also similar between P2 and P6 (mean ± SD; P2: 29506 ± 8447; P6: 36914 ± 11490; $P=0.06$) No dead somatic cells were observed in either age group. As expected, more somatic cells were recovered from P6 ovaries compared to P2 ovaries (mean ± SD; P2: 342447 ± 124431; P6: 714400 ± 238850; $P<0.0001$).

3.4.3 Follicle development in neonatal ovaries

It was important to determine the number and stage of the follicles present within P2 and P6 ovaries (P2-O and P6-O respectively) (Figure 3.2A, B). P2-O contained follicles only up to the primary stage, whereas P6-O contained more primary follicles and also secondary follicles (Figure 3.2C). Neither P2-O nor P6-O contained preantral follicles.

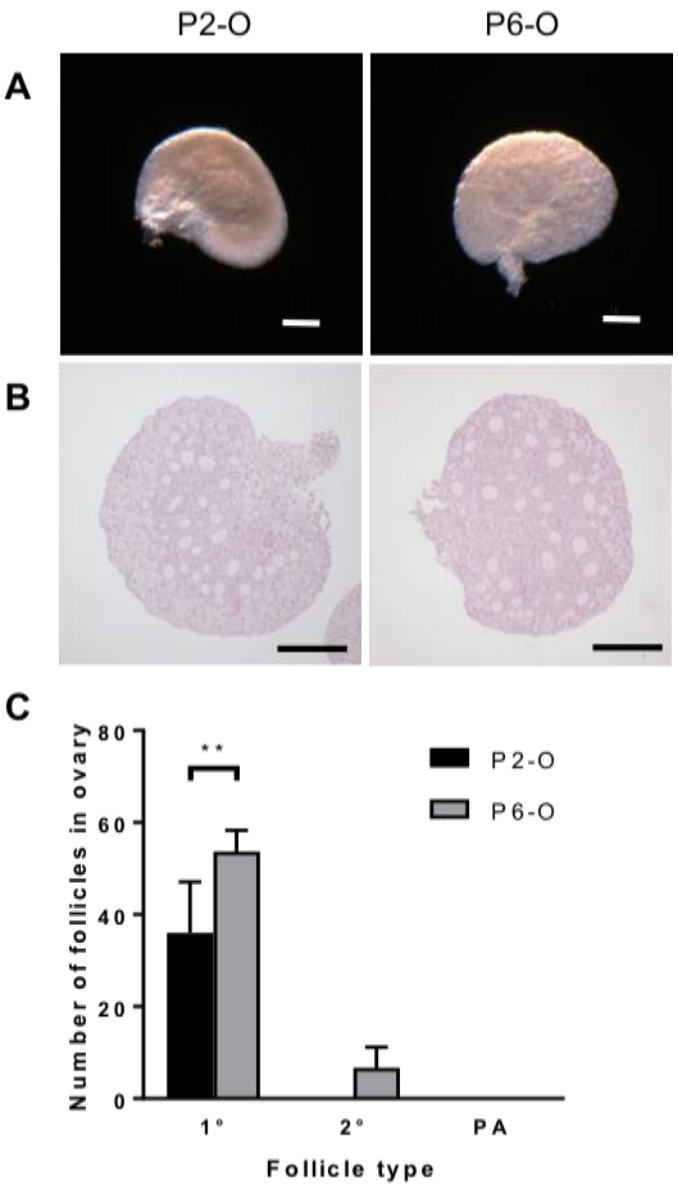


Figure 3.2 Follicle development in neonatal ovaries.

Representative images of (A) neonatal ovaries and (B) central sections stained with haematoxylin and eosin. (C) Follicle development was assessed in neonatal P2 and P6 ovaries. Scale bar: 200 µm. Data are plotted as mean values ± SD. P2-O n=4; P6-O n=3. ***P*≤0.01.

3.4.4 Age-related differences in follicle development in transplanted ROs

Since P6-O contained follicles that were more developed than P2-O, we determined whether transplanted ROs (ROt) generated from P6 ovaries contained follicles at later stages of development compared to ROs generated from P2 ovaries. We hypothesised that P6 ROs also contained more follicles as more cells within P6 ovaries were differentiated.

Only follicles from the primary follicle stage onwards were assessed, as no primordial follicles were observed in the ROs. Both P2 and P6 ROs transplanted for 21d (P2-ROt+21d and P6-ROt+21d respectively) had comparable numbers of follicles at all stages of development, up to the antral stage. P6-ROt+21d also had more developing follicles (primary follicles onwards) than P2-ROt+21d (Figure 3.3A).

However, when the ROs were collected after 14 d of transplantation (P2-ROt+14d and P6-ROt+14d), differences in follicle development emerged (Figure 3.3B). P2-ROt+14d contained follicles only up to the primary follicle stage, while P6-ROt+14d contained follicles that were more developed at the secondary follicle stage. Both P2-ROt+14d and P6-ROt+14d did not contain preantral or antral follicles, and had similar numbers of developing follicles.

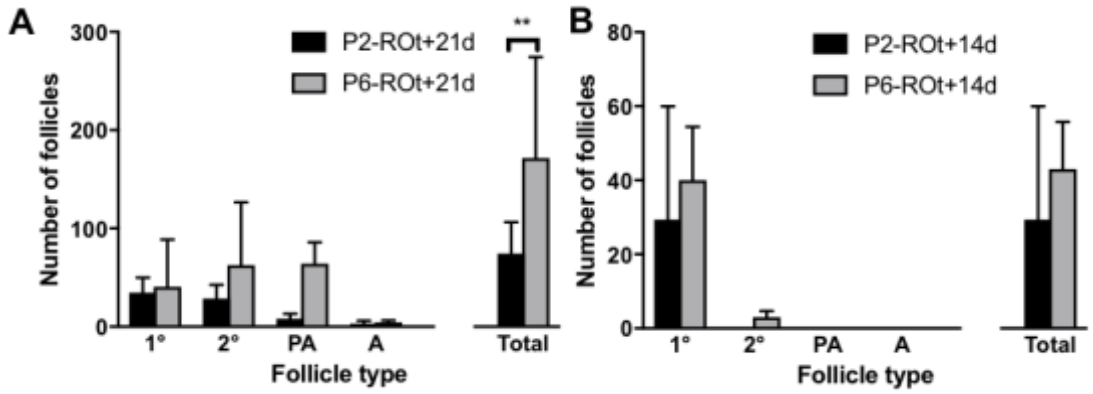


Figure 3.3 Follicle development in reaggregated ovaries transplanted for 21 days and 14 days.

Follicle development (follicle stages and total number of developing follicles) in P2 or P6 reaggregated ovaries which have been transplanted for (A) 21 and (B) 14 days was assessed. P2-ROt+14d n=3; P6-ROt+14d n=3; P2-ROt+21d n=3; P6-ROt+21d n=3.

3.4.5 Follicle development in cultured ovaries, cultured ROs, transplanted ROs and *in vivo* Control ovaries after 14 d

Since an age-related difference in follicle development was observed in transplanted ROs (Figure 3.4A), an acceleration in follicle development may also occur in cultured P6 ROs compared to P2 ROs (ROc represents cultured ROs). To control for the effects of RO generation on follicle development, P2 and P6 ovaries were also cultured for 14d (Oc represents cultured ovaries) (Figure 3.4B, C). Follicle development in transplanted ROs, cultured ROs and cultured ovaries were compared to age-matched *in vivo* Control ovaries (Figure 3.4D).

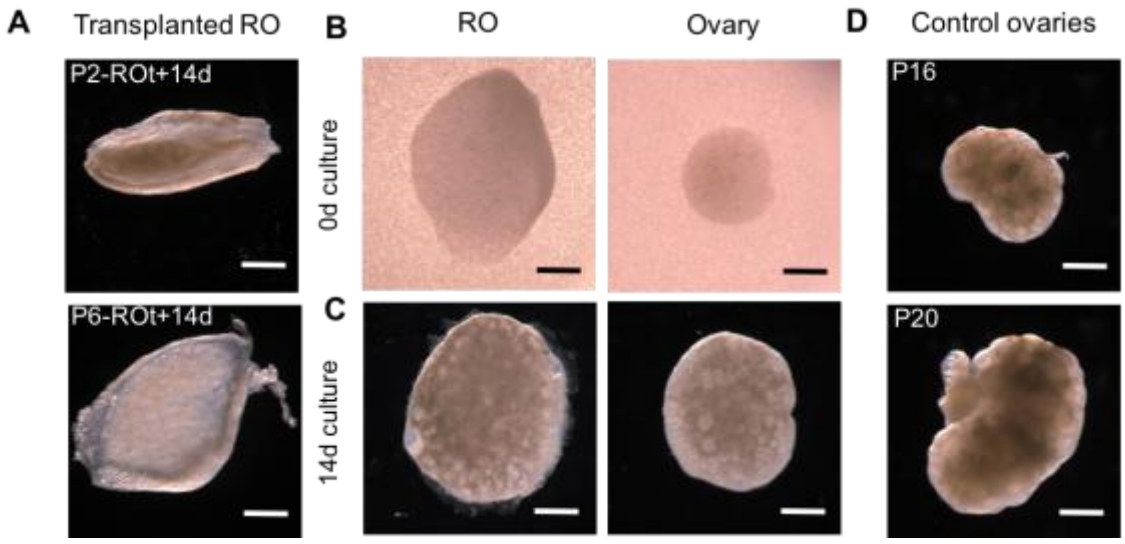


Figure 3.4 Representative images of transplanted reaggregated ovaries (ROs), cultured ROs, cultured ovaries and age-matched *in vivo* ovaries.

Representative images of (A) reaggregated ovaries (ROs) generated from P2 and P6 ovaries after 14 days of transplantation, (B) ROs and ovaries prior to culture and (C) after 14 days of culture and (D) *in vivo* Control ovaries. Scale bar: 500 µm.

Although P6 ovaries contain more developed follicles and differentiated cells, total follicle numbers between P2 and P6 groups were similar (Figure 3.5A, B). Surprisingly, even though ovaries from four neonatal mice are used to generate one RO, *in vivo* Control ovaries contained more developing follicles from the primary stage onwards (including antral follicles) compared to cultured ROs. This trend for fewer total follicles was also observed in cultured ovaries and transplanted ROs. In addition, no primordial follicles were observed within the ROs.

To assess any further differences due to the age of the ovaries, further analysis of the follicles into primary, secondary and preantral follicle stages was performed. No age-related differences were observed in cultured ROs, cultured ovaries and *in vivo* ovaries between the P2 and P6 groups, despite the advanced development of P6 ovaries (Figure 3.5C, D). The only age-related difference was observed in P6-ROt+14d, which contained secondary follicles while P2-ROt+14d only contained primary follicles. Although transplanted ROs did not contain preantral follicles, cultured ovaries and ROs from both age groups matured follicles up to the preantral stage.

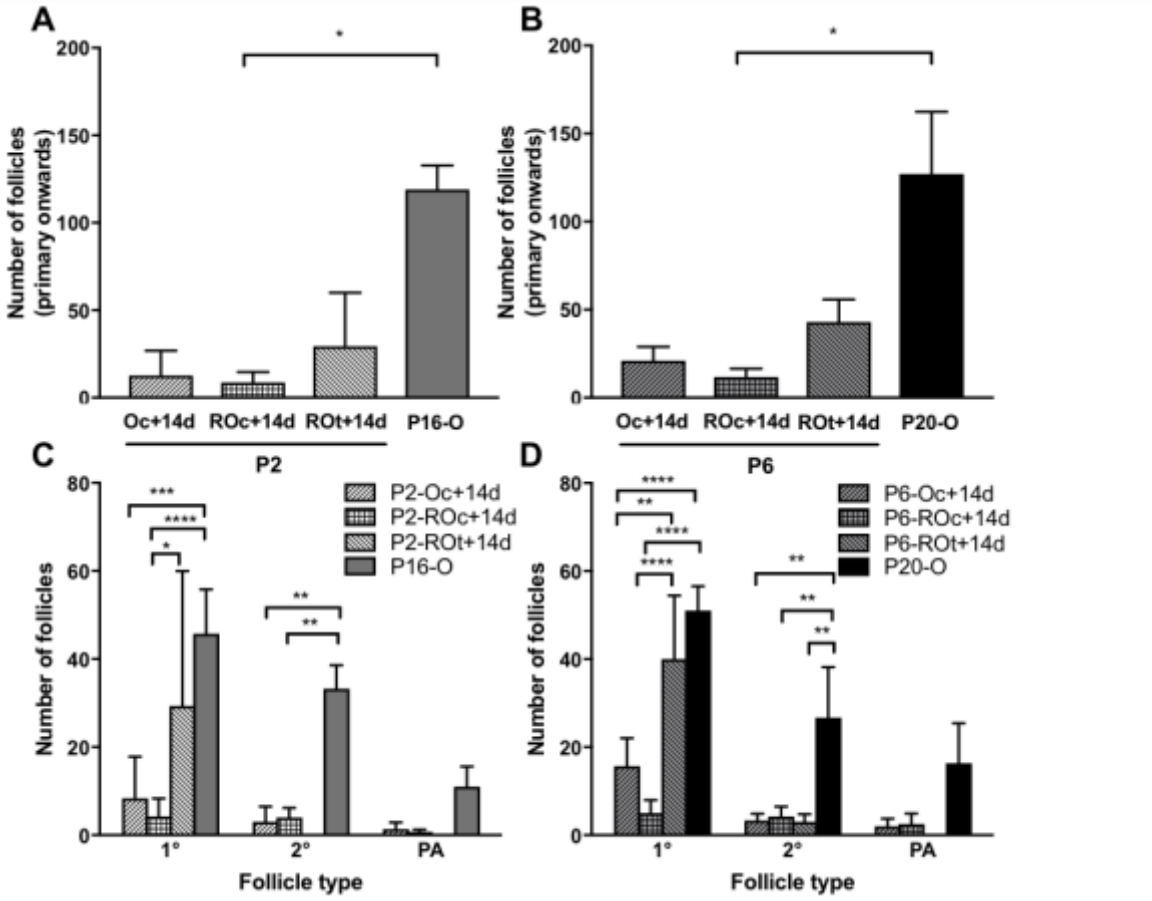


Figure 3.5 Follicle development in cultured ovaries, cultured reaggregated ovaries, transplanted reaggregated ovaries and age-matched *in vivo* ovaries.

(A) Number of developing follicles (primary, secondary, preantral and antral) in P2 ovaries (P2-Oc+14d) and P2 ROs (P2-ROc+14d) cultured for 14 days, P2 ROs transplanted for 14 days (P2-ROt+14d) and the age-matched *in vivo* control of P16 ovaries (P16-O) and (B) their equivalent in P6 ovaries and ROs (P6+Oc+14d, P6-ROc+14d, P6-RO-t+14d, P20-O). (C, D) Follicle development was assessed within these matched P2 and P6 groups, showing the number of primary (1°), secondary (2°) and preantral (PA) follicles. Data are plotted as mean values ± SD. P2-Oc+14d n=3; P2-ROc+14d n=4; P2-ROt+14d n=3; P16-

O n=4; P6-Oc+14d n=3; P6-ROc+14d n=4; P6-ROt+14d n=3; P20-O n=3. *$P \leq 0.05$; **$P \leq 0.01$; ***$P \leq 0.001$; ****$P \leq 0.0001$.

However, histological assessment of follicles revealed differences between *in vivo* ovaries and cultured ovaries, as well as transplanted ROs and cultured ovaries (Figure 3.6). Primary follicles for each condition were analysed (Figure 3.6A), and the TC layer appeared thinner in cultured follicles compared to those in transplanted tissue and *in vivo* Control ovaries (Figure 3.6A′). Furthermore, some of the cultured follicles did not appear have a complete follicle BL. A similar pattern of thinner TCs and incomplete BL emerged when secondary (Figure 3.6B, B′) and preantral follicles (Figure 3.6C, C′) were examined.

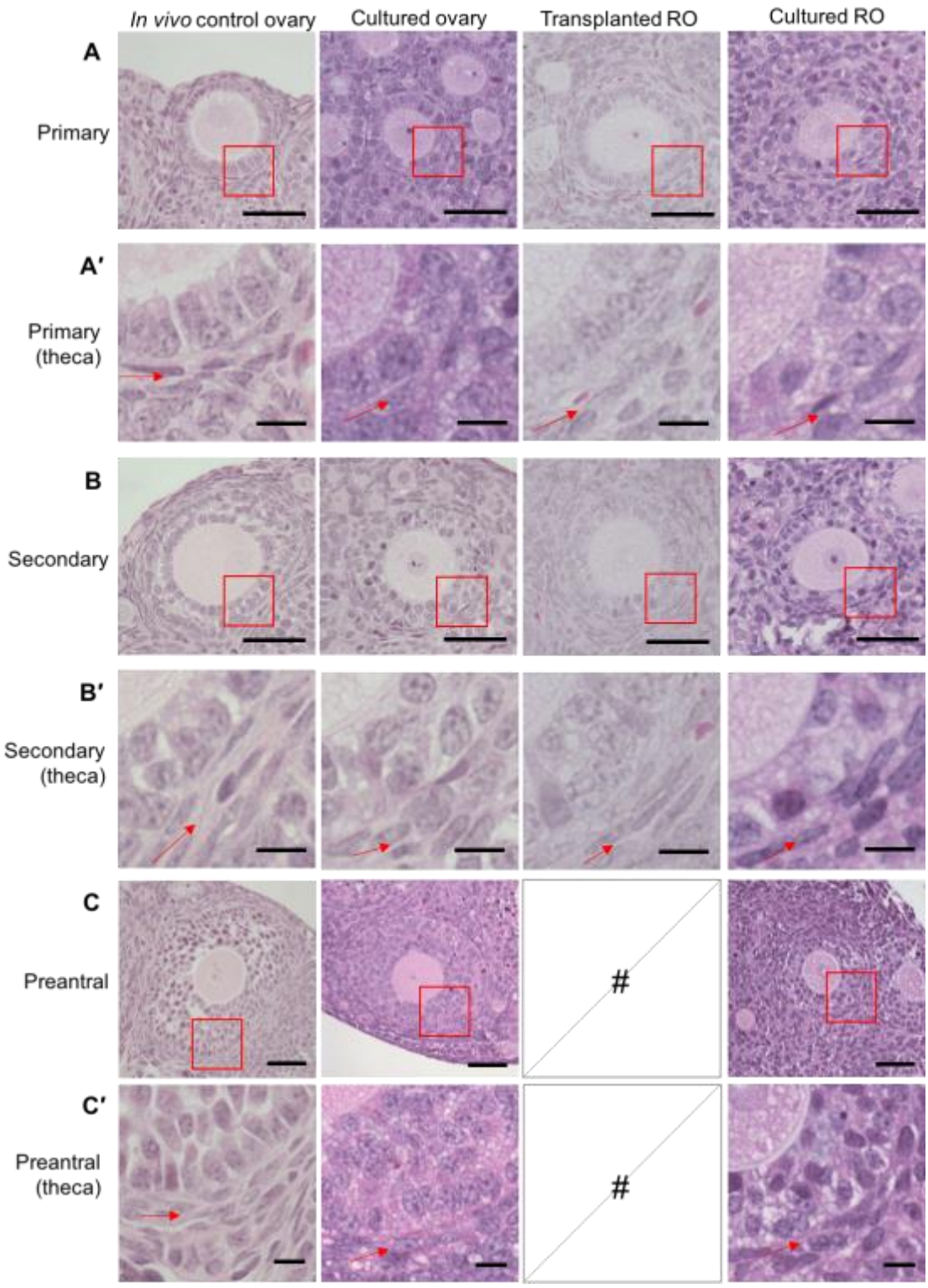


Figure 3.6 Representative images of follicles at primary, secondary and preantral stages within cultured ovaries, cultured reaggregated ovaries, transplanted reaggregated ovaries and age-matched *in vivo* ovaries.

Representative images of a (A) primary follicle from age-matched *in vivo* ovaries, cultured ovaries, transplanted reaggregated ovaries (ROs) and cultured ROs. Red box is magnified in B. (A′) Higher magnification of the red box in A, showing the theca layer of primary follicles. Red arrows are pointing at the theca layer. Representative images of (B) secondary follicles, (B′) higher magnification of secondary follicle theca layers, (C) preantral follicles and (C′) higher magnification of preantral follicle theca layers are shown. Follicle scale bar (A, B, C): 50 µm; high magnification theca scale bar (A′, B′, C′): 10 µm. #: no follicles present.

3.4.6 Follicle development in ovaries and ROs after 21 days of culture

Since antral follicles have successfully developed within ROs after 21 d of transplantation, ROs were also cultured for 21 d to assess how follicle development differed *in vitro* compared to the 21 d RO transplants (P2-ROc+21d n=4; P6-ROc+21d n=3). P2 and P6 ovaries were also cultured for 21 d to control for the effects of RO generation on follicle development (P2-Oc+21d n=5; P6-Oc+21d n=3). Although all observed follicles within the 21 d cultured ROs had abnormal morphology (unclear BL, abnormal oocytes) (Figure 3.7A, B), it was interesting to note that some follicles in 21 d cultured ovaries appeared morphologically similar to those found *in vitro* after 14 d of culture (Figure 3.7C, D). The follicles found in the 21 d cultured ovaries were still not morphologically normal, since they did not have clear BL, and appeared to have thinner TCs than follicles at the same stage of development in *in vivo* ovaries.

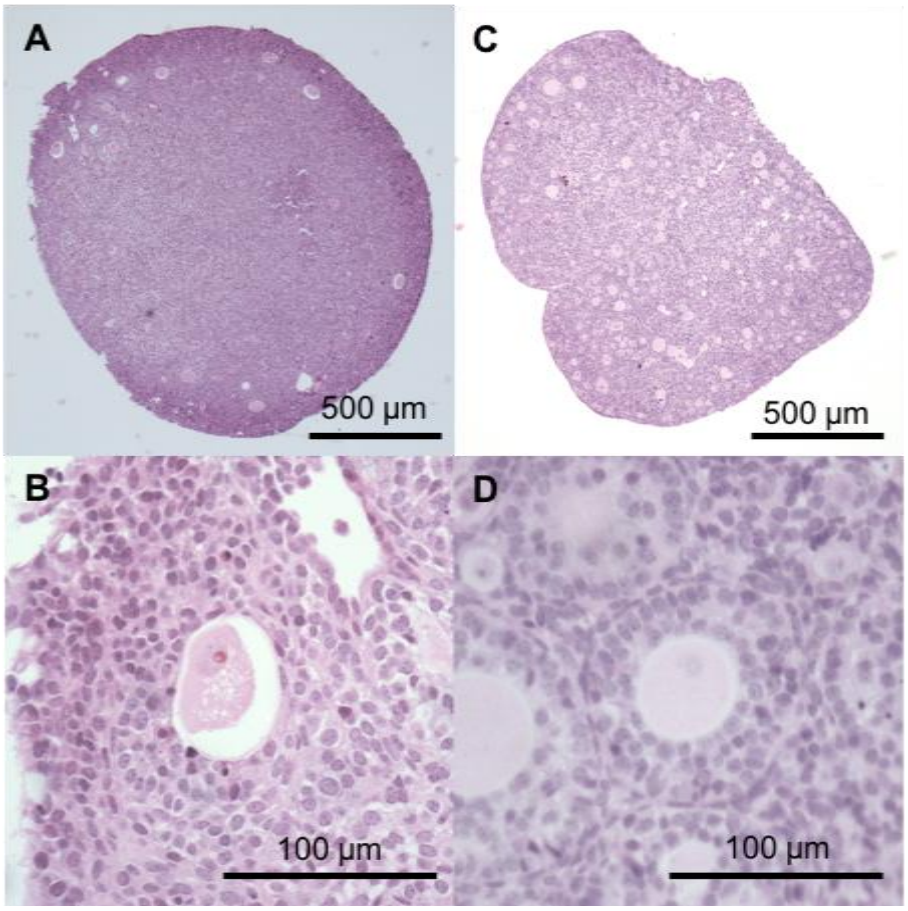


Figure 3.7 Representative images of cultured ovaries and reaggregated ovaries.

(A) A representative image of P6 reaggregated ovaries (RO) cultured for 21 d. (B) Higher magnification of an abnormal follicle within the 21 d cultured RO in A. (C) A representative image of a 21 d cultured P6 ovary, and (D) higher magnification of a follicle from panel C, similar to follicles observed in 14 d cultured ovaries.

3.5 Discussion

The RO technique, which involves the separation and reaggregation of oocytes and somatic cells, allows us to study the interactions between the two cell

compartments. However, it is important to understand how the environment (i.e. culture vs. transplantation), age and the generation of ROs affects follicle development. We have demonstrated here that culture conditions, as well as age, influence follicle development in ROs.

Initial research using the RO technique involved the transplantation of murine ROs (226) or chimeric ROs containing a mouse somatic source follicle development to occur. Since transplantation may not be a suitable option clinically, follicle development within cultured ROs must be assessed prior to transferring the technique for use with human tissues. In addition, to assess whether the somatic cell age influenced the quality and stage of follicles within an RO, ROs generated from P2 and P6 ovaries were compared.

Assessment of the cell numbers revealed more live germ cells (although not significant) isolated from P6 ovaries compared to P2 ovaries. This is unlikely due to an increase of oocytes after 4 days of aging. Since our assessment of germ cells is based on the number of cells from the non-adherent ‘germ cell’ layer, these cells could include immune cells or other bloodborne cells, which could be increased as the mice age.

Comparison of follicle development in cultured ROs and ovaries, transplanted ROs and *in vivo* Control ovaries have revealed that differences in follicle development are starkest when comparing P2 and P6 ROs transplanted for 14 d (P2-ROt+14d and P6-ROt+14d). Interestingly, the follicles present in the

transplanted ROs from P2 and P6 reflect the follicle profile in P2 and P6 ovaries (P2-O and P6-O) respectively, potentially indicating a level of delay while the oocytes and somatic cells reform follicles and restore communication, as previously hypothesised (234). The difference between P2 and P6 ROs after 21d of transplantation is not as pronounced, but there is a trend for further follicle development in P6 ROs, as evidenced by the increased number of developing follicles. The 'memory' of oocyte maturity in P6 ROs appears to be retained, driving more advanced follicle development after transplantation (228).

However, unlike the transplanted ROs which had follicles up to the secondary follicle stage, cultured ROs have developed follicles up to the preantral stage, and do not present with an age-related difference in follicle profile. This acceleration in follicle development has previously been observed in static ovary culture, and has been thought to be linked to follicle 'burn-out' (174,293). It is unclear whether the acceleration in follicle development is due to growth-promoting factors in culture compared to *in vivo* conditions (110), or whether the 'brakes' controlling follicle development are dysfunctional in culture (294); or a combination of the two. This may occur due to the disruption of regulatory factors such as PI3K/PTEN/Akt signalling in the oocyte and absence of inhibitory paracrine signals such as AMH, leading to large-scale activation of primordial follicles (294).

In addition, the digestion of whole ovaries for RO generation may also alter follicle development since the extracellular matrix surrounding follicles is known to affect follicle development, including cell morphology, proliferation, survival and

steroidogenesis (295). Ovarian fragmentation has been shown to disrupt the Hippo signalling pathway, resulting in the activation of follicle development (296), which may explain the modified follicle development in ROs. However, this alteration of the Hippo signalling pathway does not fully explain the acceleration in follicle development as transplanted ROs had slower follicle development compared to cultured ROs. The acceleration in follicle development in culture was similar between the ROs and whole ovaries cultured for 14 d, contrary to Park et al. (234), which only cultured ROs and ovaries for 4 d. This indicates that cultured ROs have developed follicles to the preantral stage despite starting culture as a mixture of oocytes and somatic cells, rather than an organised structure present in cultured ovaries.

Despite this acceleration in follicle development in cultured ROs and ovaries relative to the transplanted ROs, this could not match follicle development within the *in vivo* ovaries. *In vivo* ovaries contained antral follicles and more growing follicles compared to cultured ROs, even though eight neonatal ovaries are required for the generation of one RO. This result highlights the large germ cell loss that occurs during RO generation that will need to be reduced when developing the technique for human ovarian tissue. This loss may be attributed to death during the process of RO generation or potentially the way follicles form within the RO. In the latter case, many germ cells may not be surrounded by suitable somatic cells to reform follicles, and thus undergo apoptosis resulting in fewer follicles observed after 14 d.

After 21 d of culture, no normal follicles were observed in ROs, while 21 d cultured ovaries after 21 d contained follicles morphologically similar to those within 14 d cultured ROs and ovaries. Firstly, this highlights that the current culture system cannot support the RO for 21 d, unlike transplants collected after 21 d, which contained morphologically normal follicles up to the antral stage. Secondly, the fact that 21 d cultured ovaries contain follicles but the 21 d ROs do not reveals that the process of RO generation may be reducing the survival of follicles developing within the RO in culture. For example, the use of trypsin for cell dissociation has been shown to affect the mammalian cell proteome, resulting in the downregulation of cell growth and metabolism-related proteins (e.g. proliferating cell nuclear antigen, ATP synthase subunit beta, NADH dehydrogenase) and upregulation of proteins associated with cell apoptosis (p53, p21) (297). The multiple exposures to trypsin during RO generation may reduce the survival of the ovarian cells; but while transplantation can support the RO for 21 d, the culture system may not be supportive for follicle development beyond 14 d.

The most striking aspect of follicle development in cultured ROs and ovaries is the thinner TC layer observed surrounding follicles. Further follicle development, particularly in follicle culture, is dependent on TC association with the follicle (207). A number of defects in follicle structure have been observed in follicles from organ culture, including a lack of a complete BL, a less defined theca layer (159), along with fewer proliferating GCs and smaller primary and secondary oocytes (293). Given the importance of TCs in follicle development, further morphometric analysis of follicles within cultured ROs may reveal differences in follicle development in comparison with transplanted ROs and *in vivo* ovaries. In addition, morphometric

analysis of follicles from transplanted ROs have not been compared to age-matched *in vivo* ovaries as well. Nevertheless, the exact number of TCs required for further development may not be a critical factor, as live pups have been born from follicles generated from both transplanted ROs (226) and cultured ovaries (160).

In summary, this chapter has revealed that follicle development in accelerated in cultured ROs compared to transplanted ROs after 14 d. However, the developing follicles within the RO structure is not only fewer than the *in vivo* ovary, but the follicles present also have morphological differences. Qualitative assessment of TC number, as well as other indicators in follicle morphology (such as GC number, oocyte area etc.) can therefore be used to assess whether follicles developing within ROs and ovaries, either *in vitro* or *in vivo*, are similar.

Chapter 4: Morphological analysis of follicle development in cultured reaggregated mouse ovaries

4.1 Introduction

The results from the previous chapter revealed that follicle development is accelerated in cultured ROs and ovaries in comparison to transplanted ROs and *in vivo* ovaries, similar to the accelerated follicle development observed in other whole ovary cultures (174,293). In addition, follicles from cultured ROs and ovaries appeared to have a thinner TC layer and unclear BL, which has also been previously observed in follicles from mouse ovarian culture (159).

However, if these observations have any significance, morphological analysis of the follicles must be performed. Given the complex interplay within the follicle between the oocyte, GCs and TCs (Section 1.1.3), any perturbation with the TC layer may also affect the other two compartments. In addition, any changes to the oocyte or GCs may affect how the follicle stage is assessed. Although the follicle staging system used in this thesis is based on the number of GC layers present (298), oocyte diameter as a marker for oocyte maturity (145) and GC number have both been used to stage mouse follicles (299); altered follicle development can potentially affect how follicles are staged.

The disrupted BL observed in Chapter 3 may also affect follicle development, since the BL creates a localised microenvironment by regulating the entry of molecules into the follicle (300,301). Furthermore, the BL provides a surface for cell anchorage (302,303), enabling GC polarity and potentially a surface on which TCs can associate with. The incomplete BL may therefore be linked to the thinner TC layer observed in follicles from cultured ROs and ovaries.

Therefore, it is important to assess the previously used markers of follicle development to determine whether follicles at each stage are morphologically different in cultured ROs, cultured ovaries, transplanted ROs and age-matched *in vivo* ovaries.

4.2 Aim

- To determine if TC and GC number; follicle, granulosa and oocyte area are different at each follicle stage between cultured ROs, cultured ovaries, transplanted ROs and age-matched *in vivo* ovaries.

4.3 Materials and Methods

4.3.1 Analysis of cultured ROs, cultured ovaries, transplanted ROs and age-matched *in vivo* ovaries

The reaggregated ovaries and ovaries from Chapter 3 were used for analysis. For simplicity, since all ROs and ovaries were cultured or *in vivo* for 14 d, the 14 d suffix was removed (e.g. P2 cultured RO: P2-ROc). Follicle, granulosa and oocyte area, along with cell numbers, were analysed using ImageJ software (292).

4.3.1.1 Histological analysis

Follicles with visible nuclei within the oocyte were analysed. Theca cells were identified as thin and elongated cells separating the follicles from the surrounding stroma. Any rounded cells were excluded from the TC count. Oocyte area and follicle area (oocyte area and granulosa cell area) were assessed by directly

measuring the area using the freehand selection tool in ImageJ. Granulosa area was calculated by deducting oocyte area from follicle area.

4.3.1.2 Statistical analysis

Analysis was performed using GraphPad Prism version 7.00 (GraphPad Software, La Jolla, California, USA). Data was tested for normality using D'Agostino & Pearson normality test. The Kruskall-Wallis test with Dunn's multiple comparisons test was used to compare two variables: the total number of follicles, TC number, GC number, follicle area or oocyte area and different age and/or conditions, at each follicle stage. Results are presented as mean ± SD, with $P \leq 0.05$ considered significant.

Linear regressions were performed to correlate follicle area and granulosa area to GC number. Lines shown have $r^2 > 0.6$, which indicates the linear model fits >60% of the data plotted.

4.4 Results

4.4.1 Cultured ovaries and ROs are associated with fewer theca and granulosa cells

Quantification of TC numbers revealed that follicles from cultured ovaries and cultured ROs were associated with fewer TCs compared to *in vivo* ovaries and transplanted ROs (Figure 4.1). Although TC numbers from primary follicles in P2-O and P6-O were not compared to ROs and ovaries, it is interesting to note that primary follicles in P6-O contain more TCs than in P2-O. There was also no clear

indication of differences in TC development between follicles in cultured P2 and P6 ROs, cultured ovaries (apart from at the primary follicle stage) and *in vivo* Control ovaries.

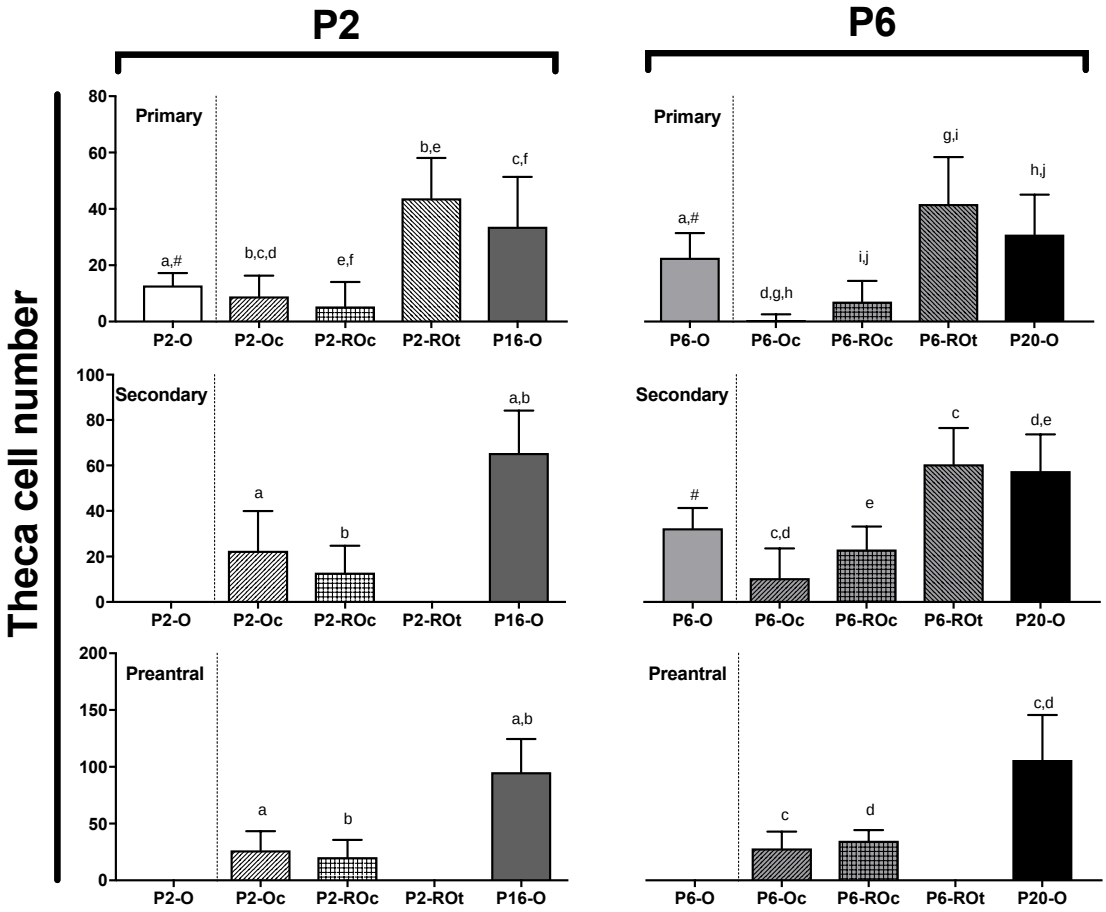


Figure 4.1 Theca cell quantification in ovaries and reaggregated ovaries.

Quantification of theca cell number was determined for primary, secondary and preantral follicles in P2 ovaries (P2-O), P2 cultured ovaries for 14 d (P2-Oc), P2 cultured reaggregated ovaries for 14 d (P2-ROc), P2 transplanted ROs for 14 d (P2-ROt) and P16 ovaries (P16-O), as well as for the P6 counterparts (P6-O, P6-Oc, P6-ROc, P6-ROt, P20-O). Data are plotted as mean values per follicle ± SD. Bars with matched

lower-case letters are significantly different to each other ($P \leq 0.05$), within a follicle stage. # P2-O and P6-O are not compared to the other conditions, as they have not been cultured for 14 d. Primary follicles: P2-O n=49; P2-Oc n=28; P2-ROc n=109; P2-ROt n=31; P16-O n=62; P6-O n=57; P6-Oc n=57; P6-ROc n=25; P6-ROt n=44; P20-O n=52. Secondary follicles: P2-Oc n=12; P2-ROc n=81; P16-O n=54; P6-O n=9; P6-Oc n=14; P6-ROc n=23; P6-ROt n=4; P20-O n=31. Preantral follicles: P2-Oc n=5; P2-ROc n=8; P16-O n=19; P6-Oc n=11; P6-ROc n=13; P20-O n=19.

Since TC recruitment and proliferation is thought to be modulated by factors secreted from GCs (26) and oocytes during the early stages of follicle development (140), any changes in the GC compartment or oocyte could affect TC numbers. The pattern of fewer GCs is not as pronounced as TCs, as primary follicles in cultured ovaries had fewer GCs than follicles from ROs and ovaries developed *in vivo* (Figure 4.2). Along with fewer GCs in cultured ovaries, primary follicles in cultured P6 ROs also had fewer GCs compared to their *in vivo* counterparts. Only secondary and preantral follicles in cultured P2 and P6 ROs, and cultured P6 ovaries had fewer GCs than their matched follicles in *in vivo* Control ovaries. Age-related differences in GC number were only observed in primary follicles from P6-O, which had more GCs than those from P2-O, and in primary follicles from cultured P6 ROs, which had fewer GCs than those from cultured P2 ROs.

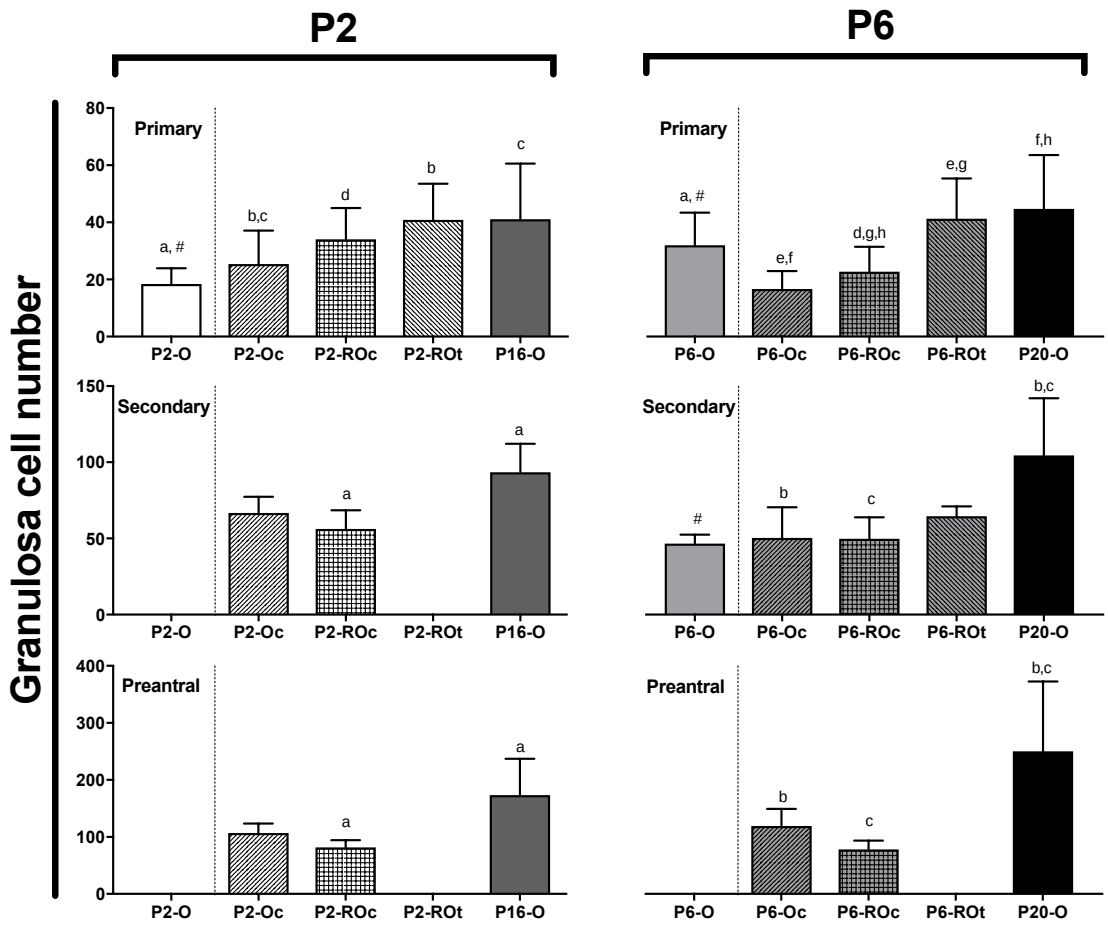


Figure 4.2 Granulosa cell quantification in ovaries and reaggregated ovaries.

Quantification of granulosa cell number was determined for primary, secondary and preantral follicles in P2 ovaries (P2-O), P2 cultured ovaries for 14 d (P2-Oc), P2 cultured reaggregated ovaries for 14 d (P2-ROc), P2 transplanted ROs for 14 d (P2-ROt) and P16 ovaries (P16-O), as well as for the P6 counterparts (P6-O, P6-Oc, P6-ROc, P6-ROt, P20-O). Data are plotted as mean values per follicle ± SD. Bars with matched lower-case letters are significantly different to each other ($P \leq 0.05$), within a follicle stage. # P2-O and P6-O are not compared to the other conditions, as they have not been cultured for 14 d. Primary follicles:

P2-O n=49; P2-Oc n=28; P2-ROc n=109; P2-ROt n=31; P16-O n=62; P6-O n=57; P6-Oc n=57; P6-ROc n=25; P6-ROt n=44; P20-O n=52. Secondary follicles: P2-Oc n=12; P2-ROc n=81; P16-O n=54; P6-O n=9; P6-Oc n=14; P6-ROc n=23; P6-ROt n=4; P20-O n=31. Preantral follicles: P2-Oc n=5; P2-ROc n=8; P16-O n=19; P6-Oc n=11; P6-ROc n=13; P20-O n=19.

4.4.2 Oocyte and follicle area in ovaries and ROs

Since follicles from cultured ovaries and ROs develop fewer TCs and GCs than their *in vivo* counterparts, they may also be developmentally slower, despite having the same number of GC layers. Since oocyte diameter has previously been used as a marker for oocyte maturity or meiotic maturity (145), comparing oocyte area between *in vitro* and *in vivo* ovaries and ROs may crudely indicate whether the follicles are developmentally comparable.

At the primary follicle stage, oocytes from primary follicles in cultured ovaries had smaller oocytes than those from cultured ROs, transplanted ROs and *in vivo* Control ovaries (Figure 4.3). Only primary oocytes from cultured P6 ROs were smaller than those in transplanted P6 ROs. Oocytes in secondary and preantral follicles from cultured ROs were smaller than their *in vivo* counterparts; this pattern was the same for cultured ovaries, apart from in preantral follicles from cultured P6 ovaries. Oocytes from P6-O primary follicles were also larger than those from P2-O.

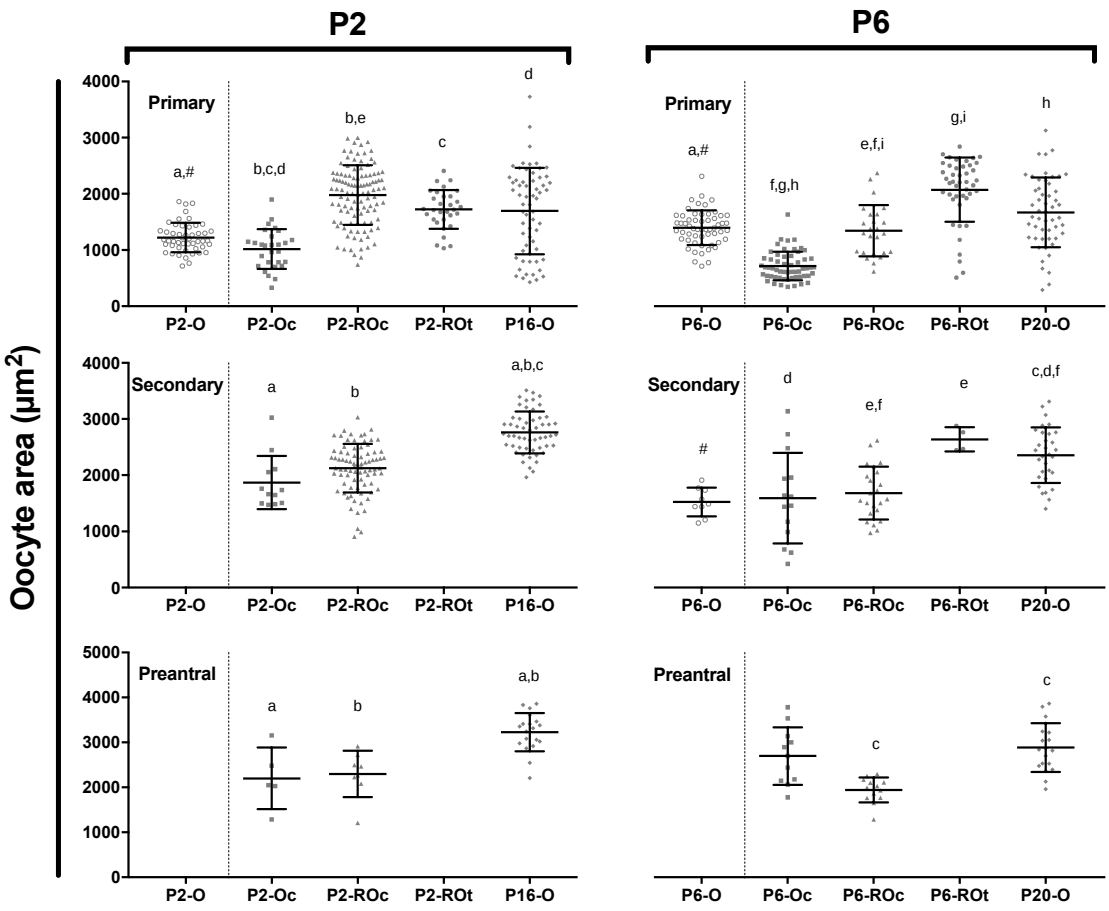


Figure 4.3 Oocyte area in ovaries and reaggregated ovaries.

Oocyte area was determined for primary, secondary and preantral follicles in P2 ovaries (P2-O), P2 cultured ovaries for 14 d (P2-Oc), P2 cultured reaggregated ovaries for 14 d (P2-ROc), P2 transplanted ROs for 14 d (P2-ROt) and P16 ovaries (P16-O), as well as for the P6 counterparts (P6-O, P6-Oc, P6-ROc, P6-ROt, P20-O). Data are plotted as mean values per follicle ± SD. Scatter plots with matched lower-case letters are significantly different to each other ($P \leq 0.05$), within a follicle stage. # P2-O and P6-O are not compared to the other conditions, as they have not been cultured for 14 d. Primary follicles: P2-O n=49; P2-Oc n=28; P2-ROc n=109; P2-ROt n=31; P16-O n=62; P6-O n=57; P6-Oc n=57; P6-ROc n=25; P6-ROt n=44; P20-O n=52. Secondary follicles: P2-

Oc n=12; P2-ROc n=81; P16-O n=54; P6-O n=9; P6-Oc n=14; P6-ROc n=23; P6-ROt n=4; P20-O n=31. Preantral follicles: P2-Oc n=5; P2-ROc n=8; P16-O n=19; P6-Oc n=11; P6-ROc n=13; P20-O n=19.

Since the oocyte and GCs contribute to the overall follicle area, any changes in the two compartments can also affect the overall size of follicles at each stage. Primary follicles in cultured P2 ovaries were smaller than those in cultured P2 ROs and P16-O; however, this pattern was not reiterated in cultured P6 ovaries, which, along with cultured P6 ROs, had smaller primary follicles than transplanted P6 ROs and P20-O (Figure 4.4). However, secondary follicles in cultured ovaries and cultured ROs were smaller than those in *in vivo* Control ovaries. Only preantral follicles in cultured ROs were smaller than those in *in vivo* Control ovaries. Analysis between the two age groups revealed that primary follicles were larger in P6-O and cultured P2 ROs compared to P2-O and P6 ROs, respectively.

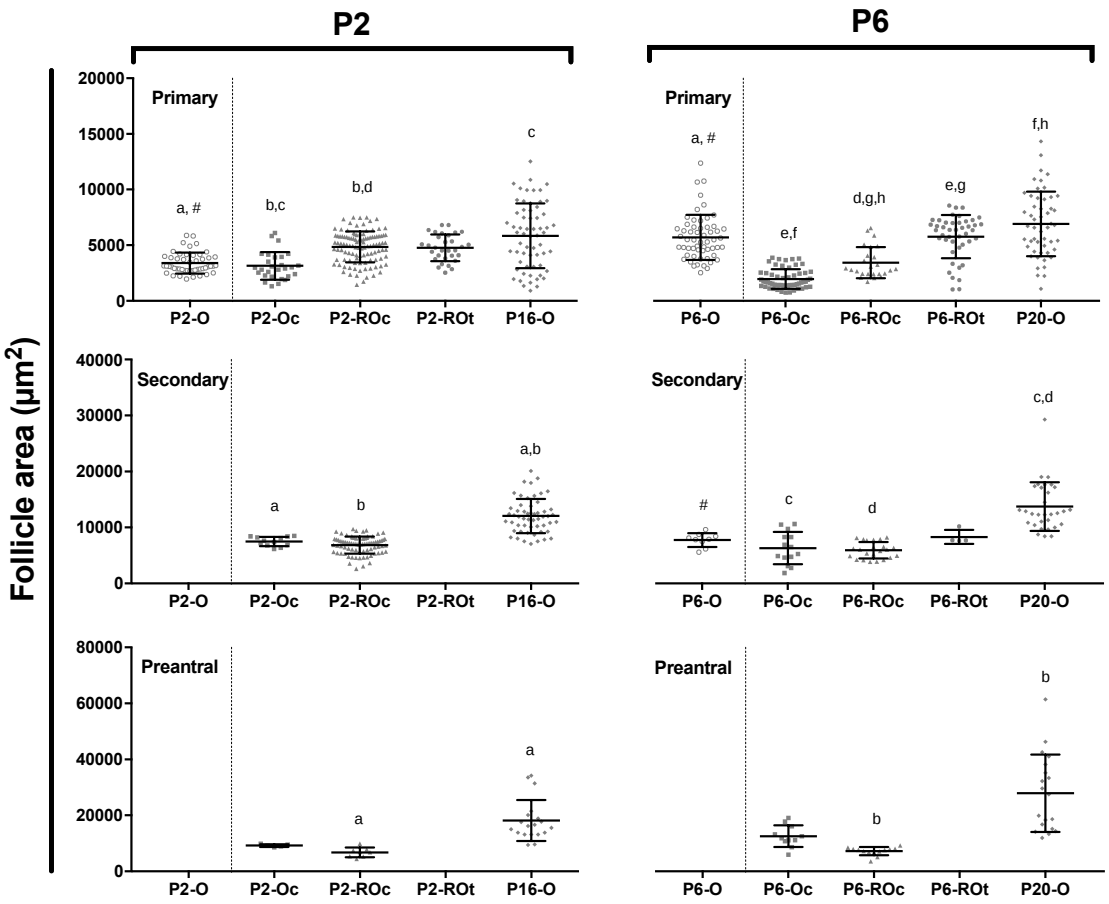


Figure 4.4 Follicle area in ovaries and reaggregated ovaries.

Follicle area was determined for primary, secondary and preantral follicles in P2 ovaries (P2-O), P2 cultured ovaries for 14 d (P2-Oc), P2 cultured reaggregated ovaries for 14 d (P2-ROc), P2 transplanted ROs for 14 d (P2-ROt) and P16 ovaries (P16-O), as well as for the P6 counterparts (P6-O, P6-Oc, P6-ROc, P6-ROt, P20-O). Data are plotted as mean values per follicle ± SD. Scatter plots with matched lower-case letters are significantly different to each other ($P \leq 0.05$), within a follicle stage. # P2-O and P6-O are not compared to the other conditions, as they have not been cultured for 14 d. Primary follicles: P2-O n=49; P2-Oc n=28; P2-ROc n=109; P2-ROt n=31; P16-O n=62; P6-O n=57; P6-Oc n=57; P6-ROc n=25; P6-ROt n=44; P20-O n=52. Secondary follicles: P2-

Oc n=12; P2-ROc n=81; P16-O n=54; P6-O n=9; P6-Oc n=14; P6-ROc n=23; P6-ROt n=4; P20-O n=31. Preantral follicles: P2-Oc n=5; P2-ROc n=8; P16-O n=19; P6-Oc n=11; P6-ROc n=13; P20-O n=19.

4.4.3 Granulosa cell area and granulosa cell density in ovaries and ROs

Since follicle area consists of oocyte area and GC area (Figure 4.5), an increased oocyte area which is not matched by a consistent increase in follicle area implies that there may be difference in GC density (the number of cells per μm^2). At the primary follicle stage, GC density was higher in cultured ovaries and cultured ROs compared to their *in vivo* Control ovaries (Figure 4.6). However, transplanted P2 ROs were denser than P16-O, despite having similar GC numbers and GC area. This pattern of denser GCs in follicles in cultured ROs compared to their *in vivo* Control ovaries was only observed in secondary follicles from cultured P2 and P6 ROs and only preantral follicles from cultured P2 ROs. The only clear age-related difference in GC density was at the primary follicle stage, where P6-O and with P20-O were less dense compared to P2-O and P16-O, respectively.

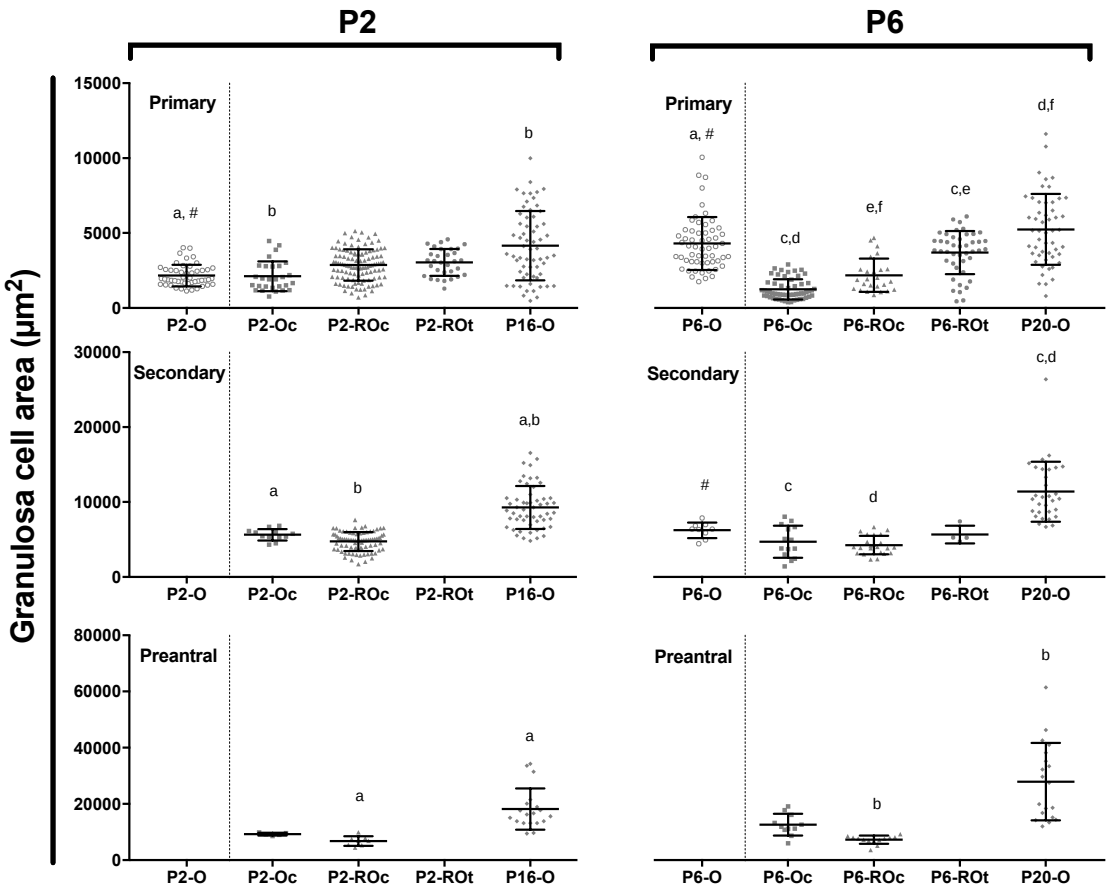


Figure 4.5 Granulosa area in ovaries and reaggregated ovaries.

Granulosa cell area was determined for primary, secondary and preantral follicles in P2 ovaries (P2-O), P2 cultured ovaries for 14 d (P2-Oc), P2 cultured reaggregated ovaries for 14 d (P2-ROc), P2 transplanted ROs for 14 d (P2-ROt) and P16 ovaries (P16-O), as well as for the P6 counterparts (P6-O, P6-Oc, P6-ROc, P6-ROt, P20-O). Data are plotted as mean values per follicle ± SD. Scatter plots with matched lower-case letters are significantly different to each other ($P \leq 0.05$), within a follicle stage. # P2-O and P6-O are not compared to the other conditions, as they have not been cultured for 14 d. Primary follicles: P2-O n=49; P2-Oc n=28; P2-ROc n=109; P2-ROt n=31; P16-O n=62; P6-O n=57; P6-Oc n=57; P6-ROc n=25; P6-ROt n=44; P20-O n=52.

Secondary follicles: P2-Oc n=12; P2-ROc n=81; P16-O n=54; P6-O n=9; P6-Oc n=14; P6-ROc n=23; P6-ROt n=4; P20-O n=31. Preantral follicles: P2-Oc n=5; P2-ROc n=8; P16-O n=19; P6-Oc n=11; P6-ROc n=13; P20-O n=19.

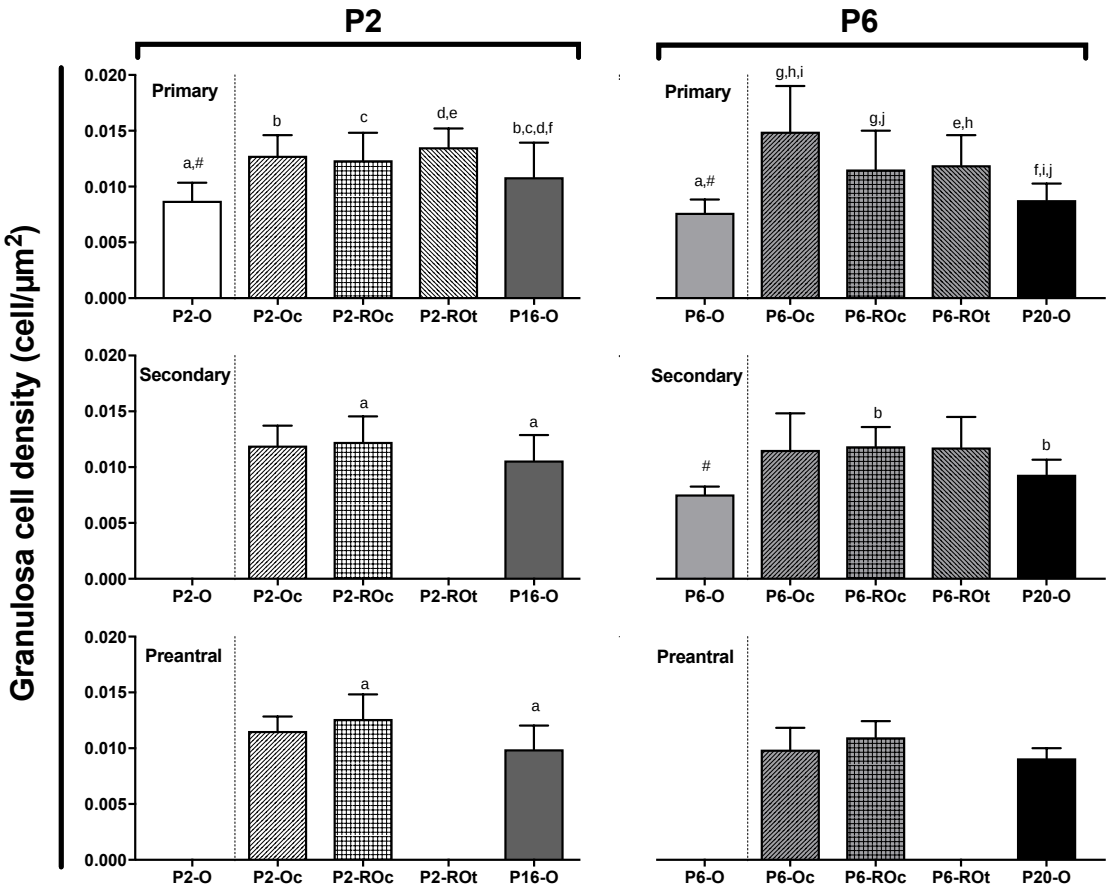


Figure 4.6 Granulosa cell density in ovaries and reaggregated ovaries.

Granulosa cell density (cells per µm^2) was determined for primary, secondary and preantral follicles in P2 ovaries (P2-O), P2 cultured ovaries for 14 d (P2-Oc), P2 cultured reaggregated ovaries for 14 d (P2-ROc), P2 transplanted ROs for 14 d (P2-ROt) and P16 ovaries (P16-O), as well as for the P6 counterparts (P6-O, P6-Oc, P6-ROc, P6-ROt, P20-O). Data are plotted as mean values per follicle ± SD. Bars with matched lower-case letters are significantly different to each other ($P \leq 0.05$), within a follicle stage. # P2-O and P6-O are not compared to the other conditions, as they have not been cultured for 14 d. Primary follicles: P2-O n=49; P2-Oc n=28; P2-ROc n=109; P2-ROt n=31; P16-O n=62; P6-O n=57; P6-Oc n=57; P6-ROc n=25; P6-ROt n=44; P20-O n=52.

Secondary follicles: P2-Oc n=12; P2-ROc n=81; P16-O n=54; P6-O n=9; P6-Oc n=14; P6-ROc n=23; P6-ROt n=4; P20-O n=31. Preantral follicles: P2-Oc n=5; P2-ROc n=8; P16-O n=19; P6-Oc n=11; P6-ROc n=13; P20-O n=19.

4.4.4 Correlations between follicle area, granulosa area and granulosa cells

As the number of GCs increase, it is expected that the GC area, and therefore the follicle area, will increase. The rate of area increase per GC can also reflect the growth rate of the follicles. For an accurate linear regression analysis, primary follicles from each condition with a GC number ranging between 9 and 65 were analysed; based on the minimum and maximum GC number from the experimental conditions (Oc, ROc, ROt). Unsurprisingly, follicle area increased rapidly per GC in P2-O (Fig 11A). However, it is interesting to note that P2-Oc, P2-ROc, as well as P2-ROt have slower growth trajectories compared to P16-O. However, this difference in growth trajectories is not evident in the P6 group (Figure 4.7A), where each condition had a different starting follicle area (i.e. different y-intercepts). Although no difference was observed in growth trajectories of follicle area in the P6 group, both the P2 and P6 groups had different growth trajectories when GC area was assessed (Figure 4.7B).

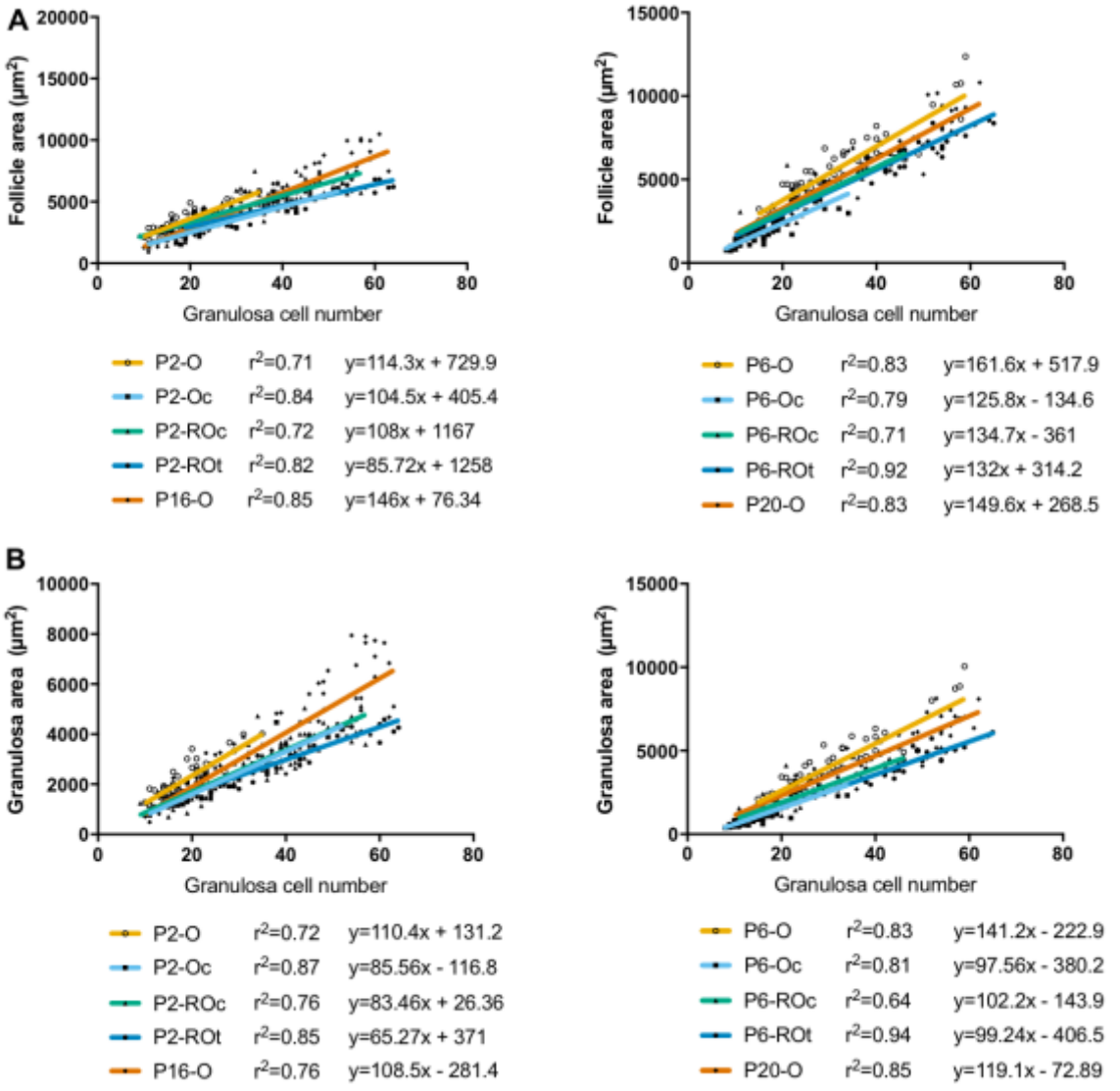


Figure 4.7 Correlations between follicle and granulosa area to granulosa cell numbers in primary follicles from ovaries and reaggregated ovaries.

Linear regressions were performed between (A) follicle area and granulosa cell number and (B) granulosa area and granulosa cell number in primary follicles from P2 whole ovaries (P2-O), P2 cultured ovaries for 14 d (P2-Oc), P2 reaggregated ovaries cultured for 14 d (P2-ROc), P2 ROs transplanted for 14 d (P2-ROt) and P16 ovaries (P16-O), as well as the P6 equivalents (P6-O, P6-Oc, P6-ROc, P6-ROt, P20-O).

Primary follicles: P2-O n=49; P2-Oc n=28; P2-ROc n=109; P2-ROt n=31; P16-O n=58; P6-O n=57; P6-Oc n=57; P6-ROc n=25; P6-ROt n=44; P20-O n=45. R-squared values and equations for each plotted line are shown next to each line, as y = (slope of the line)x + (y-intercept). All graphed lines have r^2>0.6.

4.5 Discussion

A number of defects in follicle structure have been observed in follicles from organ culture, including a lack of a complete BL (159), a less defined theca layer (159), along with fewer proliferating GCs and smaller primary and secondary oocytes (293), which are mirrored in our results. Smaller oocytes in cultured ovaries and ROs may also be indicative of oocyte immaturity (145), as oocyte diameter is used as a proxy for oocyte maturity. This change in oocytes may also affect the GC and TC numbers, and BL formation. The BL creates a localised microenvironment by regulating the entry of molecules into the follicle (300,301) and anchorage (302,303), enabling GC polarity and potentially a surface on which TCs can associate with. Aside from providing a point of anchorage, basal laminae also regulate cellular functions such as apoptosis, proliferation, differentiation and apoptosis in many tissues (304). During follicle development, the BL is constantly remodelled with the growing follicle (305); this dynamic process may be disrupted in culture, resulting in the observed incomplete BL, and therefore affect the proliferation of GCs and TCs. Slower proliferating GCs in follicles from cultured ROs and ovaries may also contribute to fewer TCs observed, as they secrete theca recruitment factors such KITL and EGF (reviewed by Young and McNeilly (26)). This is a particular concern for follicle culture; the next step after ovary culture for

follicle development, as further development in follicle culture is dependent on TC association with the follicle (207).

Since both transplanted ROs and *in vivo* Control ovaries have the same cellular components as cultured ROs and ovaries respectively, the differences in follicle development could be attributed to the culture conditions. High oxygen tension (20%, which is used in culture here) has been demonstrated to reduce oocyte survival in culture in comparison with 5% O_2 (306). The use of lower oxygen tension (2.5% O_2) improved secondary follicle survival in culture, which is hypothesised to be due to enhanced hypoxia-mediated pyruvate production for oxidative energy metabolism (244). Although a variety of factors could be added to optimise follicle development in culture, it is interesting to note that follicle co-culture with mesenchymal stem cells (MSCs) has been shown to improve preantral follicle development (307). The MSCs are thought to be promoting follicle development by acting as a 'drugstore' for the follicle and secreting factors such as activin A, transforming growth factor, vascular endothelial growth factor and fibroblast growth factor (307), which are also known to promote theca development (26).

The results presented here, and in the previous chapter, raise several important questions, which are particularly relevant given the increased interest in gamete development from ROs (232). Although cultured ROs contained the same cells as their *in vivo* counterparts prior to culture, the morphological differences, such as the fewer TCs observed, and acceleration in follicle development highlights the need for further understanding of follicle development in culture. The difference

in follicle development between transplanted P2 and P6 ROs also emphasise that the oocytes retain their developmental state to some degree, as demonstrated by Eppig et al. (2002) (228). Finally, the mechanism behind the reformation of follicles in ROs is unknown: are the somatic cells surrounding the oocyte dedifferentiated or transdifferentiated into the cells that belong in that niche (reviewed by Merrell & Stanger (308)), or do they reassemble based on their differentiated phenotype (309,310)?

In summary, the results from this chapter reveal that follicles from cultured ROs and ovaries have morphological differences compared to transplanted ROs and *in vivo* ovaries. Given the importance of GCs and TCs in follicle development, the follicles from cultured tissues with fewer TCs and GCs may have compromised development and fail to grow once dissected out for follicle culture for two step culture. This would therefore reduce the efficiency of the RO technique, which is not ideal for a clinical treatment. Further investigations into improving TC and GC development may be required to improve follicle survival.

Chapter 5: Exploration of theca cell development in different culture conditions

5.1 Introduction

The results from Chapter 3 have demonstrated that the *in vivo* reaggregated ovary (RO) technique can be adapted to a culture technique, allowing the study of follicle development outside of the 'black box' of transplantation, as well as a potential fertility treatment as an artificial ovary. However, results in Chapter 4 demonstrated that culturing both ROs and ovaries for 14 d resulted in significantly fewer theca cells (TCs) around follicles compared to their *in vivo* counterparts. In order for follicles within cultured ovaries and ROs to develop beyond the preantral stage, follicles can be isolated and cultured; the two step culture technque. Since the success of follicle culture has been linked to TC-stroma association with follicles (207), it is important to investigate factors which may improve TC development *in vitro.*

5.1.1 Theca cell development

At the primary follicle stage, the TC layer, comprising of a layer of flattened cells, are recruited from the surrounding stroma in the ovary, and envelope the basal lamina (298). By the secondary follicle stage, the TC layer is clearly present. The TC layer can be separated into two types: the theca interna and theca externa. The theca interna (approximately 3-5 cell layers thick, immediately adjacent to the basal lamina (311)) is comprised of steroidogenic cells, fibroblasts, immune cells and capillaries, while the theca externa thickness includes larger venules, lymphatic vessels, nerve fibres, and cells containing contractile filaments (312). The primary function of TCs is to produce androstenedione in response to LH, which can be

converted to testosterone and oestrogen in GCs in the presence of FSH, as part of the two-cell two-gonadotrophin hypothesis (Figure 1.2) (67).

The formation of the TC layer requires complex signals to recruit TC progenitors to the follicle, as well as signals to induce recruited TCs to proliferate (reviewed in (26), summarised in Figure 5.1).

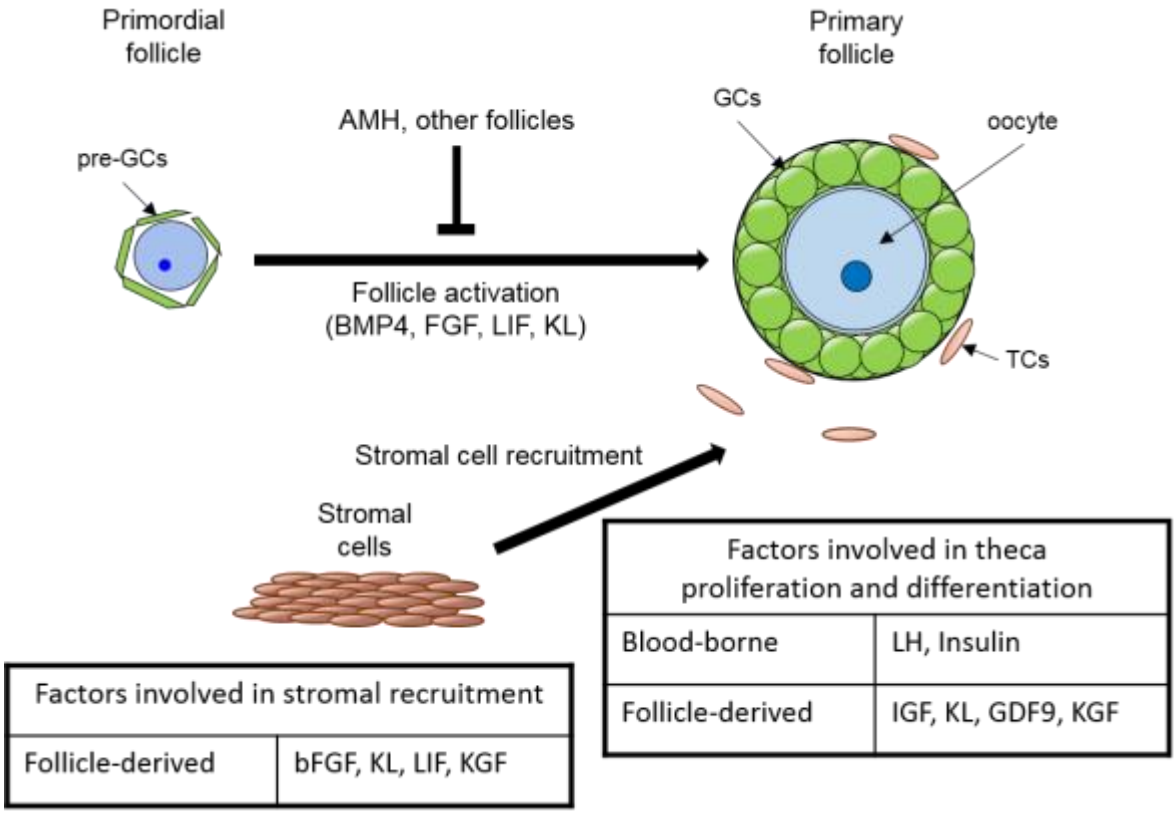


Figure 5.1 Theca cell recruitment and differentiation.

Theca progenitor cells are thought to exist in the ovarian stroma, and are recruited to follicles to differentiate into theca cells (TCs) where they proliferate. More factors may be involved in follicle development, as much is still unknown about theca recruitment and differentiation, and the exact sources of the factors are unclear. Adapted from Young et al. (2010). AMH: anti-Müllerian hormone, BMP4: bone morphogenetic protein 4; (b) FGF: (basic) fibroblast growth factor; GDF9: growth differentiation factor 9; IGF: insulin-like growth factor; LH: luteinising hormone; LIF: leukaemia inhibitory factor; KGF: keratinocyte growth factor; KL: kit ligand (also known as stem cell factor).

Theca cells are thought to originate from fibroblast-like precursors from within the stroma (67,313,314), which do not express LH receptors (314) or steroidogenic enzymes (313). It is unclear whether these theca precursors are stem cells or progenitors, as the isolated putative theca 'stem cell' colonies contain a mix of cell types (314). However, cell lineage tracking has demonstrated that mesonephros-derived *Gli1*-positive cells and ovary-derived *Wt1*-positive cells arise in the mouse ovary and contribute to the TC lineage (315).

The complexity of factors involved in the recruitment and differentiation of TCs have an additional level of intricacy, as the factors listed here are also regulated by many other factors. For example, the synthesis of IGF1 by GCs, which promotes TC proliferation *in vitro* (316,317), is regulated by FSH (318,319). Although cultured ROs are exposed to FSH in the media, and contain the same cells as transplanted ROs prior to transplantation, follicles within cultured ROs have fewer TCs. Since the cells in transplanted and cultured ROs were identical at the start, it is important to identify the differences between transplantation and culture which may influence follicle development.

5.1.2 Differences between transplantation and culture

Reaggregated ovaries can be transplanted heterotropically under the kidney capsule, which has an ample blood supply, facilitating the vascularisation of ROs, which is essential for graft establishment and follicular growth (320). The transplantation of the RO into the lateral region of the kidney beneath the kidney capsule also exposes it to pressure from both the kidney cortex and the kidney

capsule. The fibrous renal capsule surround the kidney maintains the kidney structure with a dense weave of collagen fibres (321). The quasi-static properties of the renal capsule provides the major force opposing the expansion of the kidney cortex, and enables it to act as a critical determinant of kidney volume and pressure (322). However, cultured ROs and ovaries are no longer in contact with the circulation and are not exposed to subcapsular pressure, which may influence follicle development.

5.1.2.1 Mouse serum and follicle development

Considering that transplanted and cultured ROs arise from the same cells, but have different outcomes in follicle development, the exposure to host circulation by transplanted ROs was initially investigated. The static nature of culture and lack of vascularisation *in vitro* prevents the dynamic exchange of systemic factors. Serum is added in culture as a protein source, as well as to provide other growth factors which may be involved in TC development. The RO and ovary culture media used in Chapter 3 contained foetal bovine serum (FBS), a rich source of undefined components which support cultured ovarian cells (323). Other neonatal ovary cultures which included FBS also observed thinner theca layers (159). The use of FBS may not be optimal for use in murine neonatal ovaries, as it is from a different species (xenogeneic) which have different reproductive characteristics (Section 1.2).

Mouse serum has previously been included in murine follicle culture, with mixed results. The discrepancies in results from mouse serum are unsurprising, as

each batch of mouse serum differs. The types of mouse serum used in follicle culture are summarised in Table 5.1.

Table 5.1 Types of mouse serum used in follicle culture.

Type of mouse serum	Studies
Wildtype female mice	Nayudu & Osborne 1992 (211), Spears et al. 1994 (207), Johnson et al. 1995 (324), Rose et al. 1999 (325), Durlinger et al. 2001 (326), Wycherley et al. 2004 (212), Morgan et al. 2015 (327)
Normal mouse serum (mixture of male and female serum)	Hartshorne et al. 1994 (328), Mitchell et al. 2002 (329)
Hypogonadal (*hpg*) mice	Boland et al. 1993 (330), Mitchell et al. 2002 (329)

Follicles cultured in serum derived from wildtype female mice were observed to have larger mean diameters after 6 d of culture compared to FBS, emulating the sizes observed *in vivo* (211). It was also noted that follicles cultured in FBS had abnormal TC proliferation, and 'thin' GC density, but neither were quantified (211). However, when normal mouse serum (a commercial mixture of male and female serum) was used, follicles degenerated in culture after 9 d, unlike those cultured in FBS (329). Follicles cultured in serum from hypogonadal (*hpg*) mice, which have low LH and FSH levels, had comparable growth to those cultured in FBS, when FSH was added (329). Subsequent research have used FBS rather than mouse serum (107,206,242,246,331-333), but some retain the use of mouse serum (327).

5.1.2.2 Extracellular matrix and follicle development

Along with the exposure to the host mouse circulation, transplanted ROs, which contain the same cells as cultured ROs, are also exposed to ‘tension’ from the kidney capsule after transplantation. Theca cell development may also be influenced by the subcapsular pressure which transplanted ROs are exposed to. The rigidity of the physical environment surrounding the follicle has been demonstrated to regulate follicle development in culture, and has been shown to affect parameters such as follicle growth, antrum formation, TC development, steroid production and oocyte quality (235-237).

However, the choice of a physical support for follicle development requires significant thought, as different rigidities have been shown to affect follicle development (Table 1.3). To provide physical support, or ‘tension’, for follicle development in follicle culture, several types of artificial extracellular matrices (ECMs) have been used in a variety of species (reviewed in (162)). Alginate hydrogels, which are inert, have been used to provide a 3D structure for follicle culture and mimic intraovarian rigidity. A range of alginate concentrations have been used in murine follicle development (see Table 5.2).

Table 5.2 Alginate concentrations used in murine follicle culture.

Alginate concentration	Studies
0.125%	Shikanov et al. 2011 (241), Park et al. 2012 (242)
0.15%	Dunning et al. 2011 (239)
0.25%	Xu et al. 2006 (235), Xu et al. 2006 (334), Jin et al. 2010 (238), Mainigi et al. 2011 (240), Park et al. 2012 (242), Tagler et al. 2012 (215), Jiao and Woodruff 2013 (243); Tagler et al. 2013 (217), Makanji et al. 2014 (244), Tagler et al. 2014 (218), Xiao et al. 2015 (223)
0.5%	Xu et al. 2006 (235), West-Farrell et al. 2009 (237), Shikanov et al. 2011 (241), Tingen et al. 2011 (214), Hornick et al. 2013 (216), Shiomi-Sugaya et al. 2015 (246), Skory et al. 2015 (247)
0.7%	West et al. 2007 (236), Asgari et al. 2015 (245)
1%	Xu et al. 2006 (235)
1.5%	Kreeger et al. 2005 (233), Xu et al. 2006 (235), West et al. 2007 (236), West-Farrell et al. 2009 (237), Jiao and Woodruff 2013 (243)
3%	West et al. 2007 (236)

Once alginate is exposed to milimolar concentrations of calcium or other divalent cations, crosslinking occurs (269). The resultant alginate hydrogel forms a mesh-like structure, which allows the diffusion of proteins, such as FSH (233), and provides inert mechanical support without cell adhesion (224). However, alginate hydrogels do not degrade, and any growing tissue, such as follicles, are exposed to increasing pressure from the restrictive hydrogel (271).

To provide dynamic extracellular rigidity, fibrin-alginate gels have been used in follicle culture (238,241,248,249,253); the fibrin can be degraded by proteases secreted by growing follicles (249). Fibrin is generated by the polymerisation of fibrinogen by thrombin, both of which are isolated from blood plasma. Commercially, fibrinogen and thrombin are cryoprecipitated from blood plasma, along with other

biomolecules such as fibronectin, transforming growth factor β1 (TGFβ1), basic fibroblast growth factor (bFGF), epidermal growth factor (EGF) and vascular endothelial growth factor (VEGF) (335), some of which are known to be involved in follicle development (51). Unlike with alginate, fibrin, when also bound with heparin, can reversibly bind growth factors such as bFGF, and act as a localised reservoir of biomolecules (336). When vitrified P12 ovaries were encapsulated with fibrin loaded with heparin binding protein and VEGF and grafted into the ovarian bursae of ovariectomised mice, angiogenesis was improved, and also led to the conception of healthy offspring (267).

These results may not be directly translatable to ovary culture, as the follicles in culture have been liberated from the ovarian structure to further their development. Encapsulation of mouse ovaries in culture have generally been limited to ovarian fragments (known as 'organoids') to study the ovarian surface epithelium (337-340). Alginate has also been used to encapsulate ROs generated from P1 ovaries; however, these were only cultured for 4 d (234).

Although alginate is a commonly used hydrogel, the exposure of the ovaries to millimolar concentrations of calcium ions may affect signalling within the oocyte. Calcium oscillations are vital for oocyte activation after fertilisation (341), and may influence subsequent embryo development (342,343). To avoid any effects of calcium in culture, HyStem® hydrogels may be used; these are hyaluronan (HA) hydrogels consisting of thiol-modified hyaluronan crosslinked by thiol-reactive polyethylene glycol diacrylate (Extralink®). Although HA, a polysaccharide, is the

major component of cumulus ECM of the expanded cumulus oophorous in follicles (274), it can also mediate cellular signalling, matrix organisation, wound repair and morphology in various tissues (275). The HA hydrogel does not contain any ECM proteins or cell attachment peptides, and provides mechanical support. Unlike fibrin-based hydrogels, no additional growth factors are present in the hydrogel, as the HA is generated by *Bacillus subtilis* expressing recombinant hyaluronan synthase from *Streptococcus equismilis* (344). HA hydrogel-encapsulated preantral follicles were able to reach the MII stage after 18-20 h of culture, demonstrating that follicles can develop within HA hydrogels (255). In addition, the HA hydrogel is optically transparent, and easy to gelate. Therefore, using a HA hydrogel is useful to isolate and determine whether rigidity in the environment would improve TC development *in vitro*.

5.2 Aims

- To determine if mouse serum improves theca cell development in whole ovary culture.
- To determine if HA rigidity improves theca cell development in whole ovary culture.

5.3 Materials and Methods

5.3.1 Mice

5.3.1.1 Mice for in-house serum collection

Twelve female CD-1 mice were purchased from Charles River for in-house serum collection. Cardiac puncture was performed at 8 weeks of age, to match the age at which B6Rag1 host mice received RO transplants Chapter 3.

5.3.1.2 Mice for ovary culture

Ovaries from P6 F1 mice (C57BL/6 x CD-1) were cultured in HA hydrogel or collected mouse serum. To obtain the F1 mice, C57BL/6 (CD45.2) males were purchased from Biomedical Services (University of Oxford) and mated with CD-1 females (Charles River). Ovaries from P6 F1 mice from the ROSA26*LacZ* x CD-1 cross (Chapter 3) were cultured with commercial mouse serum.

5.3.2 Mouse serum collection

5.3.2.1 Terminal blood collection by cardiac puncture

The blood was collected by Dr. Suzannah Williams via cardiac puncture, under anaesthesia established by Ms. Sairah Sheikh. Induction of anaesthesia was performed in an induction chamber using 4% isoflurane (Abbott Laboratories) and 2.5 litres per minute (LPM) of oxygen. Once fully anaesthetised, the mice were transferred to the anaesthesia mask with 2-2.5% isoflurane and 1 LPM oxygen on a heated pad (37°C). The mice were placed in a supine position and the blood collected through the sternum using a 1 ml syringe (BD Medical, Oxford, UK) with a

27-gauge needle (Terumo, Bagshot, UK). The blood was ejected into 1.5 ml microcentrifuge tubes after the needles were removed to prevent cell lysis. After blood collection was complete, the mice were cervically dislocated to confirm death.

5.3.2.2 Collection and heat inactivation of mouse serum

Mouse blood was stored in 1.5 ml microcentrifuge tubes at room temperature for 1 h to allow it to coagulate. The tubes were centrifuged for 15 min at 1500 x *g* at 4°C and the supernatant (i.e. serum) was collected without disturbing the pellet. The serum was pooled, with half heat inactivated, while the remainder was stored at -20°C until use.

To heat inactivate serum, the tubes containing serum were submerged in a 56°C water bath for 15 min. The tubes were agitated every 5 min to ensure even heating throughout all the serum. Heat inactivated serum was also stored at -20°C until use.

5.3.3 Ovary culture with mouse serum

To compare the effect of in-house produced mouse serum and the heat inactivated FBS used in Chapter 3 (FB-1550, batch number 10846, Biosera), ovaries were cultured for 14 d with culture media containing either FBS (Control), heat inactivated mouse serum or untreated mouse serum, with the media changed every 2 d (Section 2.4). Subsequent cultures to assess TC development in secondary follicles compared the addition of commercial mouse serum (MO-340,

Biosera) to FBS (FB-1550, Biosera) (Control) to the culture media. The commercial mouse serum was derived from both female and male 8-12 week old non-Swiss albino mice. All culture media was sterile filtered prior to use.

5.3.4 Ovary culture using hyaluronic acid hydrogel

Control ovaries were cultured as previously described. To create the hyaluronic acid (HA) hydrogel scaffold, the HyStem cell culture scaffold kit (HYS020; Sigma) was used to create different concentrations of HA hydrogel.

The stock solution of 1% HA was made by adding 1 ml degassed water to the HyStem vial (containing 10 mg HyStem and 9.6 mg of PBS salts). After rocking the 1% HA solution for 1h at room temperature, the varying concentrations (0.25%, 0.50% and 1.00%) were made by dilution with PBS (Table 5.3).

Table 5.3. HyStem dilutions (0.25%, 0.50% and 1.00%).

HA Concentration	1% HyStem solution (µl)	PBS (µl)	Total volume (µl)
0.25%	10	30	40
0.50%	20	20	40
1.00%	40	0	40

The cross-linker (Extralink) powder, which is required for the HA gel to form, was dissolved in 500 µl of degassed water. Prior to generating the gels, the ovaries to be cultured were collected and cleaned of bursa, and kept in warmed DPBS/BSA for less than 10 min.

To generate the gels, the diluted HA solution was mixed with the cross-linker solution. The gel mixtures and time taken to gel are listed in Table 5.4.

Table 5.4. Hyaluronic acid hydrogel formation.

HyStem Solution		Crosslinker solution (µl)	Total volume (µl)	Time taken to gel
Concentration	Volume (µl)			
0.25%	40	10	50	Does not gel
0.50%	40	10	50	24h
1.00%	40	10	50	10min

Ovaries were transferred with minimal DPBS/PBS to flat bottomed wells in µ-Slide Angiogenesis slides (Ibidi, Martinsried, Germany) and immediately covered with 10 µl of gel (Figure 5.2). For 0.25% and 0.50% HA gels, ovary culture media was added after 30 min crosslinking time in the 37°C incubator. For 1% HA gels, ovary culture media was added after 10 min of crosslinking time. 30 µl of ovary culture media was added to each well; all the media was replaced every 2 d.

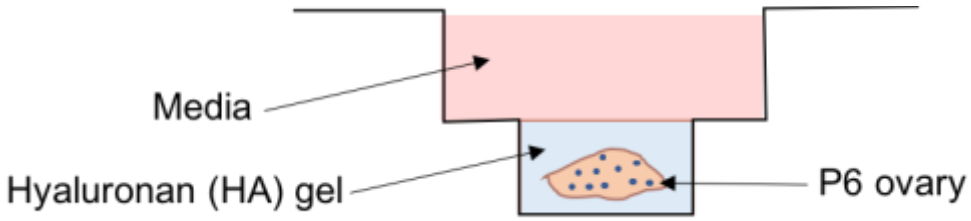


Figure 5.2 Ovary culture using hyaluronan hydrogel

Ovaries were placed on the bottom of a two-welled µ-Slide Angiogenesis slide and immediately covered with hyaluronan (HA) hydrogel to fill the first well. Once the hydrogel crosslinked, pre-equilibrated media was added to cover the HA hydrogel, filling the second well.

5.3.5 Tissue collection and processing

After the culture period, tissues were collected into 10% formalin for fixation and processed according to Section 2.3. All ovaries were sectioned at 5 µm thickness.

5.3.6 Statistical analysis

Analysis was performed using Prism 7 (GraphPad). Data was tested for normal distribution using the D'Agostino & Pearson normality test. Analysis of TC numbers per secondary follicle in ovaries cultured in either FBS or commercial mouse serum was performed using Welch's t-test or ordinary one-way ANOVA. The Mann-Whitney test was used to compare TC numbers per secondary follicle in FBS cultured ovaries sectioned at 3 µm compared to 5 µm. Results are presented as mean ± SD, with $P \leq 0.05$ considered significant.

5.3.6.1 Sample size calculation

The minimum number of analysed secondary follicles required to show a significant difference in TC numbers from FBS and commercial mouse serum cultured ovaries was calculated. This minimum was calculated in order for the results to have 80% power and a 95% confidence interval. As the data is from two independent groups (FBS vs. commercial mouse serum), with continuous results (the TC number), the following formula was used:

$$n = \frac{((\sigma_1^2 + \sigma_2^2) \div k)(z_{1-\frac{\alpha}{2}} + z_{1-\beta})^2}{\Delta^2}$$

where:

- n is the minimum sample size per condition required to detect a significant difference.
- σ_1^2 and σ_2^2 are the variances of TC numbers from secondary follicles from ovaries cultured in FBS and commercial mouse serum.
- k is the ratio of allocated samples in the two conditions. In this case, the ideal would be a ratio of 1, as the number of secondary follicles from FBS cultured ovaries should match those cultured in commercial mouse serum ovaries.
- $z_{1-\frac{\alpha}{2}}$ is the z score of $1-\frac{\alpha}{2}$, where α is the probability of making Type I errors (false positives). For a 95% confidence interval, α is 0.05.
- $z_{1-\beta}$ is the z score of the power, where β is the probability of making Type II errors (false negatives). For 80% power, β is 0.2.
- Δ is $|\mu_1 - \mu_2|$, the absolute value of the difference between the mean TC numbers in secondary follicles from ovaries cultured in FBS and commercial mouse serum.

Rearrangement of the formula to calculate the sample size required for 80% power and 95% confidence is therefore:

$$n = \frac{(\sigma_1^2 + \sigma_2^2) \times 7.84}{\Delta^2}$$

5.4 Results

5.4.1 Follicle development in ovaries cultured in collected mouse serum

To assess the effect of allogeneic serum on TC development in mouse ovary culture, neonatal ovaries cultured with FBS (Control) for 14 d (Figure 5.3A, B) were compared to those cultured in heat treated mouse serum (Figure 5.3C, D) and untreated mouse serum (Figure 5.3E, F). After 14 d, Control ovaries appeared fairly flat as usual (Figure 5.3B), while ovaries cultured in both forms of mouse serum remained relatively rounded (Figure 5.3D, F).

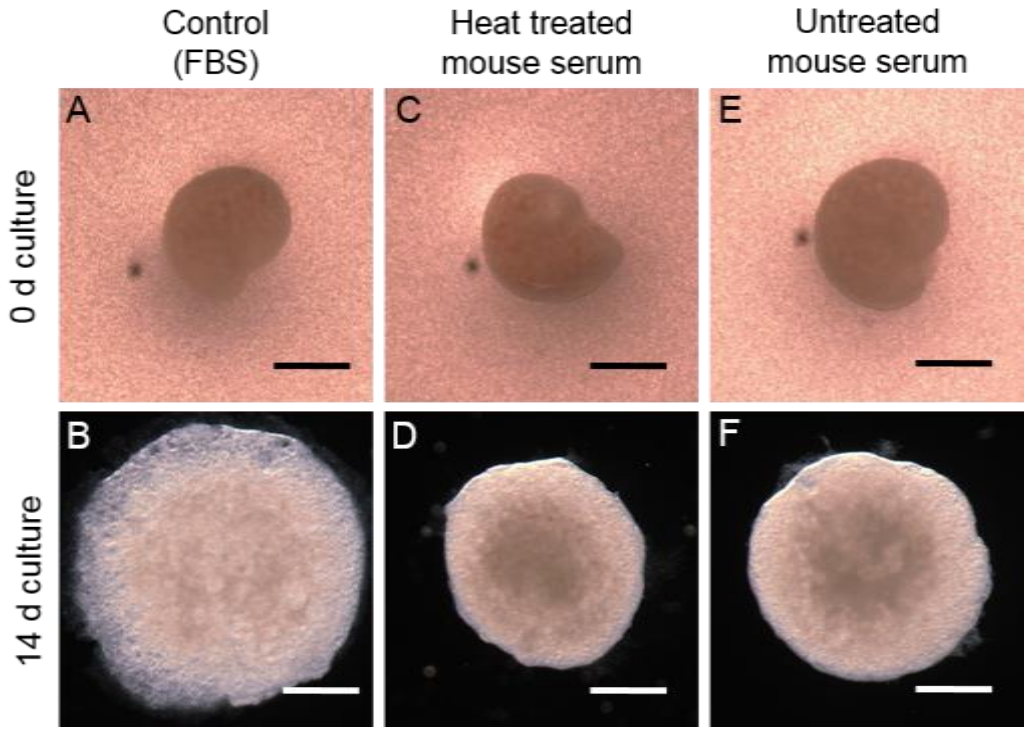


Figure 5.3. Ovaries cultured in foetal bovine serum, heat treated mouse serum and untreated mouse serum.

Representative images of ovaries cultured (A) at 0 d using foetal bovine serum (FBS) (Control) and (B) after 14 d of culture using FBS. Further representative images of ovaries cultured using heat treated mouse serum at (C) 0 d and (D) 14 d of culture; and using untreated mouse serum at (E) 0 d and (F) 14 d of culture. Scale bars: 500 µm All experiments were performed with n=4.

To compare TC development between ovaries cultured in FBS, heat treated and untreated mouse serum, TC numbers from secondary follicles were assessed, as the TC layer is clearly present by the secondary follicle stage. Analysis of follicle development after 14 d of culture revealed that some primary follicles developed in Control ovaries (Figure 5.4A, B) and ovaries cultured in heat treated mouse serum (Figure 5.4C, D). A secondary follicle was observed in an ovary cultured in untreated

mouse serum (Figure 5.4E, F). However, not enough secondary follicles were observed in the cultured ovaries (n=4 per condition) to perform a suitable analysis of TC number.

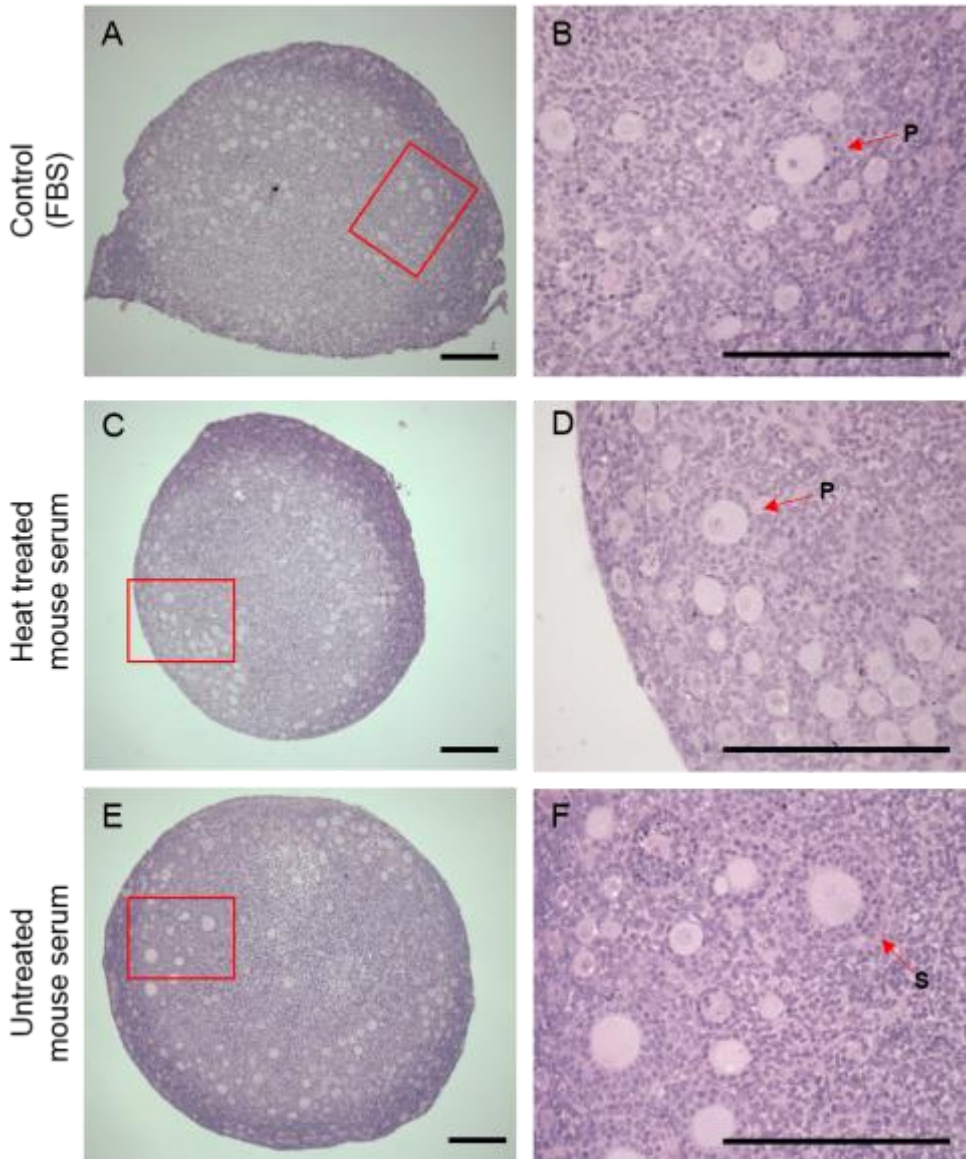


Figure 5.4. Representative sections of ovaries cultured in foetal bovine serum, heat treated and untreated mouse serum for 14 days.

Representative section of ovaries cultured in (A) foetal bovine serum (FBS) (Control). Red box is magnified in B. (B) Higher magnification of the red box in A, showing follicles which have developed in culture. The red arrow points to a primary follicle, which had at least one complete granulosa cell (GC) layer. Representative section of ovaries cultured in (C) heat treated mouse serum, (D) higher magnification of follicles. The red arrow points to a primary follicle. Representative section of ovaries cultured in (E) untreated mouse serum, (F) higher magnification of

follicles. The red arrow points to a secondary follicle, which had at least two complete GC layers. Scale bars: 200 µm. P: primary follicle; S: secondary follicle. All experiments were performed with n=4.

5.4.2 Follicle development in ovaries cultured in commercial mouse serum

Following the lack of secondary follicles present in the C57BL/6 x CD-1 F1 ovaries cultured after 14 d in FBS, the transgenic line, ROSA26*LacZ* x CD-1 F1, used in Chapter 3 was used. Unexpectedly, there were issues with processing of tissue which led to a 'shredded' appearance upon sectioning and staining, so only secondary follicles showing a clear TC layer were analysed.

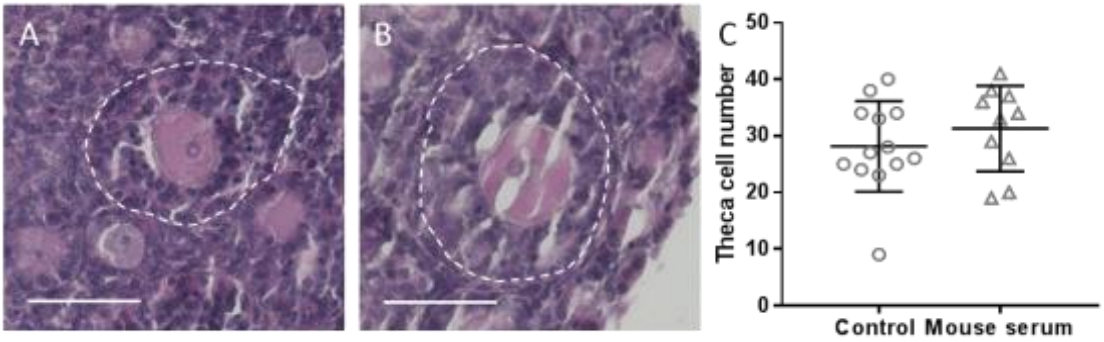


Figure 5.5 Theca cell development in secondary follicles from ovaries cultured in foetal bovine serum and commercial mouse serum after 14 days.

Representative images of secondary follicles cultured in (A) Control (FBS) and (B) commercial mouse serum for 14 d. The white dotted lines delineate the border between the theca cell (TC) layer and granulosa cells. (C) TC number in secondary follicles from ovaries cultured in FBS (Control) and commercial mouse serum for 14 d. Scale bars: 50 µm. Data are plotted as mean ± SD; *P*=0.3464. Secondary follicles in ovaries cultured in FBS (Control) n=13; and in commercial mouse serum n=10. All experiments were performed with n=4.

Despite the fewer numbers of secondary follicles which could be analysed, at least one secondary follicle was analysed from each cultured ovary (FBS (Control) n=4, commercial mouse serum n=4). Analysis of secondary follicles with a clear TC layer revealed no difference in between secondary follicle TC numbers from ovaries cultured in FBS or commercial mouse serum (Figure 5.5). However, sample size calculations indicated that a total number of 192 secondary follicles (96 secondary follicles from each group) would need to be analysed in order to observe a significant difference in TC number.

Since TC number was increased in mouse serum, it was important to determine if this increase was comparable to *in vivo* ovaries. When compared to secondary follicles from *in vivo* Control P20 ovaries (data from Chapter 4), secondary follicles from both FBS and mouse serum cultured ovaries contained fewer TCs (Figure 5.6A). However, it is important to note that the P20 ovary sections were cut at 3 µm rather than 5 µm. Therefore, to determine whether this would affect the result, we compared secondary follicle TC numbers from 5 µm FBS cultured ovaries and 3 µm FBS cultured ovaries (P6-Oc; data from Chapter 4) revealed that the ovaries sectioned at 5 µm contained more TCs (Figure 5.6B). This demonstrates that the number of secondary follicle TCs in P20 ovaries sectioned at 3 µm is an underestimation of what would have been assessed at 5 µm.

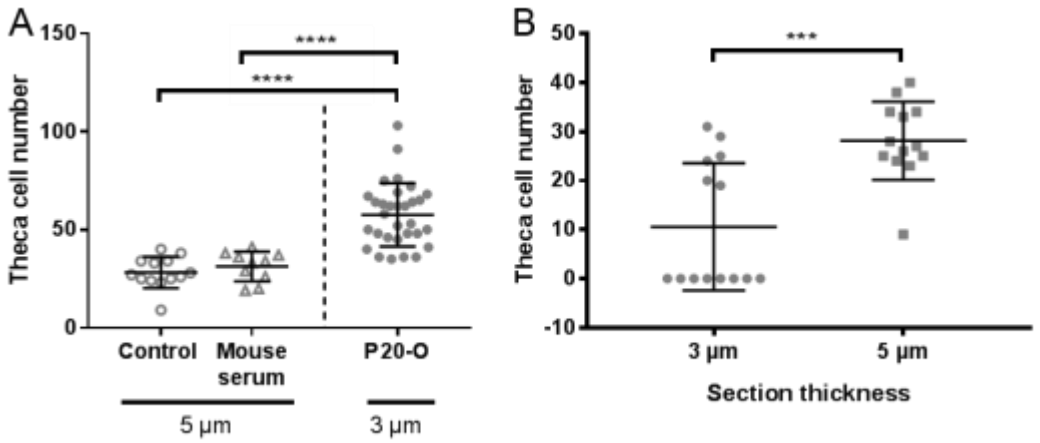


Figure 5.6 Theca cell development in secondary follicles from cultured ovaries and age-matched *in vivo* ovaries sectioned at 3 and 5 µm.

(A) Theca cell (TC) numbers in secondary follicles from ovaries cultured in mouse serum and foetal bovine serum (FBS) for 14 d, which were sectioned at 3 µm, were compared to those in the age-matched *in vivo* P20 ovary (data from Chapter 4). (B) TC numbers in secondary follicles from 14 d FBS-cultured ovaries sectioned at 3 µm (data from Chapter 4) were compared to those sectioned at 5 µm. Data are plotted as mean ± SD. ***$P \leq 0.001$; ****$P \leq 0.0001$.

5.4.3 Follicle development in ovaries cultured in hyaluronan hydrogel

To assess the effects of physical rigidity on TC development in cultured ovaries, follicle development in ovaries encapsulated and cultured on transwell membranes (Control) was compared to ovaries cultured in 0.25%, 0.50% and 1.00% HA hydrogels (Figure 5.7A). After 14d of culture, Control ovaries flattened out, while encapsulated ovaries retained their shape (Figure 5.7B). The darker centre of the ovarian tissue, which is outlined in red, appeared to be degenerated

(Figure 5.7B). Upon sectioning the tissue, follicles at various stages of development were observed in Control ovaries, with no tissue degeneration (Figure 5.7C, D). However, ovaries encapsulated by 0.25%, 0.50% and 1.00% HA hydrogels did not contain any follicles beyond the primordial follicle stage, and all presented with pyknotic cells in the degenerated cores (Figure 5.7C, D). Since no secondary follicles were not observed in HA-encapsulated ovaries, we concluded that the ovary encapsulation with HA hydrogel did not support follicle development and TC development.

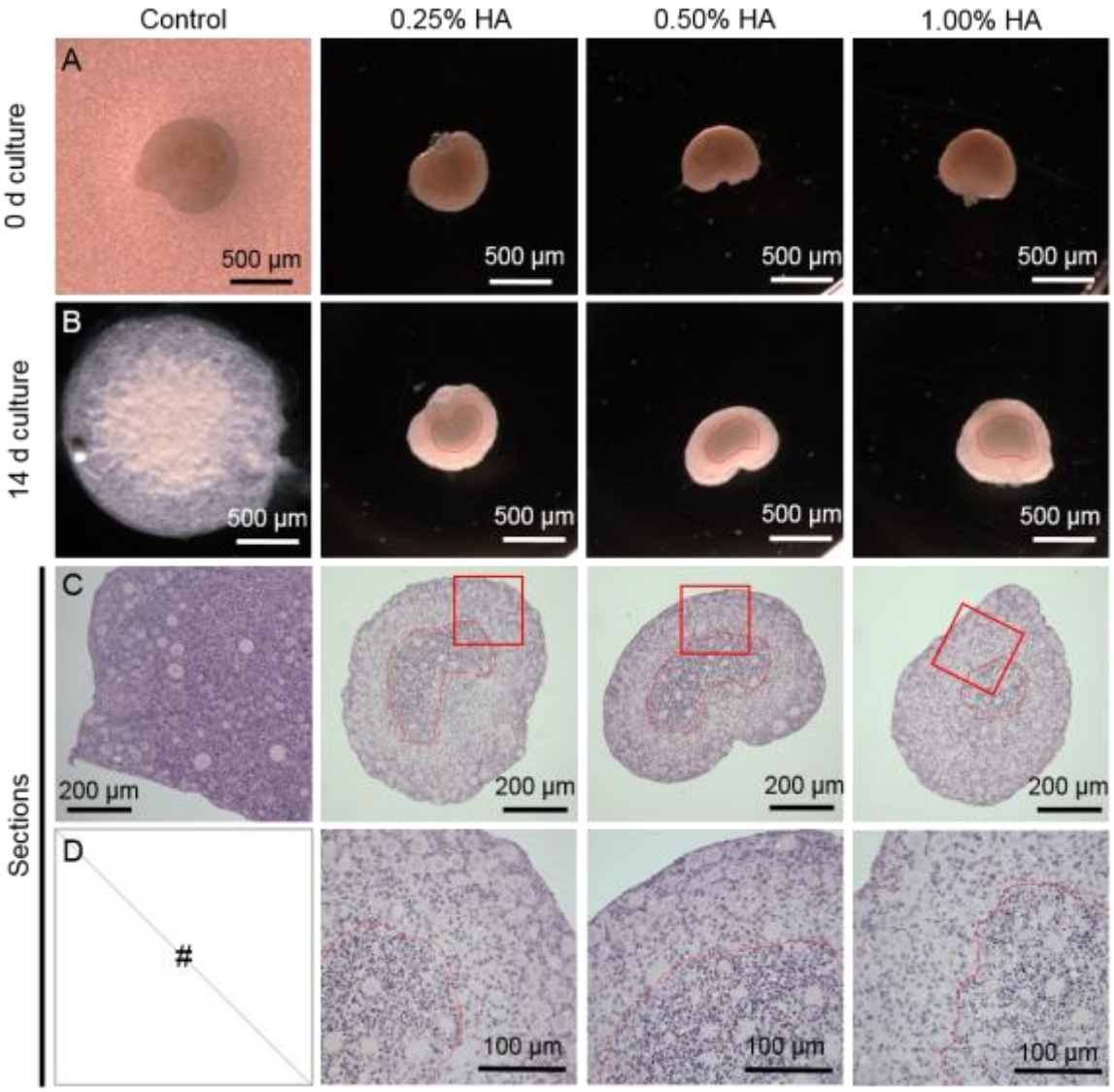


Figure 5.7. Ovaries cultured on transwell membranes, and in 0.25%, 0.50% and 1.00% hyaluronan gel after 14 days.

Representative images of ovaries cultured on transwell membranes, encapsulated in 0.25% hyaluronan (HA), 0.50% HA and 1.00% HA at (A) 0 d and (B) 14d of culture. (C) Representative section of ovaries after 14d of culture. Red box is magnified in D. (D) Higher magnification of the border between degenerating tissue and morphologically normal looking tissue. Scale bars indicate distances presented. Red dotted lines indicate the degenerated area within tissue. # No degenerated tissue present. All experiments were performed with n=4.

5.5 Discussion

After 14 d of development, TC number was higher in primary, secondary and preantral follicles in transplanted ROs and *in vivo* Control ovaries compared to cultured ROs and ovaries. Since both transplanted ROs and cultured ROs, along with *in vivo* Control ovaries and cultured ovaries contain the same cells prior to the 14 d of development, the differences between environment would be due to differences between *in vivo* and *in vitro* conditions. Transplanted ROs and *in vivo* ovaries are exposed to mouse serum, as well as rigidity from the pressure between the renal capsule and kidney (transplanted ROs) or the ovarian bursa (ovaries). We hypothesised that the addition of mouse serum to culture media or the encapsulation of ovaries in HA hydrogels may affect TC proliferation and recruitment in ovaries. To assess changes in TC number, we aimed to analyse secondary follicles, since by the secondary follicle stage, the TC layer is clearly present.

Ovaries cultured in collected generated mouse serum did not contain sufficient numbers of secondary follicles for TC analysis. This was particularly surprising, as insufficient numbers of secondary follicles were observed in the Control ovaries cultured in FBS. Ovaries cultured in Chapter 3 developed more secondary follicles after 14 d of culture than those observed here; however, they had slightly different strain background (ROSA26*LacZ* x CD-1 F1). Although the ROSA26*LacZ* mice have a predominantly C57BL/6 background (287), it appears that ovaries from the F1 cross used here (C57BL/6 x CD-1) do not support follicle development similarly. We therefore returned to using the ROSA26*LacZ* x CD-1 F1

strain from Chapters 3 and 4. Subsequent experiments culturing ovaries from the ROSA26*LacZ* x CD-1 F1 mice with either FBS or commercial mouse serum revealed similar TC numbers in secondary follicles. Although the sample size calculation indicates that TC numbers in secondary follicles from ovaries cultured in mouse serum can be higher than those cultured in FBS, the TC numbers are still significantly lower than those from *in vivo* Control P20 ovaries. This indicates there are additional aspects beyond mouse serum which are involved in TC recruitment and proliferation.

Despite the reduced number of secondary follicles present in FBS cultured ovaries, HA encapsulation of ovaries revealed several issues with our system of hydrogel encapsulation. Unlike alginate systems, which encapsulate follicles in a bead of alginate, ovaries here were covered with HA hydrogel, and the media layered over the surface of the hydrogel. After 14 d of culture within the HA hydrogels, the ovaries only contained primordial follicles, and had degenerating cells within the centre of the tissue. The presence of degradation may be due to lack of penetration of nutrients or oxygen into the centre of the ovary.

The lack of follicles developing beyond the primordial follicle stage in HA-encapsulated ovaries may be due to excess rigidity of the HA hydrogel. Increased pressure imposed by higher alginate concentration has been demonstrated to limit follicle growth in cultured encapsulated follicles, and that decreased rigidity may be allowing tensional homeostasis within the follicle, enabling a paracrine environment which promotes follicle development (236). Although the 1% HA has a modulus of

~300 Pascal after formation, which is similar to the maximal modulus considered permissive to follicle development for encapsulated follicles for culture (236,249), the experiments here involved the encapsulation of a whole ovary. It is thought the rigidity of the ovarian cortex is relatively nonpermissive to follicle growth, as it is collagen-rich area, while the medulla has a lower density of ECM, providing a gradient of rigidity (20). By encapsulating the ovary further with HA hydrogels, the intraovarian rigidity is likely to be higher, preventing further follicle development within the HA-encapsulated ovaries.

Although the results from C57BL/6 x CD-1 F1 ovaries cultured with in-house generated mouse serum proved inconclusive, ROSA26*LacZ* x CD-1 ovaries cultured with commercial mouse serum revealed that the use of allogeneic serum had no effect in TC numbers in secondary follicles, unless the sample size increased. However, the addition of mouse serum did not improve TC numbers to the numbers observed in secondary follicles from age-matched *in vivo* ovaries. The encapsulation of ovaries using HA hydrogels has also prevented follicle development beyond the primordial follicle stage, and the culture system used may have poor nutrient penetration, resulting in tissue degradation in the centre of the cultured ovary.

These results highlight that despite transplanted ROs and *in vivo* ovaries containing the same cells as cultured ROs and ovaries respectively, the addition of

mouse serum and ‘tension’ by encapsulation with HA hydrogels does not improve TC development *in vitro*.

Chapter 6: Dissection and digestion of bovine cortical tissue

6.1 Introduction

The previous chapters have focused on using murine ovaries in generating reaggregated ovaries (ROs) and developing a culture technique. However, if the RO technique is to be optimised to utilise human ovarian cortical strips, it would likely need some modifications, for example, they are more rigid and contain more ECM than mouse ovaries (personal communication, Prof. Evelyn Telfer). Therefore, since it would be wasteful to use the precious human samples for initial optimisation, bovine ovarian tissue was used. Critically, bovine ovarian tissue has similar reproductive physiology (Section 1.2) and texture to human tissues. In addition, bovine ovarian tissue is not part of the food chain and has no commercial value.

Bovine and human reproductive biology share numerous characteristics, as detailed in Table 1.1. Both cows and humans are monovular with 9 months gestation, and their ovaries are also similar in size (approximately 3 cm x 2 cm x 1.5 cm, volume 9 cm^3) (150). The cortical region of the ovary (the outermost layer), contains many primordial follicles (141), and is cryopreserved for fertility preservation (reviewed by Donnez and Dolmans (2015) (345)). Their primordial oocytes are also of similar size, with humans at approximately 36 µm (145) and bovine primordial oocytes at 29.74 µm (180) in diameter.

To isolate the primordial oocytes for the RO technique, the ovarian tissue is dissected prior to enzymatic dissociation to increase the surface area on which the enzymes can digest. Current protocols in the Ovarian Cryopreservation Tissue Bank (OCTB) at Oxford involve the dissection of human cortical strips into 1 mm x

2 mm x 5 mm strips. Although neonatal mouse ovaries do not require cutting for digestion into a single cell suspension (226), previous studies using adult ovaries in the Williams laboratory have involved cutting the ovaries into smaller pieces (approximately 1 mm^3) to ensure they can fit through the tip of a 1000 µl pipette tip during the digestion procedure (unpublished work). Optimisation of bovine ovarian cortex digestion would involve cutting the cortical strips into smaller digestible pieces, and determining the optimal enzymatic mixtures required and length of digestion time for the highest yield of live germ and somatic cells. Since the human cortical strips are cut into 1 mm x 2 mm x 5 mm strips and cryopreserved, the bovine cortical strips must also be cut into similar dimensions and cryopreserved prior to testing digestion protocols.

Optimisation of enzymatic digestion of a tissue requires knowledge of the ECM present. The ovarian ECM has been characterised in mouse (346), bovine (347-350) and human ovaries (351,352), with a particular focus on collagen type I, collagen type IV, fibronectin and laminin. The current protocol for digesting mouse tissues involve a mixture of trypsin, ethylenediaminetetraacetic acid (EDTA) and DNase I. Trypsin, an ‘aggressive’ serine protease, has a high cleavage specificity for the C-termini of arginine and lysine (353). Combined with EDTA, a chelating agent which sequesters divalent cations (e.g. Ca^{2+}, Mg^{2+}) and prevents the cation-dependent cell binding (354,355), the digest forms a single cell suspension. However a ‘gentler’, more ECM-specific enzyme mixture may result in higher live cell yields, as extended tissue incubation with trypsin can lead to the digestion of cell membranes (356) and cell death. Dispase II, which is currently used to digest human endometrial tissue (357), is a neutral protease which selectively cleaves

collagen type IV and fibrinogen, but degrades collagen type I minimally (358). Collagenases are bacterial enzymes found in certain species of the genus *Clostridium*, and proteolytically digest collagen or gelatin (a denatured collagen) (359,360). Liberase is a commercial blend of Collagenase I and II and thermolysin, a neutral metalloproteinase which cleaves peptide bonds of hydrophobic amino acids (361). Low concentrations of Liberase have previously been used to isolate follicles (362). Given the relative specificity of these enzymes, a Dispase II/Collagenase I or a Liberase enzymatic mixture may be optimal to improve the live cell yield from digesting cryopreserved bovine cortical strips.

6.2 Aims

- To establish bovine cortical strip dissection and cryopreservation method in the Williams laboratory.
- To determine whether using Dispase II/Collagenase I or Liberase mixture to enzymatically digest bovine cortical strips yields more live germ and somatic cells than 0.05% Trypsin/EDTA.

6.3 Materials and Methods

6.3.1 Collection of bovine ovaries

Bovine ovaries were collected from freshly killed cows over a period of < 1 h from the local abattoir and transported back to the laboratory (~ 30 min) based on the protocol by McLaughlin et al. (2010) (184) described below. The ovaries were transported and dissected in pre-warmed (33-37°C) Transport/Dissection media,

containing Leibovitz's L-15 medium (Gibco, Life Technologies, ThermoFisher Scientific) supplemented with 2 mM sodium pyruvate (Sigma), 2 mM glutamine (Sigma), 3 mg/ml BSA (Fraction V, Fisher Scientific), 75 µg/ml penicillin G (Sigma) and 50 µg/ml streptomycin (Sigma). Around 3-4 ovaries were collected into 50 ml conical centrifuge tubes filled with 25 ml of Transport/Dissection media. The bovine ovaries were collected with help from Dr. Suzannah Williams, Ms. Charlotte Walker and Ms. Eleni Papadopoulou.

6.3.2 Dissection of bovine cortical strips

Ovary dissection was originally performed in 35 mm non-tissue cultured Petri dishes (351008, Corning Falcon, Fisher Scientific). Borosilicate Petri dishes (10 mm; Duran Duroplan, Fisher Scientific) were later used for the dissection of the bovine cortex, to reduce the risk of creating plastic shavings to the samples during dissection.

Each ovary was placed into a Petri dish with Transport/Dissection media, and bisected through the pedicle using a pair of serrated Adson forceps (Fine Science Tools) and sterile, single use No. 24 scalpels (Swann-Morton Ltd., Sheffield, UK). During dissection, it was important to avoid grasping the cortical area with the forceps. The tissue was cut with a single clean cut, using a rocking motion with the curved scalpel blade, as this reduces damage to the cortical tissue (personal communication, OCTB). After bisecting the ovary, using the forceps to hold the medulla, each ovary was quartered. Once quartered, holding the medulla, the cortex was cut cleanly from the medulla using curved spring scissors. Cleanly isolated

cortical tissue should be barely translucent (roughly 1-2 mm thick) (Figure 6.1), and contain small follicles (which appear as ‘bubbles’), when observed under the microscope.

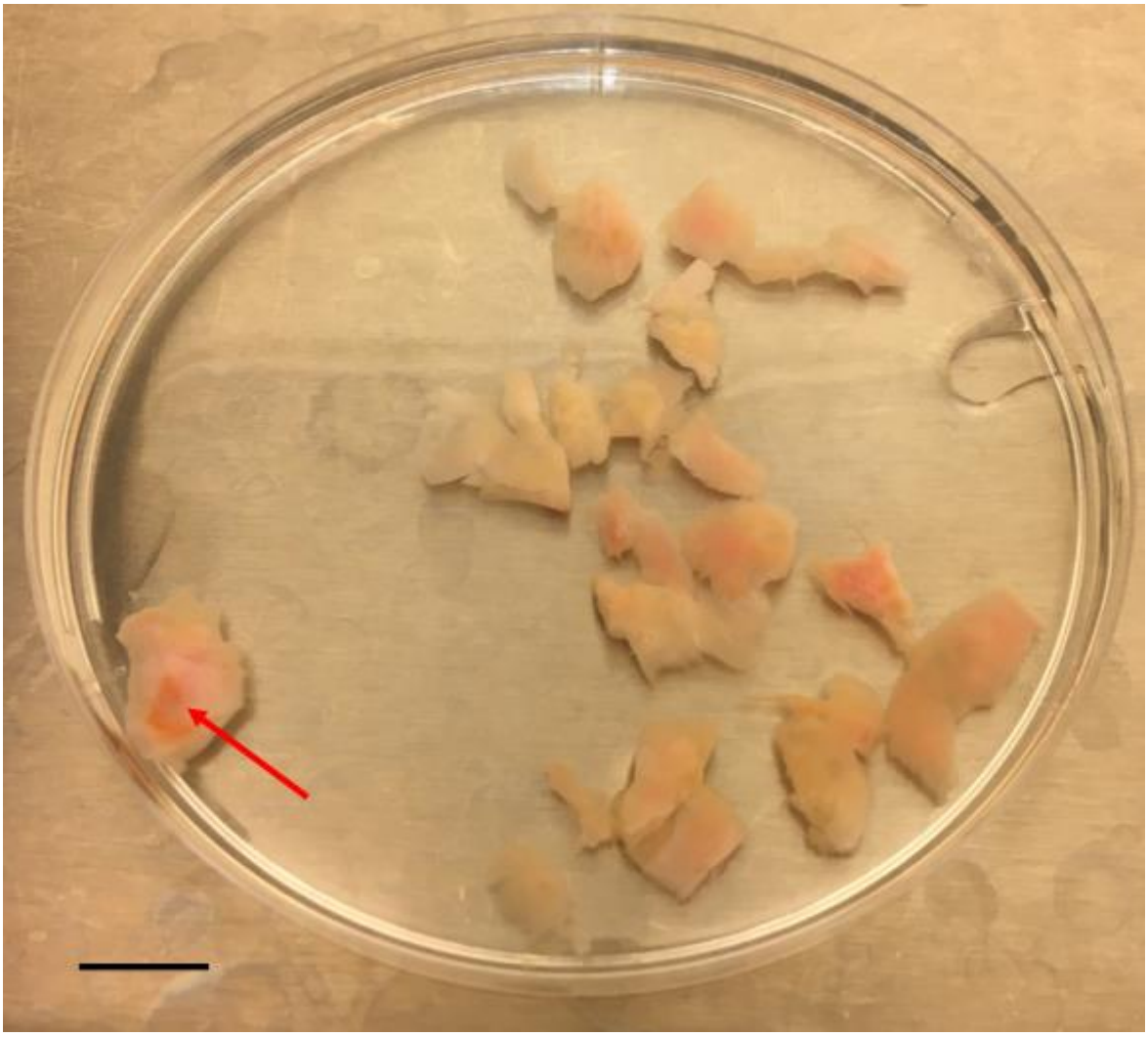


Figure 6.1 Isolated bovine cortical tissue.

The bovine cortical pieces were imaged in PBS/BSA for clearer visualisation. The bovine cortical tissue is of varying size due to variable morphology of the collected ovaries. All the pieces of tissue are approximately 1-2 mm thick and were cut into strips, aside from the piece with a remaining part of corpora luteum (pointed at by the red arrow), which was discarded. Scale bar: 1 cm

After the cortical area was cleaned, it was transferred to a new Petri dish containing fresh Transport/Dissection media. The collected cortical area was then dissected into 1 mm x 2 mm x 5 mm strips. The dissection of cortical strips was performed with the help of Ms. Eleni Papadopoulou.

6.3.3 Cryopreservation and thawing of bovine cortical strips

The cryopreservation protocol is based on the protocol established by Revel et al. (2003) ((363)) based on Gosden (2000) (364). The cryoprotectant media (CPA) consisted of L-15 medium supplemented with 10% FBS (Labtech), 1.5 M ethylene glycol (EG) (Sigma) and 0.1 M Sucrose (Sigma). To prepare for cryopreservation, the CPA was sterile filtered through 0.22 µm filters (Millex-GP Syringe Filter Unit, Merck) and aliquoted into specimen tubes (15 ml conical centrifuge tubes (Falcon, Fisher Scientific) filled with 8 ml CPA) and 2 ml cryovials (externally threaded, Corning) filled with 1 ml CPA. The specimen tubes and cryovials were pre-cooled on ice.

Five cortical strips were transferred into each specimen tube. The specimen tubes were gently shaken for 1 h on ice to promote the penetration of the cryoprotectant. After 1 h of equilibration, the strips were transferred to the cryotubes containing CPA, ensuring all five cortical strips were submerged in the CPA in each cryotube. The cryotubes were loaded into a controlled rate freezing device (Mr. Frosty, ThermoFisher Scientific) and placed into a -80°C freezer, allowing the cryovials to cool at a rate of -1°C/min overnight. Once the cortical strips were frozen at -80°C, they were transferred to storage in liquid nitrogen.

To thaw the bovine cortical strips, the cryovials were thawed in a 37°C water bath for 3 min, after which the CPA was removed and replaced with 2 ml of pre-equilibrated M199/FBS (Section 2.3), and the cryovials were incubated at 37°C for 5 min. This was repeated to ensure the CPA was removed.

6.3.4 Digestion of bovine cortical strips

The strips were washed twice in PBS/BSA (Section 2.3) and transferred to a new non-tissue culture treated 35 mm Petri dish with minimal PBS/BSA. The cortical strips in PBS/BSA were mechanically dissociated with single use No. 24 scalpels (quickly to prevent the tissue from drying out). If the tissue appeared to be drying out, additional drops of PBS/BSA were added. Using the scalpels, the cortical strips were cut so they were small enough to fit easily through wide bore 1000 µl filter tips, which were approximately 2 mm in diameter (Starlab, Milton Keynes, UK).

Once the cortical strips were of the right dimensions, 2 ml of digestion media was immediately added into the dish. The digestion mixtures tested were the 0.05% Trypsin/EDTA (Gibco, Life Technologies, ThermoFisher Scientific) with 0.02% DNase I (DN25; Sigma) (referred to as T/E), as described in Chapter 3; the Dispase II/Collagenase I/DNase I digestion mixture (referred to as D/C), detailed in Table 6.1, and 1X Liberase (Roche Life Science, Burgess Hill, UK). The enzymes were dissolved in PBS (Sigma) prior to the addition of M199 (ThermoFisher Scientific). The aliquots of Dispase II, Collagenase I and Liberase were kindly provided by the Granne/Southcombe group (Nuffield Department of Obstetrics and Gynaecology, University of Oxford).

Table 6.1 Constituents of the Dispase II/Collagenase I/DNase I digestion mixture.

Final concentrations of reagents	Aliquots of reagents added for digestion mixture
0.96 mg/ml **Dispase II** (17105-041; ThermoFisher Scientific)	500 µl of 10 mg/ml **Dispase II** dissolved in PBS
1.92 mg/ml **Collagenase I** (17018-029; ThermoFisher Scientific)	500 µl of 20 mg/ml **Collagenase I** dissolved in PBS
0.06 mg/ml **DNase I** (Sigma)	200 µl of 1.56 mg/ml **DNase I** dissolved in PBS
M199 (ThermoFisher Scientific)	4000 µl M199
Total volume	5200 µl / 5.2 ml

The cortical strips digested in T/E and Liberase were incubated at 37°C for 30 min, while those which were digested in the D/C mixture were incubated for 1 h. Originally, 30 min of D/C digestion was planned; however, after 30 min in the first experiment, minimal digestion occurred so the digestion time was extended to 1 h. Digestion was aided by frequent gentle agitation by pipetting the tissue and solution using the 1000 µl wide bore pipette tips (Starlab). The subsequent neutralisation, centrifugation, culturing and plating steps were repeated as described in Section 2.3.

After overnight culture, the unattached cell population was filtered through 100 µm cell strainers (Falcon, Fisher Scientific) to remove undigested tissue. Further culture and live/dead cell assessment was performed as described in Section 2.3.

6.3.5 Statistical analysis

Data was analysed using a paired t-test using Prism 7 (GraphPad). Results are presented as mean ± SD, with $P \leq 0.05$ considered significant.

6.4 Results

6.4.1 Dissection and cryopreservation of bovine cortical strips

Eight bovine ovaries were cleaned and dissected on the same day as collection. Between 5 to 20 strips measuring approximately 1 mm x 2 mm x 5 mm were dissected from each of the eight ovaries; a total of 80 cortical strips were cryopreserved in 16 cryovials of five strips each.

Care was taken to ensure that strips from the same ovary were cryopreserved together and noted, as strips from the same ovary were matched together for the enzymatic digestion experiments. Age and parity of the cows were unable to be recorded, as the bovine viscera were removed from the cows by abattoir staff prior to ovary collection.

6.4.2 Enzymatic digestion of bovine cortical strips

A preliminary test using fresh bovine tissue (n=1, 5 strips per condition) was performed to determine which enzymes and incubation time, were suitable for ovarian digestion (Table 6.2). The suggested incubation time with D/C was previously suggested by the Granne/Southcombe group to be approximately 1-2 h, while Liberase was suggested to be approximately 30 min. During digestion of the

ovarian tissue, it appeared that more tissue remained undigested after 30 min in D/C compared to T/E, and so the D/C incubation time was extended to 1 and 2 h. Interestingly, after enzymatic digestion of the cortical strips, there was no somatic cell adhesion to the tissue culture treated plastic Petri dishes unlike mouse somatic cells. As a result, the assessment of cell yield was made from the non-adherent cell suspension after two rounds of differential separation (see Section 2.3).

Although Liberase had a higher percentage of live cells, the overall cell yield was lower than the D/C digests, and the residual tissue appeared to be less digested compared to the other conditions after 30 min of incubation. Incubation of the bovine strips in D/C for 1 h had a similar percentage of live cells and cell yield to 2 h of incubation. However, since 2 h of incubation (along with continuous agitation) was not advantageous for performing the RO technique, subsequent experiments to test enzyme mixtures used 1 h of D/C incubation time.

Table 6.2 Digestion of fresh bovine cortical strips using Trypsin/EDTA/DNase I, Liberase and 1 or 2 hours in Dispase/Collagenase I/DNase I.

	30 min T/E		30 min Liberase		1 h D/C		2 h D/C	
Live cells	76,000	100.0%	258,400	89.5%	349,600	85.2%	304,000	83.3%
Dead cells	0	0.0%	30,400	10.5%	60,800	14.8%	60,800	16.7%
Total cell number	76,000	100.0%	288,800	100.0%	410,400	100.0%	364,800	100.0%

Following these results, the cryopreserved bovine cortical strips were tested. Using strips matched from the same ovaries, to account for differences in age and quality of ovaries, the five strips digested in T/E were compared to five matched strips digested in D/C. Again, the somatic cell adhesion was poor, so the assessment of cell yield was made from the non-adherent cell suspension after two rounds of differential separation

The number of live and dead cells were normalised to the total number of cells isolated from the tissue and expressed as a percentage (Figure 6.2). The total number of cells isolated from cortical strips digested in T/E did not differ from those digested in D/C, nor did the % of isolated live or dead cells.

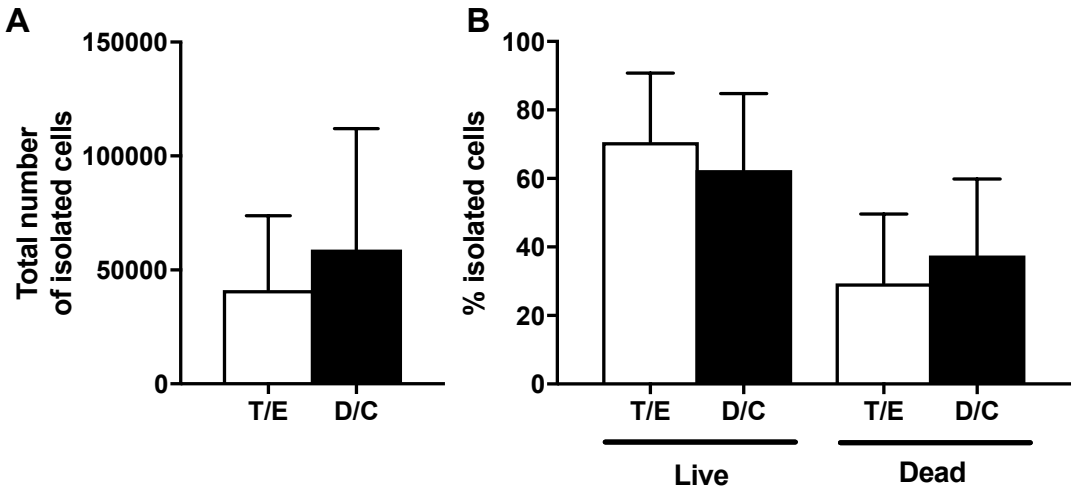


Figure 6.2 Cell yields from bovine cortical strips digested in Trypsin/EDTA/DNase I or Dispase II/Collagenase I/DNase I.

(A) The total number of cells isolated from cortical strips digested in Trypsin/EDTA/DNase (T/E) or Dispase II/Collagenase I/DNAse I (D/C). (B) The percentage of live and dead cells isolated from cortical strips, normalised to the total number of cells isolated from the cortical strips digested in T/E or D/C. Experiments involved the enzymatic digestion of five cortical strips per digestion mixture from the same ovary (T/E or D/C), with n=3 performed using strips from different ovaries. Data are presented as mean ± SD.

6.5 Discussion

Establishing the RO technique using cortical strips is dependent on optimising the mechanical and enzymatic dissociation to result in a high yield of live germ and somatic cells for reaggregation into an RO. In the Williams laboratory, ROs have been successfully generated using adult mouse ovaries, cut into approximately 1 mm^3 pieces and digested in T/E.

The primary objective of this chapter was to familiarise oneself with cortical tissue and to explore tissue digestion using bovine cortical strips as a proxy for human cortical strips. Prior to enzymatic digestion, bovine cortical strips were cut with scalpels to the size of approximately 2 mm^3; it was technically difficult to try to cut the tissue any smaller. After both digestion protocols, undigested tissue was still present, indicating that the tissue dimension may still be too big for the current enzymatic concentrations for a high cell yield.

The size of the tissue prior to enzymatic digestion is vital, as this will provide the surface area on which the enzymes can act and dissociate cells from the ovarian cortex. Ideally, the yield of cells from each cortical strip should be as high as possible, since there are only limited numbers of human cortical strips available. To ensure the tissue can be cut into smaller pieces prior to digestion, a tissue chopper can be used; this has been used to chop human medulla into 0.3-0.5 mm^3 pieces (270). Although a preliminary experiment also tested the enzymatic digestion of Liberase and 2 h of incubation with D/C, 1 h D/C was chosen as it was easier to perform the RO technique with a shorter digestion time. The enzymatic digestion of the bovine cortex revealed no difference between the use of T/E and 1 h D/C. In hindsight, weighing the cortical strips prior to digestion would allow for normalisation of tissue between the conditions. Further work will continue to use T/E, as it has a similar cell yield, and requires a shorter digestion time compared to D/C (30 min compared to 1 h).

However, the starkest result from these experiments have revealed that the bovine somatic cells do not adhere to the tissue cultured treated Petri dishes unlike mouse somatic cells, even when digested with T/E. Somatic cell adhesion allows the clean separation of the germ and somatic cell populations. By separating the germ cells cleanly from the somatic cells, patients with abnormal somatic cells (e.g. POI patients, ovarian cancer patients) can have their germ cells reaggregated with an alternative somatic source. The resultant RO could potentially develop follicles, and eventually mature fertilisable eggs for *in vitro* fertilisation (IVF).

To consider why the bovine somatic cells do not adhere to the tissue culture-treated plasticware, it is important to understand the basis of mouse somatic cell adhesion. The Petri dishes used for the differential separation of germ and somatic cells are polystyrene based, which have been treated with vacuum-plasma to promote cell attachment. Simply, the ionised plasma gas modifies the polystyrene cell growth surface to carry a negative charge, by carrying a variety of additional functional groups, such as oxygen (365). The formation of the negatively charged and hydrophilicity of the tissue culture treated surface promotes the adsorption of cell adhesion proteins (e.g. fibronectin, vitronectin) found in serum (366). Cell adhesion is commonly mediated by the tripeptide RGD (Arg-Gly-Asp), and is expressed by numerous proteins, including fibronectin and integrins (367).

In the case of our culture system, the cell adhesion proteins are derived from the FBS added in the M199/FBS. To improve somatic cell adhesion for bovine cortical strips, and potentially human cortical strips, the Petri dishes could be coated

with ECM proteins (e.g. Matrigel) or fibronectin. If human somatic cells are unable to bind to tissue culture treated plasticware alone, the improvement of somatic cell adhesion is one of the next steps required to optimise the RO technique using human tissues.

In summary, both T/E and D/C digestion of bovine cortical strips resulted in poor somatic cell adhesion, despite the success of T/E with mouse ovarian tissue. The difference in somatic cell adhesion after digestion with T/E may be species-specific, which may mean that somatic cells isolated human cortical strips using T/E may also have poor adhesion to tissue culture-treated plasticware. Since somatic cell adhesion is central to the separation of the germ and somatic cell compartments, optimisation of the somatic cell will be vital for the clinical translation of the RO technique, particularly in cases for patients with dysfunctional somatic cells which result in aberrant follicle development (e.g. POI patients).

Chapter 7: Investigating the potential of human ovarian germ cells to function in a reaggregated ovary

7.1 Introduction

To move the *in vivo* RO technique towards clinical application, the previous chapters have investigated follicle development in cultured ROs and familiarisation of cortical strips digestion using bovine ovarian tissue as a proxy for humans. However, before generating ROs containing human germ cells, it is vital to define which patients would benefit from a clinical RO technique. The RO technique is centred on the development of follicles from germ cells reaggregated with an alternate source of somatic cells. The only reason to reaggregate germ cells with an alternate source of somatic cells is for situations where the original somatic cells impede follicle development, resulting in infertility.

7.1.1 Issues in human follicle development

Patients with ovarian cancer and POI may benefit from fertility preservation (ovarian cortex cryopreservation) and the generation of fertilisable eggs using the RO technique. These conditions are characterised by dysfunctional somatic cells, which impede follicle development; by replacing the somatic cell source, normal follicle development may occur.

7.1.1.1 Ovarian cancer

Ovarian cancer is the seventh most common cancer worldwide (368), and accounts for 4.22% of all female cancer registrations in the England (289). Although over 53% of diagnoses are in females aged 65 and above (past reproductive age), (369), ovarian cancer remains one of the top three cancers for women in England

between the ages of 15 and 49 (289), with 8% of diagnoses in females below the age of 40 (369).

The different types of ovarian cancer can be divided into various histological types, with epithelial cancers accounting for approximately 90% of ovarian cancers. Non-epithelial cancers account for the remaining 10% of ovarian cancers, and include germ cell tumours and sex cord-stromal tumours (reviewed in Matulonis et al. 2016 (370)). For ovarian cancer patients with ovaries able to support follicle development, primordial follicles can be initially grown in cortical strip culture and dissected out for further follicle and oocyte development prior to IVF (Section 1.3.1.2). However, ovarian sex cord-stromal tumours develop from the somatic cells supporting follicle development, including GCs (granulosa cell tumours; GCTs) and TCs (thecomas), which may affect follicle development.

Both GCTs and thecomas are oestrogen-producing tumours; however thecomas most commonly present at an older age, with more than 80% of patients at a postmenopausal stage (371). Ovarian GCTs are further subclassified into juvenile GCT (JGCT) and adult GCT (AGCT) based on characteristics and pathology. Histologically, AGCTs present with GCs with ‘coffee bean’-shaped nuclei and little cytoplasm (372), and Call-Exner bodies (rosettes of cells surrounding a cavity) (373); while JGCTs present with immature GCs with frequent mitoses (374), with some degree of nuclear abnormalities (375). Although JGCTs normally develop before puberty, they have been diagnosed in patients from 10 months of age (376)

to 67 years of age (375). AGCTs can also occur at any age, but commonly present during the perimenopausal or postmenopausal period (377).

Although patients with GCT often present with stage I disease (growth limited to one or both ovaries; based on International Federation of Gynaecology and Obstetrics (FIGO)) (377), they may still benefit from the RO technique. Analysis of GCT patients at a fertile age range (16-45 years old) revealed a higher rate of anovulatory infertility among infertile couples with GCT (58%) (283) compared to 33% for infertile couples without GCT (378). Unkila-Kallio et al. 2000 hypothesised that the hormonal effects from GCTs disturbed the patients' menstrual cycles, resulting in oligo-amenorrhoea and anovulatory infertility (283). This indicates that the GCTs may be providing an abnormal milieu for follicle development, but that germ cells still exist within the GCT-affected ovaries. By reaggregating the germ cells from the GCT-affected ovaries with suitable somatic cells, the resultant RO may allow the development of fertilisable eggs.

7.1.1.2 Premature ovarian insufficiency (POI)

The other disorder where ROs may prove useful is premature ovarian insufficiency (POI). The size of the pool and rate of follicular activation determines the reproductive lifespan, and any modifications in the activation or development of the follicles can result in a condition known as POI, previously known as premature ovarian failure. Throughout a woman's reproductive lifespan, primordial follicles are activated from a quiescent pool for follicle development. However, once the number of quiescent follicles within the primordial follicle pool reaches ~1000, the woman

undergoes menopause. Approximately 1% of women under the age of 40 have POI, with > 74% cases presenting as idiopathic (288,379,380). Approximately 50% of POI patients still have follicles (i.e. follicular POI) (281,282,284,285); and 5-10% of patients diagnosed with POI can conceive spontaneously (381). In humans, mutations in *FOXL2*, which is localised within GCs, have been associated with POI (382). In addition to *FOXL2*, mutations in inhibin A, FSHR and LHR have been identified in POI patients (383-387). Using the RO technique to remove of the somatic cells with these mutations and reaggregating the patients' germ cells with a suitable somatic cell source may support normal follicle development.

The potential use of the RO technique to restore follicle development has been investigated in the Williams laboratory (unpublished work) using a mouse model of follicular POI, known as the Double Mutant (DM) (286). The DM mouse has abnormal follicle development, resulting in an accumulation of primary follicles, and undergoing POI by 12 weeks of age (286). Reaggregation and transplantation of germ cells from DM mice at 9 weeks of age (when they are infertile) with neonatal somatic cells rescued follicle development, with follicles reaching the antral stage.

In order for the RO technique to be applied as a fertility treatment, ROs generated using human germ cells and an alternative source of somatic cells must be used. The ROs must also be cultured rather than transplanted xenogeneically. Since follicles have developed in cultured mouse ROs (MoROs) (Chapter 3) and in chimeric ROs containing somatic cells from mice and germ cells other species such as cats (Section 1.4.4), we hypothesised that human-mouse chimeric ROs

(HuMoROs) containing human germ and mouse somatic cells would support follicle development.

Given that human germ cells would be from cryopreserved cortical strips and that our previous mouse studies used only fresh tissue, we explored whether providing recovery time before subjecting tissue to digestion would improve cell survival. We hypothesised that the additional 24 h of culture after thawing may allow the cryopreserved cortical strips to ‘recover’, before subjecting the tissue to enzymatic digestion. Preliminary work from Kingsley Ojukwu (MSc student, 2015) indicated that culturing mouse ovaries for 24 h after thawing improved live cell yield after digestion.

7.2 Aims

- To determine whether follicle development occurs in chimeric HuMoROs cultured for 7 days.
- To determine whether 24 h of cortical strip culture post-thawing improves follicle development in cultured chimeric HuMoROs.

7.3 Materials and Methods

7.3.1 Human ovarian tissue

The research performed in this chapter received approval from the NHS Research Ethics Committee (REC) (Ethics Reference Number: 14/SC/0041, R&D

Reference: 8825), and all women gave informed consent. The tissue was obtained from the OCTB.

7.3.1.1 Fresh ovarian medulla

Fresh ovarian medulla was collected on the day of the ovarian biopsy of three patients undergoing fertility preservation; these pieces of tissue were not collected for cryopreservation and were to be discarded. Further details regarding the patients are in Table 7.1.

Table 7.1 Fresh ovarian medulla donor details.

Patient	Age at ovarian tissue collection (years old)	Condition
A	24	Adenocarcinoma, familial adenomatosis polyposis
B	18	Hodgkin's lymphoma
C	9	Hodgkin's lymphoma

7.3.1.2 Cryopreserved cortical tissue

Cryopreserved cortical tissue was obtained by ovarian biopsy of three prepubertal patients undergoing fertility preservation. Prepubertal patients were defined as those who had not undergone menarche at the time of ovarian tissue collection (mean ± SD age was 10.3 ± 1.15). Further details regarding the patients are in Table 7.2.

Table 7.2 Cryopreserved ovarian cortical tissue donor details.

Patient	Age at ovarian tissue collection (years old)	Condition
D	11	Sickle cell anaemia
E	9	Medulloblastoma, with no chemotherapy before ovarian tissue collection
F	11	Sickle cell anaemia

Of the six cortical strips thawed per patient, three were used at 0 h and three were used at 24 h. Of each three strips, a piece of cortical strip (~1 mm^3) was dissected from one of the cortical strips which were immediately thawed for digestion (referred to as 0 h) and those cultured for 24 h (referred to as 24 h). The collected 1 mm^3 pieces were weighed and immediately fixed in 10% formalin for 6 h (Section 2.3).

7.3.2 Human ovary collection, dissection and cryopreservation

Human ovarian tissue collection, processing and cryopreservation were performed by the technicians in the Oxford Tissue Cryopreservation Bank (OCTB), based on the dissection and cryopreservation protocol established by Revel et al. 2003 (363), based on Gosden (2000) (364).

Ovarian tissue was collected into L-15 media, transported to the OCTB for processing and dissection into 1 mm x 2 mm x 5 mm cortical strips (Section 6.3.2). However, unlike the previous chapter, the cryoprotection agent (CPA) contained human serum substitute instead of FBS, and the cryovials (2 ml, internal thread;

Nunc, Rochester, New York, USA) were slowly frozen using the Sy-Lab Ice Cube controlled rate freezer (Sy-Lab, Neupurkersdorf, Austria). The cryovials were loaded into the pre-cooled 0ºC controlled rate freezer and set to cool at -2ºC/min until the chamber reached -9ºC, after which each tube was manually seeded to enable controlled ice crystal formation. After seeding, the cryovials were further cooled to -40ºC at a rate of -0.3ºC/min, and finally to -140ºC at -10ºC/min. Finally, the cryovials were packaged for storage and stored in liquid nitrogen tanks (-196ºC).

The medulla was kept in L-15 media and collected immediately after tissue processing for experiments.

7.3.3 Human cortical strip thawing

Prior to removing the cryovials from liquid nitrogen storage, 4 ml of each thawing media per cryovial (Solution 1, Solution 2 and Solution 3) were made and sterile filtered into 7ml bijou tubes (see Table 7.3).

Table 7.3 Thawing media constituents.

	Solution 1	**Solution 2**	**Solution 3**
Ethylene glycol (Sigma)	0.224 ml	0.112 ml	0 ml
1 M Sucrose (Sigma), dissolved in sterile water	0.4 ml	0.4 ml	0.4 ml
FBS (Batch # 1090, Labtech)	0.4 ml	0.4 ml	0.4 ml
Leibovitz's L-15 media (Gibco)	2.975 ml	3.088 ml	3.2 ml
Total volume	4 ml	4 ml	4 ml

Cryovials containing 6 cortical strips were chosen. The cryovials were transported to the laboratory in a liquid nitrogen-filled table top dewar (Dilvac; Day Impex, Colchester, Essex, UK), and rapidly thawed in a 37ºC water bath for 3 min. After thawing, the strips were transferred to the bijou tube containing Solution 1, and placed on the rocker at ~ 35 rpm for 5 min. This was repeated for Solution 2 and Solution 3.

7.3.4 Cortical strip culture

For each experiment, three of the six thawed cortical strips were cultured in Waymouth media (Sigma) supplemented with 10% FBS (FB-1090; Labtech), individually on transwell membranes (Section 2.4). The strips were cultured for 24 h before they were digested for RO formation.

7.3.5 Chimeric reaggregated ovaries using human and murine ovarian tissue

7.3.5.1 Chimeric reaggregated ovaries using fresh human medulla

The collected medulla was manually dissected using No. 24 scalpels (Swann-Morton Ltd.) as described previously (Section 6.3.4) in the L-15 collection media. The dissected medulla was transferred to a dish of DPBS/BSA using 1000 µl wide bore pipette tips (Starlabs), washed twice in DPBS/BSA and digested in 0.05% Trypsin/EDTA (Section 2.3). After overnight culture, the germ cell suspension was filtered through a 100 µm cell strainer (Falcon, Fisher Scientific) and cultured for a further 6 h for the second separation.

To generate a chimeric human-mouse RO (HuMoRO), the resultant human 'germ cell' population was reaggregated with neonatal (P0-P7) mouse somatic cells, and cultured for 7 d.

7.3.5.1.1 Red blood cell removal using a haemolytic buffer

Since many red blood cells (RBCs) were present in the germ cell suspension from the medulla, the use of a haemolytic buffer to reduce the number of red blood cells present was tested. The 10X haemolytic stock buffer (pH 7.25) was prepared containing 3.1M NH_4Cl (Sigma), 0.23M Na_2HCO_3 (Sigma) and 0.002M Na_2EDTA (Sigma) dissolved in deionised water. Prior to its use, it was diluted in deionised water to produce a 1X haemolytic buffer, and sterile filtered. The germ cell suspension after the second separation was split into three groups: Control, 1.5 min lysis and 3 min lysis.

The medulla was transferred using blunt forceps from the L-15 collection media to a Petri dish containing fresh L-15 media and dissected prior to washing in DPBS/BSA. Each cell suspension was centrifuged in 15 ml centrifuge tubes at 663 x *g* to pellet the cells. After the supernatant was removed, 4.5 ml of 1X haemolysis buffer was added to resuspend the cells in the two lysis groups, and the centrifuge tubes were repeatedly inverted for 1.5 min or 3 min. The Control cells only had 4.5 ml M199/FBS added to resuspend the cells. After exposure to the haemolysis buffer, 10.5 ml of M199/FBS was added to each tube and inverted continuously for approximately 15 sec before they were centrifuged at 500 x *g* for 5 min. The

supernatant was then removed, and the remaining cells resuspended in 200 µl of M199/FBS. Cell survival was assessed using Trypan Blue (Sigma).

7.3.5.2 Chimeric reaggregated ovaries using cryopreserved human cortexes

The remaining 0 h and 24 h cortical strips were weighed prior to digestion. To aid the enzymatic digestion of human cortical strips, the strips were cut into 250 µm pieces using a tissue chopper (McIlwain Tissue Chopper; The Mickle Laboratory Engineering Co. Ltd., Surrey, UK). The chopped cortical strips were washed twice in PBS/BSA, and digested in 0.05% Trypsin/EDTA (Section 2.3). To enhance human somatic cell adhesion to the tissue culture treated Petri dishes, the Petri dishes were pre-coated with 150 µg/ml Cultrex basement membrane extract (Cultrex RGF BME Type 2, PathClear; AMS Biotechnology Europe Ltd., Abingdon, UK). After overnight culture, the germ cell suspension was filtered through a 100 µm cell strainer (Falcon, Fisher Scientific) and cultured for a further 6 h for the second separation.

The resultant human 'germ cell' suspension was aggregated with P0-P7 *LacZ*$^{+}$-expressing somatic cells to form chimeric HuMoROs to differentiate human and mouse cells, and cultured for 7 d (Section 2.4). Cortical strips which were immediately digested post-thawing to form the HuMoROs are referred to as '0 h HuMoROs', while those which were cultured for 24 h prior to HuMoRO formation are referred to as '24 h HuMoROs'. Mouse ROs containing *LacZ*$^{+}$-expressing germ cells and *LacZ*$^{-}$-expressing somatic cells (MoROs) were cultured for 7 d as a

Control. The MoROs which were generated as matched Controls to the 0 h HuMoROs and 24 h HuMoROs were referred to as 0 h MoROs and 24 MoROs, respectively. All tissues were fixed in 10% formalin, embedded, sectioned at 5 µm and stained as described in Section 2.6. Oocyte diameter was calculated from oocyte area, which was analysed using ImageJ software (292).

7.3.6 Statistical analysis

Analysis was performed using Prism 7 (GraphPad). Data was tested for normal distribution using the D'Agostino & Pearson normality test. Analysis of cell numbers was performed using Welch's t-test, while analysis of oocyte diameter and oocyte diameter per GC was performed using ordinary one-way ANOVA. Results are presented as mean ± SD, with $P \leq 0.05$ considered significant.

7.4 Results

7.4.1 Generation of human-mouse chimeric reaggregated ovaries using fresh ovarian medulla

During the tissue processing required for cortical strip cryopreservation, the ovarian medulla is excised and discarded. Since we are limited to 10 cortical strips for research per patient (if the patient has over 50 cortical strips cryopreserved), it was decided that a preliminary study to generate HuMoROs would involve the use of the medulla.

Digestion and plating of the medulla revealed poor somatic cell adhesion to tissue culture treated plasticware, similarly to the bovine somatic cells observed in Chapter 5. However, the ‘germ cell’ suspension contained many RBCs, rendering it difficult to assess the true germ cell number. The HuMoROs (n=2) generated were cultured for 7d. However, by 4 d of culture the HuMoROs were still depositing red debris which appeared to be RBCs (arrows; Figure Figure 7.1A). After 7 d of culture, the HuMoROs retained a red tint, indicating the inclusion of RBCs within the tissue (Figure 7.1B). No follicles were observed within the HuMoROs generated from human medulla (Figure 7.1C), but many RBCs were found incorporated within the HuMoROs (Figure 7.1D).

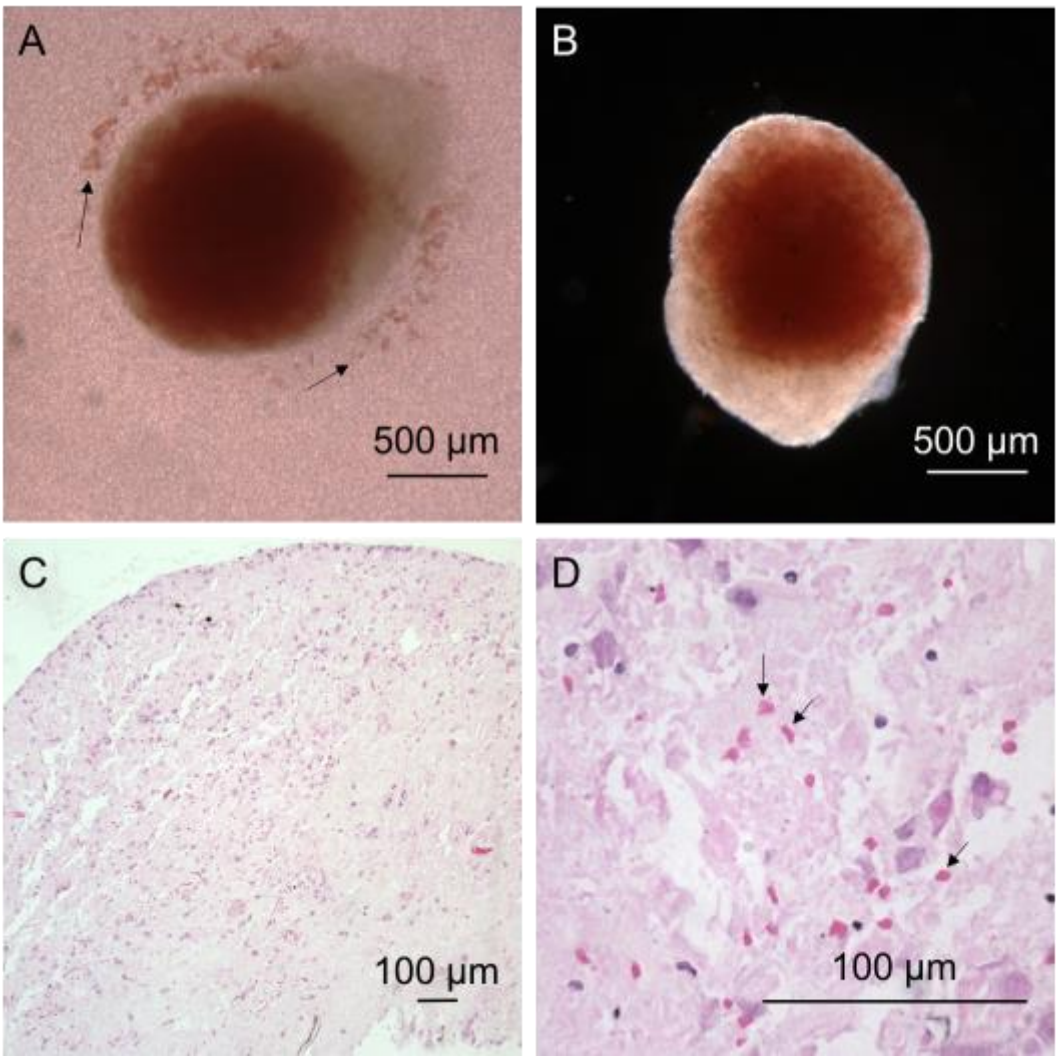


Figure 7.1 Chimeric human-mouse reaggregated ovaries generated from human medulla.

(A) Representative image of a chimeric human-mouse reaggregated ovary (HuMoRO) generated from fresh human medulla and neonatal (P0-P7) somatic cells, after 4 d of culture. Arrows are pointing at red debris, potentially RBCs, deposited by the HuMoRO. (B) Representative image of a HuMoRO after 7 d of culture. (C) A representative section of a HuMoRO after 7 d of culture, and (D) a higher magnification of the section, with arrows pointing out the red blood cells within the HuMoRO. Experiments were performed with n=2.

7.4.2 Haemolytic removal of red blood cells from the medulla cell suspension

As the RBCs were obscuring the true number of germ cells and somatic cells within the ‘germ cell’ suspension, a haemolytic buffer was tested to remove the RBCs from the ‘germ cell’ suspension prior to reaggregation (n=1). The germ cell suspension derived from one medulla suspension was split into three groups: Control, 1.5 min and 3 min exposure to the haemolytic buffer.

However, upon collection of the medulla from the OCTB, the L-15 collection media appeared to have lots of red cells in suspension, and so the medulla was transferred to a fresh dish of L-15 media prior to dissection. However, it appeared the transfer of the medulla removed a significant portion of the RBCs present, as fewer RBCs were observed. The cell counts (non-RBC) for the single experiment are in Table 7.4. The exposure of the ‘germ cell’ suspension to the haemolytic buffer resulted in a massive increase in dead cells (Table 7.4). These results indicated there was no point in continuing to use the medulla for the generation of HuMoROs.

Table 7.4 Cell numbers from a medulla 'germ cell' suspension exposed to haemolytic buffer for differing periods.

	Control		1.5 min		3 min	
Live cells	150,100	71.2%	24,700	68.4%	3,800	12.5%
Dead cells	60,800	28.8%	11,400	31.6%	26,600	87.5%
Total cell number	210,900	100.0%	36,100	100.0%	30,400	100.0%

7.4.3 Number of germ and somatic cells from digested cortical strips

Due to the high number of RBCs present and the deleterious effect of haemolytic buffer use on ovarian cells, as well as the lack of follicles present in the cultured HuMoROs (n=2), the work progressed to the use of the cortical strips. The number of cells in the germ cell suspension and adherent somatic cells from the digested human cortical strips was assessed prior to the formation of the chimeric HuMoROs using cryopreserved cortical strips. In both 0 h (Figure 7.2A) and 24 h (Figure 7.2B) human cortical pieces collected prior to digestion, primordial follicles with squamous pre-GCs were observed. The number of cells isolated were normalised to the weight of the cortical strips prior to digestion, and were assessed using Trypan Blue.

The number of live cells in the germ cell suspension and the adhered somatic pool per gram of cortical strip were similar between 0 h and 24 h cortical strips (Figure 7.2C). The number of dead Trypan blue-positive cells in the germ cell suspension were also similar between the 0 h and 24 h cortical strips, but no dead somatic cells were found from 0 h cortical strips (Figure 7.2D). Since poor human

somatic cell adhesion was observed after the medulla was digested, Petri dishes were pre-coated with ECM to encourage somatic cell adhesion. However, fewer human somatic cells in total were adhered to the ECM-coated dishes than expected, compared to the number of adhered somatic cells from 4 P0-P7 neonatal mice which were digested at the same time for HuMoRO and MoRO generation (Figure 7.2E).

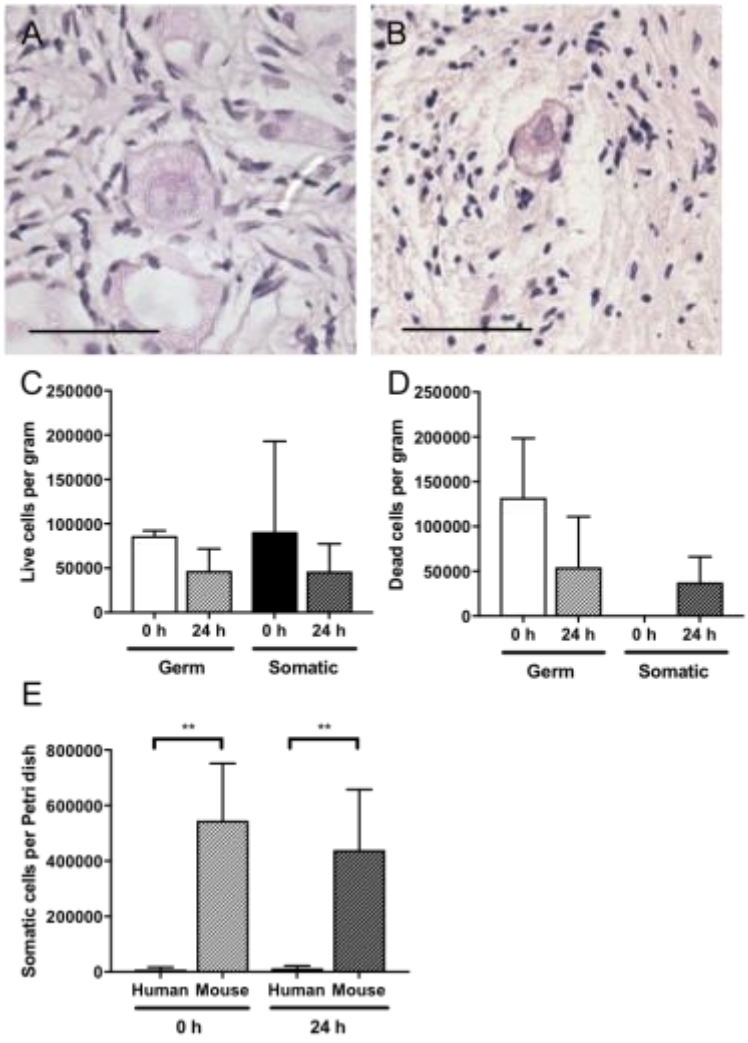


Figure 7.2 Cells from 0 h and 24 h human cortical strips

Representative images of a human primordial follicle from (A) 0 h cortical strips and (B) 24 h cortical strips. The number of (C) live and (D) dead cells in the germ cell suspension and adhered somatic population were normalised to the weight (gram) of 0 h or 24 h cortical strips and assessed. (E) The total number of adhered somatic cells (including live and dead cells) per Petri dish from 0 h cortical strips and neonatal (P0-P7) mouse ovaries from four mice; and 24 h cortical strips and the neonatal ovaries. Scale bar: 50 µm. Data are plotted as mean values ± SD 0 h human cortical strip digests n=3, 24 h human cortical

strip digests n=3; 0 h mouse ovarian digests n=3; 24 h mouse ovarian digests n=3. **$P \leq 0.01$.

7.4.4 Follicle development in chimeric human-mouse reaggregated ovaries (HuMoROs) generated from cortical strips

The human germ cell suspension was reaggregated with *LacZ*$^{+}$-expressing mouse somatic cells into a HuMoRO to differentiate human cells from mouse cells, the latter of which were stained with a blue precipitate after exposing the HuMoRO to X-gal. Experiments were repeated in triplicate, with MoROs cultured alongside (0 h HuMoROs n=3; 0 h MoROs n=3; 24 h HuMoROs n=3; 24 h MoROs n=3). The MoROs (containing *LacZ*$^{+}$ germ cells and *LacZ*$^{-}$ somatic cells) were cultured for 7 d and demonstrated clear separation of the germ and somatic cells. After 7 d of culture, the HuMoROs developed primary follicles containing *LacZ*$^{+}$ blue oocytes (Figure 7.3A, B), as well as some containing non-blue oocytes *LacZ*$^{-}$ (Figure 7.3C, D).

However, due to varying shades of blue precipitate observed within an oocyte (Figure 7.3E-H), every single section was analysed to establish whether an oocyte was blue and whether the blue *LacZ*$^{+}$ oocytes within the HuMoROs were mouse oocytes or human oocytes. The HuMoROs also contained patches of non-blue somatic cells, which were morphologically similar to luteinised cells.

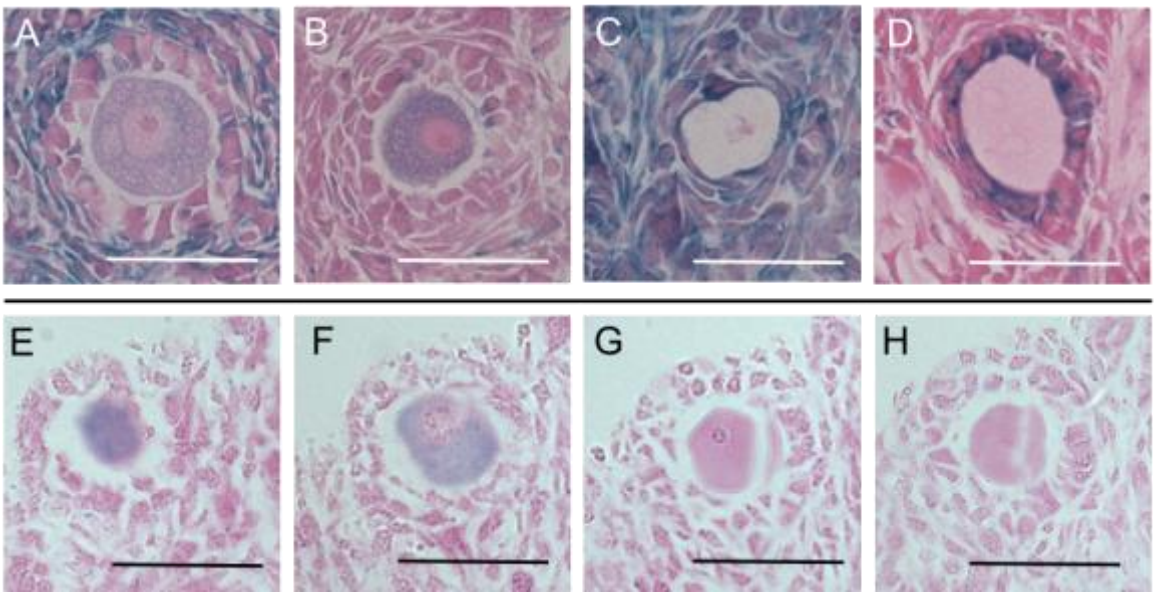


Figure 7.3 Follicles exposed to X-gal in human-mouse chimeric reaggregated ovaries and mouse reaggregated ovaries.

Representative images of follicles exposed to X-gal and counterstained with eosin. (A, B) Images of follicles with blue-stained oocytes (i.e. *LacZ*$^{+}$) and (C, D) non-blue stained oocytes (i.e. *LacZ*$^{-}$) in human-mouse chimeric reaggregated ovaries (HuMoROs). (E, F, G, H) Representative images of the variable X-gal staining (blue) within the same oocyte in sequential sections in a mouse reaggregated ovary (MoRO). Scale bar: 50 µm.

Since human oocytes are larger, oocyte diameters were normalised to GC number from blue oocytes in HuMoROs were compared to those from MoROs to determine whether they were human or mouse derived. All blue oocytes within the HuMOROs were analysed (0h HROs n=31; 24h HROs n=9). Due to the large number of follicles which had developed within the MoROs, only oocytes with a clear nucleus in each 5th section were analysed. For an accurate comparison, only

primary follicles containing 17 to 49 GCs (the minimum and maximum number of GCs in primary follicles in HuMoROs) were analysed.

No differences in oocyte diameter normalised to GC number were observed, when comparing the blue oocytes in 0 h HuMoROs and MoROs, as well as 24 h HuMoROs and MoROs (Figure 7.4A). Even when the 0 h and 24 h groups were combined for analysis, the oocyte diameter per GC was still comparable between oocytes in HuMoROs and MoROs, (Figure 7.4B).

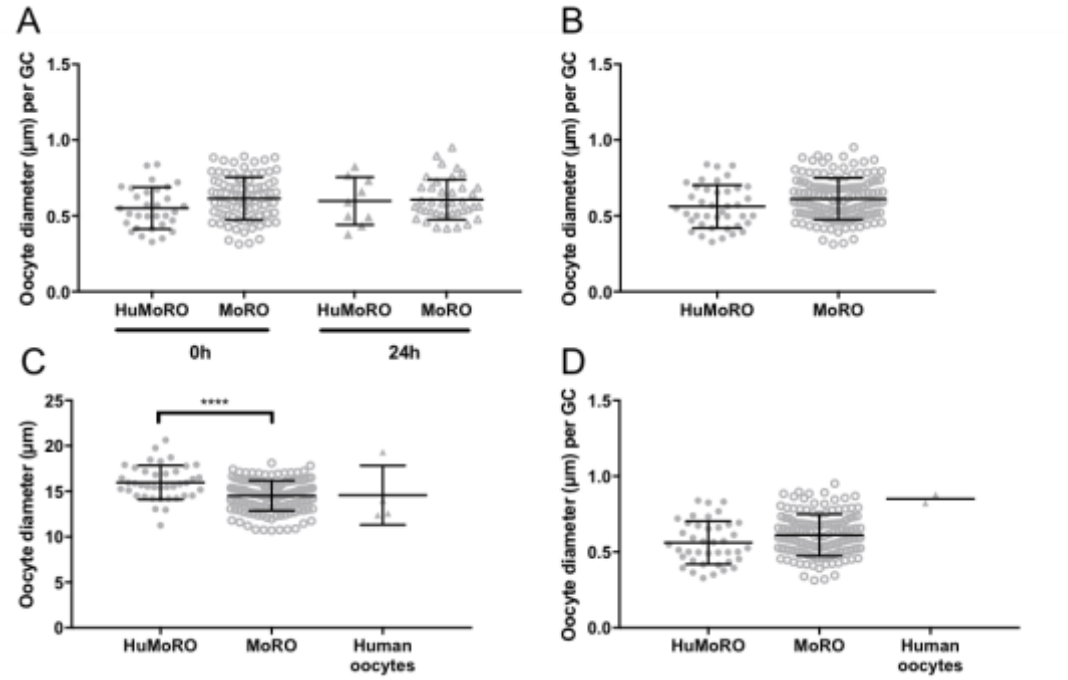


Figure 7.4 Oocyte diameters of follicles in human-mouse chimeric reaggregated oocytes and mouse reaggregated ovaries.

(A) Oocyte diameter normalised to GC number in primary follicles (17-49 GCs) was assessed for all blue-stained oocytes (i.e. *LacZ*$^{+}$) in 0 h human-mouse chimeric reaggreagated ovaries (HuMoROs) and the 0 h Control mouse reaggregated ovaries (MoRO), 24 h HuMoROs and 24 h MoROs. (B) Oocyte diameter normalised to GC number was assessed in *LacZ*$^{+}$ oocytes the grouped HuMoROs and MoROs (0 h and 24 h). (C) Oocyte diameters of non-blue stained 'human' oocytes (i.e. *LacZ*$^{-}$) in HuMoROs were compared to blue-stained oocytes in HuMoROs and MoROs. (D) Oocyte diameters of 'human' oocytes normalised to GC numbers were analysed and plotted alongside data from blue-stained oocytes in HuMoROs and MoROs. Data are plotted as mean values ± SD Blue *LacZ*$^{+}$ oocytes analysed in 0 h HuMoROs n=31, 0 h MoROs n=107; 24 h HuMoROs n=9; 24 h MoROs n=42. 'Human' oocytes analysed in 0 h HuMoROs n=2; 24 h HuMoROs n=2. ****P<0.0001.

Only four non-blue *LacZ*$^{-}$ oocytes were observed; two oocytes in one 0 h HuMoRO, and one from each 24 h HuMoRO. As human oocytes should not express *LacZ*, no blue precipitate should be formed upon exposure to X-gal; these were therefore referred to as 'human oocytes'. Although the nuclei were not clear for all the oocytes, the largest oocyte diameter was measured by selecting the section with the largest oocyte visible. Analysis revealed similar oocyte diameters between the human oocytes and the blue oocytes within HuMoROs and MoROs, but significantly larger oocyte diameter in HuMoROs than MoROs (Figure 7.4C). The pattern of larger oocytes in HuMoROs was not present when the oocyte diameters are normalised to GCs (Figure 7.4B, D). Only two human oocytes were clearly associated with GCs (Figure 7.4C); the data points were plotted as a reference, as there was not enough data for analysis (Figure 7.4D). Follicle counts of the collected cortical strips were unnecessary, since there were so few potential human oocytes in the HuMoROs, there was nothing to compare follicle development to.

7.5 Discussion

Ovaries from patients with GCTs and POI may not support follicle development to produce a fertilisable oocyte due to an abnormal environment within the tissue. By providing an alternative somatic cell source to their germ cells, follicle development may resume within the resultant ROs. The RO technique has been shown to rescue follicle development in a mouse model of POI by replacing the somatic cells with a new source; we therefore hypothesised that the RO technique could be adapted for use with human tissue. Since previous chimeric ROs supported follicle development using mouse cells as a somatic source, we also

hypothesised that mouse somatic cells would support follicle development when reaggregated with human germ cells.

Prior to the use of the valuable cortical strips, the first HuMoROs generated used human cells digested from the medulla. The medulla is a highly vascularised portion of the ovary (388,389), and also contains some primordial follicles (390), but is discarded as a by-product of cortical strip cryopreservation. Due to the high vascularity of the medulla, the initial HuMoROs generated contained many RBCs, and depositing them during the 7 d of culture. A second experiment to test whether exposure of the 'germ cell' suspension to a haemolytic buffer revealed that the initial transfer of the tissue considerably reduced the number of RBCs observed. However, the exposure of the cells to the haemolytic buffer for 1.5 min and 3 min appeared to reduce germ or somatic cell survival. Although the medulla was useful for preliminary experiments, the tissue of interest for future fertility preservation is the cortex. The ovarian cortex also has less vascularisation (391), and therefore we turned our attention to cortical tissue.

Subsequent experiments involved the reaggregation of cells from cryopreserved cortical strips and neonatal mouse *LacZ*$^{+}$ somatic cells. After 7 d of culture, more *LacZ*$^{+}$ blue oocytes were present within the HuMoROs compared to *LacZ*$^{-}$ non-blue oocytes. Since it has been shown that transzonal processes facilitate RNA transfer between the oocyte and its surrounding cumulus cells (392), the β-galactosidase mRNA may have transferred from mouse *LacZ*$^{+}$ GCs to the human oocytes, resulting in the synthesis of β-galactosidase and production of blue

precipitate in human oocytes. However, this has previously not been observed in our mouse ROs. To determine whether the *LacZ*$^{+}$ oocytes were of human or mouse origin, the diameters of the blue oocytes from primary follicles within the HuMoROs were compared to the blue oocytes within the MoROs, since human oocytes are larger than mouse oocytes at the primordial (mouse = 12.6 µm, human = 36 µm) and primary follicle stages (mouse = 28.8 µm, human = 42.1µm) (145). Our results indicate the blue oocytes within the HuMoROs are mouse-derived, as the maximum oocyte diameter measured was only 20.64 µm. Interestingly, no *LacZ*$^{-}$ oocytes were observed in the MoROs, with all follicles containing *LacZ*$^{+}$ oocytes, indicating a clean separation of the *LacZ*$^{-}$ somatic cells from the germ cells. Although not a direct comparison, this demonstrates that the RO technique does cleanly separate the germ and somatic cells, and therefore the *LacZ*$^{+}$ oocytes should have come from the *LacZ*$^{+}$ somatic cell pool within the HuMoROs. To determine whether the *LacZ*$^{+}$ oocytes in the HuMoROs arise from contaminating oocytes, or even oocyte-like stem cells (reviewed by Yazdekhasti et al. 2016 (393)), further analysis of the somatic cell population is needed.

Only four *LacZ*$^{-}$ non-blue oocytes developed within the HuMoROs, despite reaggregation with all the ‘germ cell’ suspension with *LacZ*$^{+}$ mouse somatic cells. Although the plates were coated with ECM, human somatic cell adhesion was still poor compared to the number of adhered mouse neonatal somatic cells. This meant that the somatic cells remained in the germ cell suspension, and were therefore reaggregated with the *LacZ*$^{+}$ mouse somatic cells to form the HuMoROs. This addition of human somatic cells may have inhibited the formation of follicles

containing human oocytes, or potentially even promoted the development of follicles containing mouse *LacZ*$^{+}$ oocytes.

These experiments have revealed the need for further optimisation for HuMoRO generation, and to determine whether the mouse somatic cells inhibit follicle development with human oocytes. A clearer method to identify human cells is required; such as immunohistochemistry using antibodies specific for human nuclear antigen to determine whether the oocytes within follicles are human or mouse, and to investigate the fate of the non-adherent human somatic cells within the HuMoRO structure. In addition, it would be useful to confirm the source of the clusters of cells with a luteinised appearance.

In summary, without clean separation of human germ and somatic cells, the human germ cells in an RO will still be exposed to the somatic cells from the premature ovarian insufficiency and granulosa cell tumour patients. In order for the RO technique to become useful for GCT and POI patients, the human somatic cells should be completely separated from the patients' germ cells, so they can be reaggregated with alternative somatic cells which can support follicle development. Further work on optimising the RO technique for human tissue must focus on improving somatic cell adhesion, or investigate other methods to effectively separate the patients' germ cells from their somatic cells.

Chapter 8: Conclusions

The overall aims of this thesis were to assess follicle development in cultured ROs and to transfer the RO technique from using mouse ovarian tissue to human ovarian tissue. Although the initial methods to develop follicles within the RO involved transplantation into the kidney capsule of immunocompromised mice (226), we have demonstrated that follicle development progresses to the preantral stage in cultured ROs. Interestingly, ROs generated from P6 ovaries had comparable follicle development to *in vitro* P2 ovaries even though P6 ovaries are more developed. Consequently, further work was performed with P6 neonatal ovaries as this allowed for easier dissection and more time for planning experiments.

Despite requiring eight neonatal mouse ovaries to generate one RO, the total number of growing follicles within the single RO cultured for 14 d was fewer than in a single age-matched *in vivo* ovary. This result highlights the large cell loss that occurs during RO generation that will need to be reduced when developing the technique for human ovarian tissue. The number of developing follicles within the RO structure is not only fewer than the *in vivo* ovary, but the follicles present also have morphological differences: fewer TCs and GCs, incomplete BL and smaller oocytes, which is consistent with previous observations regarding follicle development in cultured ovaries (159,293).

Poor TC development associated with follicles from cultured ROs can potentially affect the next step in follicle development *in vitro*, as the success of isolated preantral follicle culture has been linked to theca-stroma cell association

with follicles (207). While secondary follicle TC numbers can be improved by supplementation with mouse serum in ovary culture, they were still significantly lower than the 'normal' TC number from *in vivo* ovaries. Disappointingly, hyaluronan hydrogels did not support follicle development or TC development. Since an 'adequate' number of TCs required for successful follicle culture has not been quantified and follicle culture was not performed in this thesis, improvement of TC development in culture was not pursued. However, this may be relevant for future work if follicle survival is poor after isolation from cultured ROs for follicle culture.

After competent dissection and digestion of cortical strips using bovine ovarian tissue, we generated chimeric human-mouse reaggregated ovaries (HuMoROs) by aggregating the human 'germ cell' suspension with mouse *LacZ*$^{+}$ somatic cells. To improve the poor bovine and human somatic adhesion to tissue culture treated plasticware, Petri dishes were coated to ECM prior to the digestion of human cortical strips. Despite the addition of ECM, human somatic cells still adhered poorly to the Petri dishes compared to mouse somatic cells.

Aside from improving the culture surface for human somatic cell adhesion, the method of tissue dissociation may also need to be investigated. Trypsinisation of bovine and human ovarian tissue may result in the cleavage of collagen, fibronectin and laminin which initiate attachment to substrates (i.e. the tissue culture treated plasticware or the ECM) (394). The 'recovery' of molecules associated with cell adhesion in bovine and human ovarian cells may be impaired, as proteomic analysis of human cancer cell lines exposed to trypsin have revealed the

downregulation of proteins regulating cell metabolism, cell growth and cell adhesion, while apoptosis-related proteins are upregulated (297). Alternatively, the M199/FBS media used routinely for mouse studies may be suboptimal for bovine and human ovarian cell culture, resulting in stressed cells which adhere poorly to the substrates (394). Without adhesion and therefore complete removal of somatic cells from the germ cell population, follicle development may be affected within ROs when using ovarian tissue from patients with dysfunctional follicle development (e.g. POI and granulosa cell tumours); clearly further optimisation is required.

Although the human somatic cells were not separated from the germ cells, some potential human oocytes, based on the absence of X-gal staining, were found in the cultured HuMoROs. However, these HuMoROs contained many X-gal positive oocytes which was surprising since all controls indicated that there should be no mouse oocytes present. Therefore, further work is required to confirm the source of these oocytes. Since the number of potential human oocytes was so low, there was no point relating the number of oocytes found in the cortical strips to the number found in the HuMoROs. Nevertheless, the fate of the human germ cells added to the HuMoROs is unclear, particularly since the cortical strips were rich in primordial follicles. This massive cell loss could partially be attributed to the cell loss observed during mouse RO generation. However, suboptimal media may have also affected human cell survival during the generation and culture of the HuMoROs, as the media used was based on murine RO generation and culture. Though only four potential human oocytes were observed in the cultured HuMoROs, these initial steps to transfer the RO technique for human tissues have indicated its potential as a fertility treatment.

Further considerations exist to translate the RO technique for clinical use, including assessing an alternate source of human somatic cells for human RO generation for POI and granulosa cell tumour patients. Despite the potential of using iPSCs as a potential somatic cell source, since they can be patient-derived, iPSCs derived from a POI patients and differentiated into GCs appear to have differential and reduced expression of GC-associated genes such as AMH, AMHR2 and CYP19A1 when compared to control iPSCs and ES cells (395). This demonstrates that these iPSC-derived GCs they may already have compromised cell function and affect follicle development, reflecting the patient's POI phenotype. In addition to being functional, the somatic cells used must also fulfil the good manufacturing practice (GMP) criteria for clinical use if the RO technique is to be used for fertility treatment.

Aside from its clinical applications, the RO technique may also allow us to examine how follicle formation occurs over time. Since the RO, prior to transplantation or culture, is a heterogeneous mixture of germ and somatic cells, we hypothesise there are three methods by which follicle formation occurs: i) that the somatic cells surrounding the oocytes are dedifferentiated or transdifferentiated into cells belonging to that niche, ii) the differentiated cells (e.g. GCs) migrate through the RO to reassemble follicles based on their differentiated phenotype, or iii) a mixture of both mechanisms. To investigate how the follicles reform within the RO, cell lineage tracing can be used. For example, using a marker which only activates permanently once a cell-specific gene is activated, such as the red fluorescence-based reporter of theca-specific *Gli1* used by Liu et al. 2015 (315), the fate of the cells can be assessed. If murine TCs expressing this *Gli1* reporter are

incorporated within an RO, the eventual location of the red fluorescence within the RO will reveal the mechanism of follicle formation. If GCs are fluorescing red, the oocyte will have reprogrammed the TCs; however, if the TC layer contain all the fluorescent cells, the TCs may have migrated to their original niches and/or those in other niches will have died. Additional analyses will be required to validate the final function of these murine fluorescent cells before a definitive answer can be reached. Any mechanisms elucidated from this may help improve TC development in cultured human tissue, and enable improved follicle development *in vitro*.

In summary, this thesis explores follicle development *in vitro* using the RO technique, both as a method to assess follicle development in real time and as a potential fertility treatment. Neonatal mouse RO culture developed follicles up to the preantral stage, fulfilling the first step in two-step culture (ovary culture and follicle culture). However, the adaptation of the RO technique human cortical tissue has revealed the need for further optimisation in order for follicle development within the chimeric tissue.

References

1. Hirshfield AN. Development of Follicles in the Mammalian Ovary. Elsevier; 1991. pp. 43–101. (International Review of Cytology; vol. 124).

2. McGee EA, Hsueh AJ. Initial and cyclic recruitment of ovarian follicles. Endocrine Reviews. 2000 Apr;21(2):200–14.

3. Smitz JEJ, Cortvrindt RG. The earliest stages of folliculogenesis in vitro. Reproduction. 2002 Feb;123(2):185–202.

4. Edson MA, Nagaraja AK, Matzuk MM. The mammalian ovary from genesis to revelation. Endocrine Reviews. Endocrine Society; 2009 Oct;30(6):624–712.

5. Gondos B, Westergaard L, Byskov AG. Initiation of oogenesis in the human fetal ovary: ultrastructural and squash preparation study. Am J Obstet Gynecol. 1986 Jul;155(1):189–95.

6. McLaren A. Meiosis and differentiation of mouse germ cells. Symp Soc Exp Biol. 1984;38:7–23.

7. Ohkubo Y, Shirayoshi Y, Nakatsuji N. Autonomous regulation of proliferation and growth arrest in mouse primordial germ cells studied by mixed and clonal cultures. Exp Cell Res. 1996 Feb 1;222(2):291–7.

8. McLaren A, Southee D. Entry of mouse embryonic germ cells into meiosis. Developmental Biology. 1997 Jul 1;187(1):107–13.

9. Byskov AG. Differentiation of mammalian embryonic gonad. Physiological Reviews. 1986 Jan;66(1):71–117.

10. Salha O, Abusheikha N, Sharma V, Abusheika N. Dynamics of human follicular growth and in-vitro oocyte maturation. Hum Reprod Update. 1998 Nov;4(6):816–32.

11. Gondos B, Zamboni L. Ovarian development: the functional importance of germ cell interconnections. Fertil Steril. 1969 Jan;20(1):176–89.

12. Pepling ME, Spradling AC. Female mouse germ cells form synchronously dividing cysts. Development. 1998 Sep;125(17):3323–8.

13. Motta PM, Makabe S, Nottola SA. The ultrastructure of human reproduction. I. The natural history of the female germ cell: origin, migration and differentiation inside the developing ovary. Hum Reprod Update. 1997 May;3(3):281–95.

14. Pepling ME, Spradling AC. Mouse ovarian germ cell cysts undergo programmed breakdown to form primordial follicles. Developmental

Biology. Academic Press; 2001 Jun 15;234(2):339–51.

15. Chen Y, Jefferson WN, Newbold RR, Padilla-Banks E, Pepling ME. Estradiol, progesterone, and genistein inhibit oocyte nest breakdown and primordial follicle assembly in the neonatal mouse ovary in vitro and in vivo. Endocrinology. Endocrine Society; 2007 Aug;148(8):3580–90.

16. Maheshwari A, Fowler PA. Primordial follicular assembly in humans--revisited. Zygote. Cambridge University Press; 2008 Nov;16(4):285–96.

17. Bristol-Gould SK, Kreeger PK, Selkirk CG, Kilen SM, Cook RW, Kipp JL, et al. Postnatal regulation of germ cells by activin: the establishment of the initial follicle pool. Developmental Biology. 2006 Oct 1;298(1):132–48.

18. Tingen C, Kim A, Woodruff TK. The primordial pool of follicles and nest breakdown in mammalian ovaries. Mol Hum Reprod. Oxford University Press; 2009 Dec;15(12):795–803.

19. Byskov AG, Guoliang X, Andersen CY. The cortex-medulla oocyte growth pattern is organized during fetal life: an in-vitro study of the mouse ovary. Mol Hum Reprod. 1997 Sep;3(9):795–800.

20. Woodruff TK, Shea LD. A new hypothesis regarding ovarian follicle development: ovarian rigidity as a regulator of selection and health. J Assist Reprod Genet. Springer US; 2011 Jan;28(1):3–6.

21. Peters H. The development of the mouse ovary from birth to maturity. Acta Endocrinol. 1969 Sep;62(1):98–116.

22. Qvist R, Blackwell LF, Bourne H, Brown JB. Development of mouse ovarian follicles from primary to preovulatory stages in vitro. J Reprod Fertil. 1990 May;89(1):169–80.

23. Lintern-Moore S, Moore GPM. The Initiation of Follicle and Oocyte Growth in the Mouse Ovary. Biol Reprod. Biology of Reproduction; 1979 May 1;20(4):773–8.

24. Picton HM. Activation of follicle development: the primordial follicle. Theriogenology. Elsevier; 2001 Apr 1;55(6):1193–210.

25. Hutt KJ, Albertini DF. An oocentric view of folliculogenesis and embryogenesis. Reprod Biomed Online. 2007 Jun;14(6):758–64.

26. Young JM, McNeilly AS. Theca: the forgotten cell of the ovarian follicle. Reproduction. Society for Reproduction and Fertility; 2010 Oct;140(4):489–504.

27. Philpott CC, Ringuette MJ, Dean J. Oocyte-specific expression and developmental regulation of ZP3, the sperm receptor of the mouse zona pellucida. Developmental Biology. 1987 Jun;121(2):568–75.

28. Kumar TR, Wang Y, Lu N, Matzuk MM. Follicle stimulating hormone is

required for ovarian follicle maturation but not male fertility. Nat Genet. Nature Publishing Group; 1997 Feb;15(2):201–4.

29. Dierich A, Sairam MR, Monaco L, Fimia GM, Gansmuller A, LeMeur M, et al. Impairing follicle-stimulating hormone (FSH) signaling in vivo: targeted disruption of the FSH receptor leads to aberrant gametogenesis and hormonal imbalance. PNAS. National Academy of Sciences; 1998 Nov 10;95(23):13612–7.

30. Abel MH, Wootton AN, Wilkins V, Huhtaniemi I, Knight PG, Charlton HM. The effect of a null mutation in the follicle-stimulating hormone receptor gene on mouse reproduction. Endocrinology. 2000 May;141(5):1795–803.

31. Smith SS, Ojeda SR. Neonatal release of gonadotropins is essential for development of ovarian follicle-stimulating hormone receptors. Biol Reprod. 1986 Feb;34(1):219–27.

32. Shalgi R, Kraicer PF, Soferman N. Gases and electrolytes of human follicular fluid. Reproduction. Society for Reproduction and Fertility; 1972 Mar 1;28(3):335–40.

33. Gosden RG, Hunter RH, Telfer E, Torrance C, Brown N. Physiological factors underlying the formation of ovarian follicular fluid. J Reprod Fertil. 1988 Mar;82(2):813–25.

34. Rodgers RJ, Irving-Rodgers HF. Formation of the ovarian follicular antrum and follicular fluid. Biol Reprod. 2010 Jun;82(6):1021–9.

35. Baerwald AR, Adams GP, Pierson RA. A new model for ovarian follicular development during the human menstrual cycle. Fertil Steril. 2003 Jul;80(1):116–22.

36. Zhuo L, Yoneda M, Zhao M, Yingsung W, Yoshida N, Kitagawa Y, et al. Defect in SHAP-hyaluronan complex causes severe female infertility. A study by inactivation of the bikunin gene in mice. J Biol Chem. American Society for Biochemistry and Molecular Biology; 2001 Mar 16;276(11):7693–6.

37. Diaz FJ, Wigglesworth K, Eppig JJ. Oocytes determine cumulus cell lineage in mouse ovarian follicles. J Cell Sci. The Company of Biologists Ltd; 2007 Apr 15;120(Pt 8):1330–40.

38. Chen L, Russell PT, Larsen WJ. Functional significance of cumulus expansion in the mouse: Roles for the preovulatory synthesis of hyaluronic acid within the cumulus mass. Mol Reprod Dev. Wiley Subscription Services, Inc., A Wiley Company; 1993 Jan;34(1):87–93.

39. Chen L, Zhang H, Powers RW, Russell PT, Larsen WJ. Covalent linkage between proteins of the inter-alpha-inhibitor family and hyaluronic acid is mediated by a factor produced by granulosa cells. J Biol Chem. 1996 Aug 9;271(32):19409–14.

40. Stocco C, Telleria C, Gibori G. The Molecular Control of Corpus Luteum Formation, Function, and Regression. Endocrine Reviews. 2007 Feb;28(1):117–49.

41. Devoto L, Fuentes A, Kohen P, Céspedes P, Palomino A, Pommer R, et al. The human corpus luteum: life cycle and function in natural cycles. Fertil Steril. Elsevier; 2009 Sep;92(3):1067–79.

42. Baker TG. A Quantitative and Cytological Study of Germ Cells in Human Ovaries. Proc R Soc Lond, B, Biol Sci. 1963 Oct 22;158:417–33.

43. Hsueh AJ, Billig H, Tsafriri A. Ovarian follicle atresia: a hormonally controlled apoptotic process. Endocrine Reviews. 1994 Dec;15(6):707–24.

44. Hirshfield AN, Midgley AR. Morphometric analysis of follicular development in the rat. Biol Reprod. 1978 Oct;19(3):597–605.

45. Richards JS, Fitzpatrick SL, Clemens JW, Morris JK, Alliston T, Sirois J. Ovarian cell differentiation: a cascade of multiple hormones, cellular signals, and regulated genes. Recent Prog Horm Res. 1995;50:223–54.

46. Drummond AE. The role of steroids in follicular growth. Reprod Biol Endocrinol. BioMed Central; 2006 Apr 10;4(1):16.

47. Elvin JA, Clark AT, Wang P, Wolfman NM, Matzuk MM. Paracrine actions of growth differentiation factor-9 in the mammalian ovary. Mol Endocrinol. 1999 Jun;13(6):1035–48.

48. Knight PG, Glister C. Potential local regulatory functions of inhibins, activins and follistatin in the ovary. Reproduction. 2001 Apr;121(4):503–12.

49. Shimasaki S, Moore RK, Otsuka F, Erickson GF. The bone morphogenetic protein system in mammalian reproduction. Endocrine Reviews. 2004 Feb;25(1):72–101.

50. Drummond AE. TGFbeta signalling in the development of ovarian function. Cell Tissue Res. 2005 Oct;322(1):107–15.

51. Knight PG, Glister C. TGF-beta superfamily members and ovarian follicle development. Reproduction. Society for Reproduction and Fertility; 2006 Aug;132(2):191–206.

52. Antunes JL, Carmel PW, Housepian EM, Ferin M. Luteinizing hormone-releasing hormone in human pituitary blood. Journal of Neurosurgery. 1978 Sep;49(3):382–6.

53. Levine JE, Ramirez VD. Luteinizing hormone-releasing hormone release during the rat estrous cycle and after ovariectomy, as estimated with push-pull cannulae. Endocrinology. 1982 Nov;111(5):1439–48.

54. Baba Y, Matsuo H, Schally AV. Structure of the porcine LH- and FSH-releasing hormone. II. Confirmation of the proposed structure by

conventional sequential analyses. Biochemical and Biophysical Research Communications. 1971 Jul;44(2):459–63.

55. Schally AV, Arimura A, Kastin AJ, Matsuo H, Baba Y, Redding TW, et al. Gonadotropin-releasing hormone: one polypeptide regulates secretion of luteinizing and follicle-stimulating hormones. Science. 1971 Sep 10;173(4001):1036–8.

56. Belchetz PE, Plant TM, Nakai Y, Keogh EJ, Knobil E. Hypophysial responses to continuous and intermittent delivery of hypopthalamic gonadotropin-releasing hormone. Science. 1978 Nov 10;202(4368):631–3.

57. Collins TJ, Parkening TA, Smith ER. Plasma and pituitary concentrations of LH, FSH and prolactin after injection of GnRH in aged female C57BL/6 mice. Neurobiol Aging. 1981;2(2):125–31.

58. Burns KH, Matzuk MM. Minireview: genetic models for the study of gonadotropin actions. Endocrinology. 2002 Aug;143(8):2823–35.

59. Baenziger JU, Green ED. Pituitary glycoprotein hormone oligosaccharides: structure, synthesis and function of the asparagine-linked oligosaccharides on lutropin, follitropin and thyrotropin. Biochim Biophys Acta. 1988 Jun 9;947(2):287–306.

60. Dorrington JH, Moon YS, Armstrong DT. Estradiol-17beta biosynthesis in cultured granulosa cells from hypophysectomized immature rats; stimulation by follicle-stimulating hormone. Endocrinology. 1975 Nov;97(5):1328–31.

61. Fortune JE, Armstrong DT. Androgen production by theca and granulosa isolated from proestrous rat follicles. Endocrinology. 1977 May;100(5):1341–7.

62. Brown JB. Pituitary control of ovarian function--concepts derived from gonadotrophin therapy. Aust N Z J Obstet Gynaecol. 1978 Feb;18(1):46–54.

63. Moon YS, Tsang BK, Simpson C, Armstrong DT. 17 beta-Estradiol biosynthesis in cultured granulosa and thecal cells of human ovarian follicles: stimulation by follicle-stimulating hormone. J Clin Endocrinol Metab. 1978 Aug;47(2):263–7.

64. Leung PC, Armstrong DT. Interactions of steroids and gonadotropins in the control of steroidogenesis in the ovarian follicle. Annu Rev Physiol. Annual Reviews 4139 El Camino Way, P.O. Box 10139, Palo Alto, CA 94303-0139, USA; 1980;42(1):71–82.

65. Hillier SG, De Zwart FA. Evidence that granulosa cell aromatase induction/activation by follicle-stimulating hormone is an androgen receptor-regulated process in-vitro. Endocrinology. 1981 Oct;109(4):1303–5.

66. Camp TA, Rahal JO, Mayo KE. Cellular localization and hormonal regulation of follicle-stimulating hormone and luteinizing hormone receptor messenger RNAs in the rat ovary. Mol Endocrinol. 1991 Oct;5(10):1405–17.

67. Erickson GF, Magoffin DA, Dyer CA, Hofeditz C. The ovarian androgen producing cells: a review of structure/function relationships. Endocrine Reviews. Endocrine Society; 1985;6(3):371–99.

68. Drummond AE, Findlay JK. The role of estrogen in folliculogenesis. Mol Cell Endocrinol. 1999 May;151(1-2):57–64.

69. Billig H, Furuta I, Hsueh AJ. Estrogens inhibit and androgens enhance ovarian granulosa cell apoptosis. Endocrinology. 1993 Nov;133(5):2204–12.

70. Richards JS. Maturation of ovarian follicles: actions and interactions of pituitary and ovarian hormones on follicular cell differentiation. Physiological Reviews. 1980 Jan;60(1):51–89.

71. Zhuang L-Z, Adashi EY, Hsueh AJW. Direct enhancement of gonadotropin-stimulated ovarian estrogen biosynthesis by estrogen and clomiphene citrate. Endocrinology. 1982 Jun;110(6):2219–21.

72. Wang XN, Greenwald GS. Synergistic effects of steroids with FSH on folliculogenesis, steroidogenesis and FSH- and hCG-receptors in hypophysectomized mice. J Reprod Fertil. 1993 Nov;99(2):403–13.

73. Green S, Walter P, Kumar V, Krust A, Bornert JM, Argos P, et al. Human oestrogen receptor cDNA: sequence, expression and homology to v-erb-A. Nature. Nature Publishing Group; 1986 Mar;320(6058):134–9.

74. Greene GL, Gilna P, Waterfield M, Baker A, Hort Y, Shine J. Sequence and expression of human estrogen receptor complementary DNA. Science. American Association for the Advancement of Science; 1986 Mar 7;231:1150–5.

75. Kuiper GG, Enmark E, Pelto-Huikko M, Nilsson S, Gustafsson JA. Cloning of a novel receptor expressed in rat prostate and ovary. PNAS. National Acad Sciences; 1996 Jun 11;93(12):5925–30.

76. Chu S, Fuller PJ. Identification of a splice variant of the rat estrogen receptor β gene. Mol Cell Endocrinol. 1997 Sep;132(1-2):195–9.

77. Petersen DN, Tkalcevic GT, Koza-Taylor PH, Turi TG, Brown TA. Identification of estrogen receptor beta2, a functional variant of estrogen receptor beta expressed in normal rat tissues. Endocrinology. 1998 Mar;139(3):1082–92.

78. Byers M, Kuiper GG, Gustafsson JA, Park-Sarge OK. Estrogen receptor-beta mRNA expression in rat ovary: down-regulation by gonadotropins. Mol Endocrinol. 1997 Feb;11(2):172–82.

79. Drummond AE, Baillie AJ, Findlay JK. Ovarian estrogen receptor α and β mRNA expression: impact of development and estrogen. Mol Cell Endocrinol. 1999 Mar;149(1-2):153–61.

80. Lubahn DB, Moyer JS, Golding TS, Couse JF, Korach KS, Smithies O. Alteration of reproductive function but not prenatal sexual development after insertional disruption of the mouse estrogen receptor gene. PNAS. National Academy of Sciences; 1993 Dec 1;90(23):11162–6.

81. Krege JH, Hodgin JB, Couse JF, Enmark E, Warner M, Mahler JF, et al. Generation and reproductive phenotypes of mice lacking estrogen receptor beta. PNAS. National Academy of Sciences; 1998 Dec 22;95(26):15677–82.

82. Schomberg DW, Couse JF, Mukherjee A, Lubahn DB, Sar M, Mayo KE, et al. Targeted disruption of the estrogen receptor-alpha gene in female mice: characterization of ovarian responses and phenotype in the adult. Endocrinology. 1999 Jun;140(6):2733–44.

83. Hegele-Hartung C, Siebel P, Peters O, Kosemund D, Müller G, Hillisch A, et al. Impact of isotype-selective estrogen receptor agonists on ovarian function. PNAS. 2004 Apr 6;101(14):5129–34.

84. Fisher CR, Graves KH, Parlow AF, Simpson ER. Characterization of mice deficient in aromatase (ArKO) because of targeted disruption of the cyp19 gene. PNAS. National Academy of Sciences; 1998 Jun 9;95(12):6965–70.

85. Britt KL, Drummond AE, Cox VA, Dyson M, Wreford NG, Jones ME, et al. An age-related ovarian phenotype in mice with targeted disruption of the Cyp 19 (aromatase) gene. Endocrinology. 2000 Jul;141(7):2614–23.

86. Britt K, Kerr J, O'Donnell L, Jones M, Drummond A. Defining the roles of sex steroid hormones in the control of differentiation in somatic cells of mammalian gonads. Proc USA Endocr Soc. Proc USA Endocr Soc; 2001.

87. Britt KL, Drummond AE, Dyson M, Wreford NG, Jones ME, Simpson ER, et al. The ovarian phenotype of the aromatase knockout (ArKO) mouse. J Steroid Biochem Mol Biol. 2001 Dec;79(1-5):181–5.

88. Britt KL, Saunders PK, McPherson SJ, Misso ML, Simpson ER, Findlay JK. Estrogen actions on follicle formation and early follicle development. Biol Reprod. 2004 Nov;71(5):1712–23.

89. Graham JD, Clarke CL. Physiological action of progesterone in target tissues. Endocrine Reviews. 1997 Aug;18(4):502–19.

90. Spelsberg TC, Steggles AW, Chytil F, O'Malley BW. Progesterone-binding components of chick oviduct. V. Exchange of progesterone-binding capacity from target to nontarget tissue chromatins. J Biol Chem. 1972 Mar 10;247(5):1368–74.

91. Kastner P, Krust A, Turcotte B, Stropp U, Tora L, Gronemeyer H, et al.

Two distinct estrogen-regulated promoters generate transcripts encoding the two functionally different human progesterone receptor forms A and B. The EMBO Journal. European Molecular Biology Organization; 1990 May;9(5):1603–14.

92. Conneely OM, Mulac-Jericevic B, DeMayo F, Lydon JP, O'Malley BW. Reproductive functions of progesterone receptors. Recent Prog Horm Res. 2002;57:339–55.

93. Conneely OM, Mulac-Jericevic B, Lydon JP. Progesterone-dependent regulation of female reproductive activity by two distinct progesterone receptor isoforms. Steroids. 2003 Nov;68(10-13):771–8.

94. Tung L, Mohamed MK, Hoeffler JP, Takimoto GS, Horwitz KB. Antagonist-occupied human progesterone B-receptors activate transcription without binding to progesterone response elements and are dominantly inhibited by A-receptors. Mol Endocrinol. 1993 Oct;7(10):1256–65.

95. Vegeto E, Shahbaz MM, Wen DX, Goldman ME, O'Malley BW, McDonnell DP. Human progesterone receptor A form is a cell- and promoter-specific repressor of human progesterone receptor B function. Mol Endocrinol. 1993 Oct;7(10):1244–55.

96. Mulac-Jericevic B, Mullinax RA, DeMayo FJ, Lydon JP, Conneely OM. Subgroup of reproductive functions of progesterone mediated by progesterone receptor-B isoform. Science. 2000 Sep 8;289(5485):1751–4.

97. Mulac-Jericevic B, Lydon JP, DeMayo FJ, Conneely OM. Defective mammary gland morphogenesis in mice lacking the progesterone receptor B isoform. PNAS. National Acad Sciences; 2003 Aug 19;100(17):9744–9.

98. Jia XC, Kessel B, Welsh TH, Hsueh AJ. Androgen inhibition of follicle-stimulating hormone-stimulated luteinizing hormone receptor formation in cultured rat granulosa cells. Endocrinology. 1985 Jul;117(1):13–22.

99. Nandedkar TD, Munshi SR. Effect of dihydrotestosterone on follicular development, ovulation and reproductive capacity of mice. J Reprod Fertil. 1981 May;62(1):21–4.

100. Hu Y-C, Wang P-H, Yeh S, Wang R-S, Xie C, Xu Q, et al. Subfertility and defective folliculogenesis in female mice lacking androgen receptor. PNAS. 2004 Aug 3;101(31):11209–14.

101. Vale W, Rivier J, Vaughan J, McClintock R, Corrigan A, Woo W, et al. Purification and characterization of an FSH releasing protein from porcine ovarian follicular fluid. Nature. Nature Publishing Group; 1986 Jun 19;321(6072):776–9.

102. Rabinovici J, Goldsmith PC, Roberts VJ, Vaughan J, Vale W, Jaffe RB. Localization and secretion of inhibin/activin subunits in the human and subhuman primate fetal gonads. J Clin Endocrinol Metab. 1991 Nov;73(5):1141–9.

103. McNatty KP, Fidler AE, Juengel JL, Quirke LD, Smith PR, Heath DA, et al. Growth and paracrine factors regulating follicular formation and cellular function. Mol Cell Endocrinol. 2000 May 25;163(1-2):11–20.

104. Pangas SA. Localization of the Activin Signal Transduction Components in Normal Human Ovarian Follicles: Implications for Autocrine and Paracrine Signaling in the Ovary. J Clin Endocrinol Metab. 2002 Jun 1;87(6):2644–57.

105. Drummond AE, Le MT, Ethier J-F, Dyson M, Findlay JK. Expression and localization of activin receptors, Smads, and beta glycan to the postnatal rat ovary. Endocrinology. 2002 Apr;143(4):1423–33.

106. Li R, Phillips DM, Mather JP. Activin promotes ovarian follicle development in vitro. Endocrinology. 1995 Mar;136(3):849–56.

107. Smitz J, Cortvrindt R, Hu Y, Vanderstichele H. Effects of recombinant activin A on in vitro culture of mouse preantral follicles. Mol Reprod Dev. Wiley Subscription Services, Inc., A Wiley Company; 1998 Jul;50(3):294–304.

108. Liu X, Andoh K, Abe Y, Kobayashi J, Yamada K, Mizunuma H, et al. A comparative study on transforming growth factor-beta and activin A for preantral follicles from adult, immature, and diethylstilbestrol-primed immature mice. Endocrinology. 1999 Jun;140(6):2480–5.

109. Zhao J, Taverne MA, van der Weijden GC, Bevers MM, van den Hurk R. Effect of activin A on in vitro development of rat preantral follicles and localization of activin A and activin receptor II. Biol Reprod. 2001 Sep;65(3):967–77.

110. Fortune JE, Cushman RA, Wahl CM, Kito S. The primordial to primary follicle transition. Mol Cell Endocrinol. 2000 May;163(1-2):53–60.

111. Young JM, Henderson S, Souza C, Ludlow H, Groome N, McNeilly AS. Activin B is produced early in antral follicular development and suppresses thecal androgen production. Reproduction. Society for Reproduction and Fertility; 2012 May;143(5):637–50.

112. Robertson DM, Burger HG, Fuller PJ. Inhibin/activin and ovarian cancer. Endocrine Related Cancer. BioScientifica; 2004 Mar;11(1):35–49.

113. O WS, Robertson DM, de Kretser DM. Inhibin as an oocyte meiotic inhibitor. Mol Cell Endocrinol. 1989 Apr;62(2):307–11.

114. Woodruff TK, Borree J, Attie KM, Cox ET, Rice GC, Mather JP. Stage-specific binding of inhibin and activin to subpopulations of rat germ cells. Endocrinology. 1992 Feb;130(2):871–81.

115. Hsueh AJ, Dahl KD, Vaughan J, Tucker E, Rivier J, Bardin CW, et al. Heterodimers and homodimers of inhibin subunits have different paracrine action in the modulation of luteinizing hormone-stimulated androgen

biosynthesis. PNAS. National Academy of Sciences; 1987 Jul;84(14):5082–6.

116. Shimonaka M, Inouye S, Shimasaki S, Ling N. Follistatin binds to both activin and inhibin through the common subunit. Endocrinology. 1991 Jun;128(6):3313–5.

117. Mathews LS. Activin receptors and cellular signaling by the receptor serine kinase family. Endocrine Reviews. 1994 Jun 1;15(3):310–25.

118. Josso N, Lamarre I, Picard JY, Berta P, Davies N, Morichon N, et al. Anti-müllerian hormone in early human development. Early Hum Dev. 1993 Jun;33(2):91–9.

119. Durlinger AL, Kramer P, Karels B, de Jong FH, Uilenbroek JT, Grootegoed JA, et al. Control of primordial follicle recruitment by anti-Müllerian hormone in the mouse ovary. Endocrinology. 1999 Dec;140(12):5789–96.

120. Münsterberg A, Lovell-Badge R. Expression of the mouse anti-müllerian hormone gene suggests a role in both male and female sexual differentiation. Development. 1991 Oct;113(2):613–24.

121. Durlinger ALL, Gruijters MJG, Kramer P, Karels B, Ingraham HA, Nachtigal MW, et al. Anti-Müllerian hormone inhibits initiation of primordial follicle growth in the mouse ovary. Endocrinology. 2002 Mar;143(3):1076–84.

122. Hirobe S, He WW, Gustafson ML, Maclaughlin DT, Donahoe PK. Müllerian inhibiting substance gene expression in the cycling rat ovary correlates with recruited or graafian follicle selection. Biol Reprod. 1994 Jun;50(6):1238–43.

123. Hayes E, Kushnir V, Ma X, Biswas A, Prizant H, Gleicher N, et al. Intra-cellular mechanism of Anti-Müllerian hormone (AMH) in regulation of follicular development. Mol Cell Endocrinol. 2016 Sep;433:56–65.

124. McPherron AC, Lee SJ. GDF-3 and GDF-9: two new members of the transforming growth factor-beta superfamily containing a novel pattern of cysteines. J Biol Chem. American Society for Biochemistry and Molecular Biology; 1993 Feb 15;268(5):3444–9.

125. Dong J, Albertini DF, Nishimori K, Kumar TR, Lu N, Matzuk MM. Growth differentiation factor-9 is required during early ovarian folliculogenesis. Nature. Nature Publishing Group; 1996 Oct 10;383(6600):531–5.

126. Dube JL, Wang P, Elvin J, Lyons KM, Celeste AJ, Matzuk MM. The bone morphogenetic protein 15 gene is X-linked and expressed in oocytes. Mol Endocrinol. 1998 Dec;12(12):1809–17.

127. Kaivo-Oja N, Bondestam J, Kämäräinen M, Koskimies J, Vitt U, Cranfield M, et al. Growth differentiation factor-9 induces Smad2 activation and inhibin B production in cultured human granulosa-luteal cells. J Clin Endocrinol Metab. 2003 Feb;88(2):755–62.

128. Roh J-S, Bondestam J, Mazerbourg S, Kaivo-Oja N, Groome N, Ritvos O, et al. Growth differentiation factor-9 stimulates inhibin production and activates Smad2 in cultured rat granulosa cells. Endocrinology. 2003 Jan;144(1):172–8.

129. Moore RK, Otsuka F, Shimasaki S. Molecular basis of bone morphogenetic protein-15 signaling in granulosa cells. J Biol Chem. American Society for Biochemistry and Molecular Biology; 2003 Jan 3;278(1):304–10.

130. Peng J, Li Q, Wigglesworth K, Rangarajan A, Kattamuri C, Peterson RT, et al. Growth differentiation factor 9:bone morphogenetic protein 15 heterodimers are potent regulators of ovarian functions. Proc Natl Acad Sci USA. National Acad Sciences; 2013 Feb 19;110(8):E776–85.

131. Hayashi M, McGee EA, Min G, Klein C, Rose UM, van Duin M, et al. Recombinant growth differentiation factor-9 (GDF-9) enhances growth and differentiation of cultured early ovarian follicles. Endocrinology. 1999 Mar;140(3):1236–44.

132. Wang J, Roy SK. Growth differentiation factor-9 and stem cell factor promote primordial follicle formation in the hamster: modulation by follicle-stimulating hormone. Biol Reprod. 2004 Mar;70(3):577–85.

133. Otsuka F, Yao Z, Lee T, Yamamoto S, Erickson GF, Shimasaki S. Bone morphogenetic protein-15. Identification of target cells and biological functions. J Biol Chem. American Society for Biochemistry and Molecular Biology; 2000 Dec 15;275(50):39523–8.

134. Yan C, Wang P, DeMayo J, DeMayo FJ, Elvin JA, Carino C, et al. Synergistic roles of bone morphogenetic protein 15 and growth differentiation factor 9 in ovarian function. Mol Endocrinol. 2001 Jun;15(6):854–66.

135. Elvin JA, Yan C, Wang P, Nishimori K, Matzuk MM. Molecular characterization of the follicle defects in the growth differentiation factor 9-deficient ovary. Mol Endocrinol. 1999 Jun;13(6):1018–34.

136. Wu X, Chen L, Brown CA, Yan C, Matzuk MM. Interrelationship of growth differentiation factor 9 and inhibin in early folliculogenesis and ovarian tumorigenesis in mice. Mol Endocrinol. Endocrine Society; 2004 Jun;18(6):1509–19.

137. Eppig JJ. Oocyte control of ovarian follicular development and function in mammals. Reproduction. Society for Reproduction and Fertility; 2001 Dec 1;122(6):829–38.

138. Matzuk MM, Lamb DJ. The biology of infertility: research advances and clinical challenges. Nat Med. Nature Publishing Group; 2008 Nov;14(11):1197–213.

139. McLaughlin EA, McIver SC. Awakening the oocyte: controlling primordial

follicle development. Reproduction. Society for Reproduction and Fertility; 2009 Jan;137(1):1–11.

140. Orisaka M, Tajima K, Tsang BK, Kotsuji F. Oocyte-granulosa-theca cell interactions during preantral follicular development. J Ovarian Res. BioMed Central; 2009;2(1):9.

141. Kerr JB, Myers M, Anderson RA. The dynamics of the primordial follicle reserve. Reproduction. 2013 Dec;146(6):R205–15.

142. Zhang H, Liu K. Cellular and molecular regulation of the activation of mammalian primordial follicles: somatic cells initiate follicle activation in adulthood. Hum Reprod Update. Oxford University Press; 2015 Nov;21(6):779–86.

143. Campbell BK, Souza C, Gong J, Webb R, Kendall N, Marsters P, et al. Domestic ruminants as models for the elucidation of the mechanisms controlling ovarian follicle development in humans. Reprod Suppl. 2003;61:429–43.

144. Brambell FWR. The Development and Morphology of the Gonads of the Mouse. Part III.--The Growth of the Follicles. Proceedings of the Royal Society of London B: Biological Sciences. The Royal Society; 1928 Aug 1;103(724):258–72.

145. Griffin J, Emery BR, Huang I, Peterson CM, Carrell DT. Comparative analysis of follicle morphology and oocyte diameter in four mammalian species (mouse, hamster, pig, and human). J Exp Clin Assist Reprod. 2006;3(1):2.

146. Hyttel P, Fair T, Callesen H, Greve T. Oocyte growth, capacitation and final maturation in cattle. Theriogenology. Elsevier; 1997 Jan;47(1):23–32.

147. Allen E. The oestrous cycle in the mouse. American Journal of Anatomy. Wiley Subscription Services, Inc., A Wiley Company; 1922 May;30(3):297–371.

148. Caligioni CS. Assessing reproductive status/stages in mice. Curr Protoc Neurosci. Hoboken, NJ, USA: John Wiley & Sons, Inc; 2009 Jul;Appendix 4:Appendix4I–A.4I.8.

149. Milligan SR, Khan AA, Thorne BC. Delayed pseudopregnancy in the mouse. Reproduction. Society for Reproduction and Fertility; 1980 Sep 1;60(1):49–51.

150. Adams GP, Pierson RA. Bovine model for study of ovarian follicular dynamics in humans. Theriogenology. 1995 Jan;43(1):113–20.

151. Singh J, Adams GP, Pierson RA. Promise of new imaging technologies for assessing ovarian function. Anim Reprod Sci. PMC Canada manuscript submission; 2003 Oct 15;78(3-4):371–99.

152. Adams GP, Singh J, Baerwald AR. Large animal models for the study of ovarian follicular dynamics in women. Theriogenology. 2012 Nov;78(8):1733–48.

153. Mihm M, Gangooly S, Muttukrishna S. The normal menstrual cycle in women. Anim Reprod Sci. Elsevier; 2011 Apr;124(3-4):229–36.

154. Del Canto F, Sierralta W, Kohen P. Features of natural and gonadotropin-releasing hormone antagonist-induced corpus luteum regression and effects of in vivo human chorionic gonadotropin. The Journal of Physical Chemistry B. 2007.

155. Peter AT, Levine H, Drost M, Bergfelt DR. Compilation of classical and contemporary terminology used to describe morphological aspects of ovarian dynamics in cattle. Theriogenology. Elsevier; 2009 Jun 1;71(9):1343–57.

156. Baerwald AR, Adams GP, Pierson RA. Characterization of ovarian follicular wave dynamics in women. Biol Reprod. 2003 Sep;69(3):1023–31.

157. Adams GP. Comparative patterns of follicle development and selection in ruminants. J Reprod Fertil Suppl. 1999;54:17–32.

158. Ginther OJ, Kastelic JP, Knopf L. Composition and characteristics of follicular waves during the bovine estrous cycle. Anim Reprod Sci. 1989 Sep;20(3):187–200.

159. Eppig JJ, O'Brien MJ. Development in vitro of mouse oocytes from primordial follicles. Biol Reprod. 1996 Jan;54(1):197–207.

160. O'Brien MJ, Pendola JK, Eppig JJ. A revised protocol for in vitro development of mouse oocytes from primordial follicles dramatically improves their developmental competence. Biol Reprod. Society for the Study of Reproduction; 2003 May;68(5):1682–6.

161. Telfer EE, McLaughlin M, Ding C, Thong KJ. A two-step serum-free culture system supports development of human oocytes from primordial follicles in the presence of activin. Hum Reprod. Oxford University Press; 2008 May;23(5):1151–8.

162. Vanacker J, Amorim CA. Alginate: A Versatile Biomaterial to Encapsulate Isolated Ovarian Follicles. Ann Biomed Eng. Springer US; 2017 Feb 28;68:682–17.

163. Devine PJ, Rajapaksa KS, Hoyer PB. In vitro ovarian tissue and organ culture: a review. Front Biosci. 2002 Sep 1;7:d1979–89.

164. Blandau R, Warrick E, Rumery RE. In vitro cultivation of fetal mouse ovaries. Fertil Steril. 1965 Nov;16(6):705–15.

165. Stefansdottir A, Fowler PA, Powles-Glover N, Anderson RA, Spears N. Use of ovary culture techniques in reproductive toxicology. Reprod Toxicol.

2014 Nov;49:117–35.

166. Sadeu JC, Adriaenssens T, Smitz J. Expression of growth differentiation factor 9, bone morphogenetic protein 15, and anti-Müllerian hormone in cultured mouse primary follicles. Reproduction. Society for Reproduction and Fertility; 2008 Aug;136(2):195–203.

167. Abdi S, Salehnia M, Hosseinkhani S. Evaluation of apoptosis in long-term culture of vitrified mouse whole ovaries. Res Vet Sci. 2014 Feb;96(1):1–4.

168. Terada N, Kuroda H, Namiki M, Kitamura Y, Matsumoto K. Augmentation of aromatase activity by FSH in ovaries of fetal and neonatal mice in organ culture. Journal of Steroid Biochemistry. Pergamon; 1984 Mar;20(3):741–5.

169. Adhikari D, Gorre N, Risal S, Zhao Z, Zhang H, Shen Y, et al. The safe use of a PTEN inhibitor for the activation of dormant mouse primordial follicles and generation of fertilizable eggs. Kim S, editor. PLoS ONE. Public Library of Science; 2012;7(6):e39034.

170. Roh J, Pi W. Regulation of follicle growth and apoptosis in cultured mouse ovaries by NGF and oxygen. Gynecol Endocrinol. Taylor & Francis; 2013 Jun;29(6):574–9.

171. Barilovits SJ, Newsom KJ, Bickford JS, Beachy DE, Rhoton-Vlasak A, Nick HS. Characterization of a mechanism to inhibit ovarian follicle activation. Fertil Steril. 2014 May;101(5):1450–7.

172. Chen C-L, Fu X-F, Wang L-Q, Wang J-J, Ma H-G, Cheng S-F, et al. Primordial follicle assembly was regulated by notch signaling pathway in the mice. Mol Biol Rep. Springer Netherlands; 2014;41(3):1891–9.

173. Komatsu K, Koya T, Wang J, Yamashita M, Kikkawa F, Iwase A. Analysis of the Effect of Leukemia Inhibitory Factor on Follicular Growth in Cultured Murine Ovarian Tissue. Biol Reprod. Society for the Study of Reproduction; 2015 Jul;93(1):18–8.

174. Winkler-Crepaz K, Nederegger V, Ayuandari S, Rosenfellner D, Zervomanolakis I, Hofer S, et al. Novel dynamic culture system to support initiation of primordial follicle growth in prepubertal mouse ovaries. Fertil Steril. 2014 Sep;102(3):864–870.e2.

175. Shen W, Li L, Bai Z, Pan Q, Ding M, Deng H. In vitro development of mouse fetal germ cells into mature oocytes. Reproduction. Society for Reproduction and Fertility; 2007 Aug 1;134(2):223–31.

176. Morohaku K, Tanimoto R, Sasaki K, Kawahara-Miki R, Kono T, Hayashi K, et al. Complete in vitro generation of fertile oocytes from mouse primordial germ cells. Proc Natl Acad Sci USA. National Acad Sciences; 2016 Aug 9;113(32):9021–6.

177. Scott JE, Carlsson IB, Bavister BD, Hovatta O. Human ovarian tissue

cultures: extracellular matrix composition, coating density and tissue dimensions. Reprod Biomed Online. 2004 Sep;9(3):287–93.

178. Picton HM, Harris SE, Muruvi W, Chambers EL. The in vitro growth and maturation of follicles. Reproduction. Society for Reproduction and Fertility; 2008 Dec;136(6):703–15.

179. Wandji SA, Srsen V, Voss AK, Eppig JJ, Fortune JE. Initiation in vitro of growth of bovine primordial follicles. Biol Reprod. 1996 Nov;55(5):942–8.

180. Braw-Tal R, Yossefi S. Studies in vivo and in vitro on the initiation of follicle growth in the bovine ovary. J Reprod Fertil. 1997 Jan;109(1):165–71.

181. Wandji SA, Srsen V, Nathanielsz PW, Eppig JJ, Fortune JE. Initiation of growth of baboon primordial follicles in vitro. Human Reproduction. 1997 Sep;12(9):1993–2001.

182. Fortune JE, Kito S, Wandji SA, Srsen V. Activation of bovine and baboon primordial follicles in vitro. Theriogenology. 1998 Jan 15;49(2):441–9.

183. Gigli I, Byrd DD, Fortune JE. Effects of oxygen tension and supplements to the culture medium on activation and development of bovine follicles in vitro. Theriogenology. 2006 Jul 15;66(2):344–53.

184. McLaughlin M, Telfer EE. Oocyte development in bovine primordial follicles is promoted by activin and FSH within a two-step serum-free culture system. Reproduction. Society for Reproduction and Fertility; 2010 Jun;139(6):971–8.

185. Castro SV, Carvalho AA, Silva CMG, Santos FW, Campello CC, de Figueiredo JR, et al. Frozen and fresh ovarian tissue require different culture media to promote in vitro development of bovine preantral follicles. Biopreserv Biobank. Mary Ann Liebert, Inc. 140 Huguenot Street, 3rd Floor New Rochelle, NY 10801 USA; 2014 Oct;12(5):317–24.

186. Tepekoy F, Akkoyunlu G. The effect of FSH and activin A on Akt and MAPK1/3 phosphorylation in cultured bovine ovarian cortical strips. J Ovarian Res. BioMed Central; 2016 Mar 11;9(1):200.

187. Hovatta O, Silye R, Abir R, Krausz T, Winston RM. Extracellular matrix improves survival of both stored and fresh human primordial and primary ovarian follicles in long-term culture. Hum Reprod. 1997 May;12(5):1032–6.

188. Wright CS, Hovatta O, Margara R, Trew G, Winston RM, Franks S, et al. Effects of follicle-stimulating hormone and serum substitution on the in-vitro growth of human ovarian follicles. Hum Reprod. 1999 Jun;14(6):1555–62.

189. Morimoto Y, Oku Y, Sonoda M, Haruki A, Ito K, Hashimoto S, et al. High oxygen atmosphere improves human follicle development in organ cultures of ovarian cortical tissues in vitro. Human Reproduction. Oxford University

Press; 2007 Dec 1;22(12):3170–7.

190. Liebenthron J, Köster M, Drengner C, Reinsberg J, van der Ven H, Montag M. The impact of culture conditions on early follicle recruitment and growth from human ovarian cortex biopsies in vitro. Fertil Steril. 2013 Aug;100(2):483–5.

191. Stubbs SA, Webber LJ, Stark J, Rice S, Margara R, Lavery S, et al. Role of Insulin-like growth factors in initiation of follicle growth in normal and polycystic human ovaries. J Clin Endocrinol Metab. Endocrine Society Chevy Chase, MD; 2013 Aug;98(8):3298–305.

192. Anderson RA, McLaughlin M, Wallace WHB, Albertini DF, Telfer EE. The immature human ovary shows loss of abnormal follicles and increasing follicle developmental competence through childhood and adolescence. Hum Reprod. Oxford University Press; 2014 Jan;29(1):97–106.

193. Laronda MM, Duncan FE, Hornick JE, Xu M, Pahnke JE, Whelan KA, et al. Alginate encapsulation supports the growth and differentiation of human primordial follicles within ovarian cortical tissue. J Assist Reprod Genet. Springer US; 2014 Aug;31(8):1013–28.

194. McLaughlin M, Kinnell HL, Anderson RA, Telfer EE. Inhibition of phosphatase and tensin homologue (PTEN) in human ovary in vitro results in increased activation of primordial follicles but compromises development of growing follicles. Mol Hum Reprod. Oxford University Press; 2014 Aug;20(8):736–44.

195. Asadi E, Najafi A, Moeini A, Pirjani R, Hassanzadeh G, Mikaeili S, et al. Ovarian tissue culture in presence of VEGF and fetuin stimulates follicle growth and steroidogenesis. Journal of Endocrinology. BioScientifica; 2016 Nov 16;232(2):JOE–16–0368–219.

196. Hovatta O. Human primordial, primary and secondary ovarian follicles in long-term culture: effect of partial isolation. Human Reproduction. Oxford University Press; 1999 Oct 1;14(10):2519–24.

197. Hulshof SC, Figueiredo JR, Beckers JF, Bevers MM, van der Donk JA, van den Hurk R. Effects of fetal bovine serum, FSH and 17beta-estradiol on the culture of bovine preantral follicles. Theriogenology. Elsevier; 1995 Jul 15;44(2):217–26.

198. Young LE, Sinclair KD, Wilmut I. Large offspring syndrome in cattle and sheep. Rev Reprod. 1998 Sep;3(3):155–63.

199. van Wagtendonk-de Leeuw AM, Mullaart E, de Roos AP, Merton JS, Daas den JH, Kemp B, et al. Effects of different reproduction techniques: AI MOET or IVP, on health and welfare of bovine offspring. Theriogenology. 2000 Jan 15;53(2):575–97.

200. Kleinman HK, McGarvey ML, Hassell JR, Star VL, Cannon FB, Laurie GW, et al. Basement membrane complexes with biological activity.

Biochemistry. 1986 Jan 28;25(2):312–8.

201. Vukicevic S, Kleinman HK, Luyten FP, Roberts AB, Roche NS, Reddi AH. Identification of multiple active growth factors in basement membrane Matrigel suggests caution in interpretation of cellular activity related to extracellular matrix components. Exp Cell Res. 1992 Sep;202(1):1–8.

202. Kleinman HK, Martin GR. Matrigel: basement membrane matrix with biological activity. Semin Cancer Biol. 2005 Oct;15(5):378–86.

203. Gougeon A. Dynamics of follicular growth in the human: a model from preliminary results. Human Reproduction. 1986 Feb;1(2):81–7.

204. Smitz J, Dolmans MM, Donnez J, Fortune JE, Hovatta O, Jewgenow K, et al. Current achievements and future research directions in ovarian tissue culture, in vitro follicle development and transplantation: implications for fertility preservation. Hum Reprod Update. Oxford University Press; 2010 Jul 1;16(4):395–414.

205. Eppig JJ, Schroeder AC. Capacity of mouse oocytes from preantral follicles to undergo embryogenesis and development to live young after growth, maturation, and fertilization in vitro. Biol Reprod. 1989 Aug;41(2):268–76.

206. Cortvrindt R, Smitz J, Van Steirteghem AC. In-vitro maturation, fertilization and embryo development of immature oocytes from early preantral follicles from prepuberal mice in a simplified culture system. Hum Reprod. 1996 Dec;11(12):2656–66.

207. Spears N, Boland NI, Murray AA, Gosden RG. Mouse oocytes derived from in vitro grown primary ovarian follicles are fertile. Hum Reprod. 1994 Mar;9(3):527–32.

208. Gutierrez CG, Ralph JH, Telfer EE, Wilmut I, Webb R. Growth and antrum formation of bovine preantral follicles in long-term culture in vitro. Biol Reprod. 2000 May;62(5):1322–8.

209. Walters KA, Binnie JP, Campbell BK, Armstrong DG, Telfer EE. The effects of IGF-I on bovine follicle development and IGFBP-2 expression are dose and stage dependent. Reproduction. Society for Reproduction and Fertility; 2006 Mar;131(3):515–23.

210. Thomas FH, Campbell BK, Armstrong DG, Telfer EE. Effects of IGF-I bioavailability on bovine preantral follicular development in vitro. Reproduction. Society for Reproduction and Fertility; 2007 Jul 16;133(6):1121–8.

211. Nayudu PL, Osborn SM. Factors influencing the rate of preantral and antral growth of mouse ovarian follicles in vitro. J Reprod Fertil. 1992 Jul;95(2):349–62.

212. Wycherley G, Downey D, Kane MT, Hynes AC. A novel follicle culture

system markedly increases follicle volume, cell number and oestradiol secretion. Reproduction. Society for Reproduction and Fertility; 2004 Jun;127(6):669–77.

213. Picton HM, Gosden RG. In vitro growth of human primordial follicles from frozen-banked ovarian tissue. Mol Cell Endocrinol. 2000 Aug 15;166(1):27–35.

214. Tingen CM, Kiesewetter SE, Jozefik J, Thomas C, Tagler D, Shea L, et al. A macrophage and theca cell-enriched stromal cell population influences growth and survival of immature murine follicles in vitro. Reproduction. Society for Reproduction and Fertility; 2011 Jun;141(6):809–20.

215. Tagler D, Tu T, Smith RM, Anderson NR, Tingen CM, Woodruff TK, et al. Embryonic Fibroblasts Enable the Culture of Primary Ovarian Follicles Within Alginate Hydrogels. Tissue Eng Part A. Mary Ann Liebert, Inc. 140 Huguenot Street, 3rd Floor New Rochelle, NY 10801 USA; 2012 Jun;18(11-12):1229–38.

216. Hornick JE, Duncan FE, Shea LD, Woodruff TK. Multiple follicle culture supports primary follicle growth through paracrine-acting signals. Reproduction. Society for Reproduction and Fertility; 2013 Jan;145(1):19–32.

217. Tagler D, Makanji Y, Anderson NR, Woodruff TK, Shea LD. Supplemented αMEM/F12-based medium enables the survival and growth of primary ovarian follicles encapsulated in alginate hydrogels. Biotechnol Bioeng. 2013 Jul 15;110(12):3258–68.

218. Tagler D, Makanji Y, Tu T, Bernabé BP, Lee R, Zhu J, et al. Promoting extracellular matrix remodeling via ascorbic acid enhances the survival of primary ovarian follicles encapsulated in alginate hydrogels. Biotechnol Bioeng. 2014 Jul;111(7):1417–29.

219. Abir R, Fisch B, Nitke S, Okon E, Raz A, Ben Rafael Z. Morphological study of fully and partially isolated early human follicles. Fertil Steril. 2001 Jan;75(1):141–6.

220. Wang T-R, Yan L-Y, Yan J, Lu C-L, Xia X, Yin T-L, et al. Basic fibroblast growth factor promotes the development of human ovarian early follicles during growth in vitro. Hum Reprod. Oxford University Press; 2014 Jan 9;29(3):det465–576.

221. Telfer EE, McLaughlin M. Strategies to support human oocyte development in vitro. The International Journal of Developmental Biology. 2012;56(10-11-12):901–7.

222. Guzel Y, Oktem O. Understanding follicle growth in vitro: are we getting closer to obtaining mature oocytes from in vitro-grown human follicles of humans? Mol Reprod Dev. 2017 Apr 27.

223. Xiao S, Zhang J, Romero MM, Smith KN, Shea LD, Woodruff TK. In vitro

follicle growth supports human oocyte meiotic maturation. Sci Rep. 2015;5:17323.

224. Kreeger PK, Woodruff TK, Shea LD. Murine granulosa cell morphology and function are regulated by a synthetic Arg–Gly–Asp matrix. Mol Cell Endocrinol. 2003 Jul;205(1-2):1–10.

225. Gilchrist RB, Ritter LJ, Armstrong DT. Oocyte-somatic cell interactions during follicle development in mammals. Anim Reprod Sci. 2004 Jul;82-83:431–46.

226. Eppig JJ, Wigglesworth K. Development of mouse and rat oocytes in chimeric reaggregated ovaries after interspecific exchange of somatic and germ cell components. Biol Reprod. 2000 Oct;63(4):1014–23.

227. Wang H, Xia G, Wang Q, Li M, Lu Z. Follicles were reconstituted from dissociated mouse fetal ovarian cells in vitro. Chinese Science Bulletin. 2001 Apr;46(8):672–4.

228. Eppig JJ, Wigglesworth K, Pendola FL. The mammalian oocyte orchestrates the rate of ovarian follicular development. PNAS. 2002 Mar 5;99(5):2890–4.

229. Gittens JEI, Kidder GM. Differential contributions of connexin37 and connexin43 to oogenesis revealed in chimeric reaggregated mouse ovaries. J Cell Sci. 2005 Nov 1;118(Pt 21):5071–8.

230. Lei L, Zhang H, Jin S, Wang F, Fu M, Wang H, et al. Stage-specific germ-somatic cell interaction directs the primordial folliculogenesis in mouse fetal ovaries. J Cell Physiol. Wiley Subscription Services, Inc., A Wiley Company; 2006 Sep;208(3):640–7.

231. Tong D, Li TY, Naus KE, Bai D, Kidder GM. In vivo analysis of undocked connexin43 gap junction hemichannels in ovarian granulosa cells. J Cell Sci. The Company of Biologists Ltd; 2007 Nov 15;120(Pt 22):4016–24.

232. Hikabe O, Hamazaki N, Nagamatsu G, Obata Y, Hirao Y, Hamada N, et al. Reconstitution in vitro of the entire cycle of the mouse female germ line. Nature. 2016 Oct 17.

233. Kreeger PK, Fernandes NN, Woodruff TK, Shea LD. Regulation of mouse follicle development by follicle-stimulating hormone in a three-dimensional in vitro culture system is dependent on follicle stage and dose. Biol Reprod. Society for the Study of Reproduction; 2005 Nov;73(5):942–50.

234. Park C-E, Lee D, Kim K-H, Lee K-A. Establishment of ovarian reconstruction system in culture for functional genomic analysis. J Biosci Bioeng. 2006 Nov;102(5):396–401.

235. Xu M, West E, Shea LD, Woodruff TK. Identification of a stage-specific permissive in vitro culture environment for follicle growth and oocyte development. Biol Reprod. Society for the Study of Reproduction; 2006

Dec;75(6):916–23.

236. West ER, Xu M, Woodruff TK, Shea LD. Physical properties of alginate hydrogels and their effects on in vitro follicle development. Biomaterials. 2007 Oct;28(30):4439–48.

237. West-Farrell ER, Xu M, Gomberg MA, Chow YH, Woodruff TK, Shea LD. The mouse follicle microenvironment regulates antrum formation and steroid production: alterations in gene expression profiles. Biol Reprod. 2009 Mar;80(3):432–9.

238. Jin SY, Lei L, Shikanov A, Shea LD, Woodruff TK. A novel two-step strategy for in vitro culture of early-stage ovarian follicles in the mouse. Fertil Steril. 2010 May 15;93(8):2633–9.

239. Dunning KR, Akison LK, Russell DL, Norman RJ, Robker RL. Increased beta-oxidation and improved oocyte developmental competence in response to l-carnitine during ovarian in vitro follicle development in mice. Biol Reprod. 2011 Sep;85(3):548–55.

240. Mainigi MA, Ord T, Schultz RM. Meiotic and Developmental Competence in Mice Are Compromised Following Follicle Development In Vitro Using an Alginate-Based Culture System. Biol Reprod. Biology of reproduction; 2011 Aug 1;85(2):269–76.

241. Shikanov A, Xu M, Woodruff TK, Shea LD. A method for ovarian follicle encapsulation and culture in a proteolytically degradable 3 dimensional system. J Vis Exp. 2011;(49):e2695–5.

242. Park KE, Kim YY, Ku S-Y, Baek SM, Huh Y, Kim YJ, et al. Effects of alginate hydrogels on in vitro maturation outcome of mouse preantral follicles. Tissue Engineering and Regenerative Medicine. Springer Netherlands; 2012 May 21;9(3):170–4.

243. Jiao Z-X, Woodruff TK. Follicle microenvironment-associated alterations in gene expression in the mouse oocyte and its polar body. Fertil Steril. 2013 Apr;99(5):1453–1459.e1.

244. Makanji Y, Tagler D, Pahnke J, Shea LD, Woodruff TK. Hypoxia-mediated carbohydrate metabolism and transport promote early-stage murine follicle growth and survival. Am J Physiol Endocrinol Metab. American Physiological Society; 2014 Apr 15;306(8):E893–903.

245. Asgari F, Valojerdi MR, Ebrahimi B, Fatehi R. Three dimensional in vitro culture of preantral follicles following slow-freezing and vitrification of mouse ovarian tissue. Cryobiology. 2015 Dec;71(3):529–36.

246. Shiomi-Sugaya N, Komatsu K, Wang J, Yamashita M, Kikkawa F, Iwase A. Regulation of secondary follicle growth by theca cells and insulin-like growth factor 1. J Reprod Dev. 2015;61(3):161–8.

247. Skory RM, Xu Y, Shea LD, Woodruff TK. Engineering the ovarian cycle

using in vitro follicle culture. Human Reproduction. Oxford University Press; 2015 Jun 1;30(6):1386–95.

248. Kreeger PK, Deck JW, Woodruff TK, Shea LD. The in vitro regulation of ovarian follicle development using alginate-extracellular matrix gels. Biomaterials. 2006 Feb;27(5):714–23.

249. Shikanov A, Xu M, Woodruff TK, Shea LD. Interpenetrating fibrin-alginate matrices for in vitro ovarian follicle development. Biomaterials. 2009 Oct;30(29):5476–85.

250. Luyckx V, Dolmans M-M, Vanacker J, Legat C, Fortuño Moya C, Donnez J, et al. A new step toward the artificial ovary: survival and proliferation of isolated murine follicles after autologous transplantation in a fibrin scaffold. Fertil Steril. 2014 Apr;101(4):1149–56.

251. Smith RM, Shikanov A, Kniazeva E, Ramadurai D, Woodruff TK, Shea LD. Fibrin-mediated delivery of an ovarian follicle pool in a mouse model of infertility. Tissue Eng Part A. 2014 Nov;20(21-22):3021–30.

252. Kniazeva E, Hardy AN, Boukaidi SA, Woodruff TK, Jeruss JS, Shea LD. Primordial Follicle Transplantation within Designer Biomaterial Grafts Produce Live Births in a Mouse Infertility Model. Sci Rep. Nature Publishing Group; 2015;5:17709.

253. Zhou H, Malik MA, Arab A, Hill MT, Shikanov A. Hydrogel Based 3-Dimensional (3D) System for Toxicity and High-Throughput (HTP) Analysis for Cultured Murine Ovarian Follicles. Rosenfeld CS, editor. PLoS ONE. Public Library of Science; 2015;10(10):e0140205.

254. Chiti MC, Dolmans MM, Orellana R, Soares M, Paulini F, Donnez J, et al. Influence of follicle stage on artificial ovary outcome using fibrin as a matrix. Hum Reprod. Oxford University Press; 2016 Feb;31(2):427–35.

255. Desai N, Abdelhafez F, Calabro A, Falcone T. Three dimensional culture of fresh and vitrified mouse pre-antral follicles in a hyaluronan-based hydrogel: a preliminary investigation of a novel biomaterial for in vitro follicle maturation. Reprod Biol Endocrinol. BioMed Central; 2012 Jun 13;10(1):29.

256. Shikanov A, Smith RM, Xu M, Woodruff TK, Shea LD. Hydrogel network design using multifunctional macromers to coordinate tissue maturation in ovarian follicle culture. Biomaterials. 2011 Apr;32(10):2524–31.

257. Kim J, Perez AS, Claflin J, David A, Zhou H, Shikanov A. Synthetic hydrogel supports the function and regeneration of artificial ovarian tissue in mice. npj Regenerative Medicine. Nature Publishing Group; 2016 Jul 7;1(1):218.

258. Krotz SP, Robins JC, Ferruccio T-M, Moore R, Steinhoff MM, Morgan JR, et al. In vitro maturation of oocytes via the pre-fabricated self-assembled artificial human ovary. J Assist Reprod Genet. 2010 Dec;27(12):743–50.

259. Laronda MM, Rutz AL, Xiao S, Whelan KA, Duncan FE, Roth EW, et al. A bioprosthetic ovary created using 3D printed microporous scaffolds restores ovarian function in sterilized mice. Nat Commun. 2017 May 16;8:15261.

260. Laronda MM, Jakus AE, Whelan KA, Wertheim JA, Shah RN, Woodruff TK. Initiation of puberty in mice following decellularized ovary transplant. Biomaterials. 2015 May;50:20–9.

261. Shea LD, Woodruff TK, Shikanov A. Bioengineering the ovarian follicle microenvironment. Annu Rev Biomed Eng. Annual Reviews; 2014 Jul 11;16(1):29–52.

262. Chan BP, Leong KW. Scaffolding in tissue engineering: general approaches and tissue-specific considerations. Eur Spine J. Springer-Verlag; 2008 Dec;17 Suppl 4(S4):467–79.

263. Brännström M, Flaherty S. Methodology and characterization of an in vitro perfusion model for the mouse ovary. J Reprod Fertil. Society for Reproduction and Fertility; 1995 Nov;105(2):177–83.

264. Zanotelli MR, Henningsen JD, Hopkins PM, Dederich AP, Herman T, Puccinelli TJ, et al. An ovarian bioreactor for in vitro culture of the whole bovine ovary: a preliminary report. J Ovarian Res. BioMed Central; 2016 Aug 4;9(1):47.

265. Vanacker J, Dolmans M-M, Luyckx V, Donnez J, Amorim CA. First transplantation of isolated murine follicles in alginate. Regenerative Medicine. Future Medicine Ltd London, UK; 2014 Sep;9(5):609–19.

266. Joo S, Oh S-H, Sittadjody S, Opara EC, Jackson JD, Lee SJ, et al. The effect of collagen hydrogel on 3D culture of ovarian follicles. Biomed Mater. IOP Publishing; 2016 Nov 11;11(6):065009.

267. Shikanov A, Zhang Z, Xu M, Smith RM, Rajan A, Woodruff TK, et al. Fibrin encapsulation and vascular endothelial growth factor delivery promotes ovarian graft survival in mice. Tissue Eng Part A. 2011 Dec;17(23-24):3095–104.

268. Donati I, Mørch YA, Strand BL, Skjåk-Bræk G, Paoletti S. Effect of Elongation of Alternating Sequences on Swelling Behavior and Large Deformation Properties of Natural Alginate Gels. The Journal of Physical Chemistry B. American Chemical Society; 2009 Oct;113(39):12916–22.

269. Haug A, Smidsrod O. Strontium-calcium selectivity of alginates. Nature. 1967 Aug 12;215(5102):757.

270. Yin H, Kristensen SG, Jiang H, Rasmussen A, Andersen CY. Survival and growth of isolated pre-antral follicles from human ovarian medulla tissue during long-term 3D culture. Human Reproduction. Oxford University Press; 2016 Jul 1;31(7):1531–9.

271. Xu M, West-Farrell ER, Stouffer RL, Shea LD, Woodruff TK, Zelinski MB. Encapsulated three-dimensional culture supports development of nonhuman primate secondary follicles. Biol Reprod. 2009 Sep;81(3):587–94.

272. LaPolt PS, Yamoto M, Veljkovic M, Sincich C, Ny T, Tsafriri A, et al. Basic fibroblast growth factor induction of granulosa cell tissue-type plasminogen activator expression and oocyte maturation: potential role as a paracrine ovarian hormone. Endocrinology. The Endocrine Society; 1990 Nov;127(5):2357–63.

273. Dahlbäck B. Blood coagulation. Lancet. 2000 May 6;355(9215):1627–32.

274. Salustri A, Yanagishita M, Underhill CB, Laurent TC, Hascall VC. Localization and synthesis of hyaluronic acid in the cumulus cells and mural granulosa cells of the preovulatory follicle. Developmental Biology. 1992 Jun;151(2):541–51.

275. Toole BP. Hyaluronan: from extracellular glue to pericellular cue. Nat Rev Cancer. Nature Publishing Group; 2004 Jul;4(7):528–39.

276. and MPL, Hubbell JA. Synthesis and Physicochemical Characterization of End-Linked Poly(ethylene glycol)-co-peptide Hydrogels Formed by Michael-Type Addition. Biomacromolecules. American Chemical Society; 2003 Feb 26;4(3):713–22.

277. Kim J, Kong YP, Niedzielski SM, Singh RK, Putnam AJ, Shikanov A. Characterization of the crosslinking kinetics of multi-arm poly(ethylene glycol) hydrogels formed via Michael-type addition. Soft Matter. The Royal Society of Chemistry; 2016 Feb 21;12(7):2076–85.

278. Hern DL, Hubbell JA. Incorporation of adhesion peptides into nonadhesive hydrogels useful for tissue resurfacing. Journal of Biomedical Materials Research. John Wiley & Sons, Inc; 1998 Feb;39(2):266–76.

279. Howe A, Aplin AE, Alahari SK, Juliano RL. Integrin signaling and cell growth control. Current Opinion in Cell Biology. 1998 Apr;10(2):220–31.

280. Pecins-Thompson M, Bethea CL. RU 486 blocks and fluoxetine augments progesterone-induced prolactin secretion in monkeys. Neuroendocrinology. 1997 May;65(5):335–43.

281. Mehta AE, Matwijiw I, Lyons EA, Faiman C. Noninvasive diagnosis of resistant ovary syndrome by ultrasonography. Fertil Steril. 1992 Jan;57(1):56–61.

282. Nelson LM, Anasti JN, Kimzey LM, Defensor RA, Lipetz KJ, White BJ, et al. Development of luteinized graafian follicles in patients with karyotypically normal spontaneous premature ovarian failure. J Clin Endocrinol Metab. 1994 Nov;79(5):1470–5.

283. Unkila-Kallio L, Tiitinen A, Wahlström T, Lehtovirta P, Leminen A.

Reproductive features in women developing ovarian granulosa cell tumour at a fertile age. Human Reproduction. 2000 Mar;15(3):589–93.

284. Massin N, Gougeon A, Meduri G, Thibaud E, Laborde K, Matuchansky C, et al. Significance of ovarian histology in the management of patients presenting a premature ovarian failure. Human Reproduction. 2004 Nov;19(11):2555–60.

285. Suzuki N, Yoshioka N, Takae S, Sugishita Y, Tamura M, Hashimoto S, et al. Successful fertility preservation following ovarian tissue vitrification in patients with primary ovarian insufficiency. Hum Reprod. Oxford University Press; 2015 Mar;30(3):608–15.

286. Williams SA, Stanley P. Premature ovarian failure in mice with oocytes lacking core 1-derived O-glycans and complex N-glycans. Endocrinology. 2011 Mar;152(3):1057–66.

287. Friedrich G, Soriano P. Promoter traps in embryonic stem cells: a genetic screen to identify and mutate developmental genes in mice. Genes Dev. 1991 Sep;5(9):1513–23.

288. Coulam CB, Adamson SC, Annegers JF. Incidence of premature ovarian failure. Obstet Gynecol. 1986 Apr;67(4):604–6.

289. Office for National Statistics. Cancer Registration Statistics, England: 2015 [Internet]. Office for National Statistics. 2017 May. Available from: https://www.ons.gov.uk/peoplepopulationandcommunity/healthandsocialcare/conditionsanddiseases/bulletins/cancerregistrationstatisticsengland/2015

290. Abdi S, Salehnia M, Hosseinkhani S. Steroid Production and Follicular Development of Neonatal Mouse Ovary during in vitro Culture. Int J Fertil Steril. Royan Institute; 2013 Oct;7(3):181–6.

291. Abercrombie M. Estimation of nuclear population from microtome sections. Anat Rec. 1946 Feb;94:239–47.

292. Schneider CA, Rasband WS, Eliceiri KW. NIH Image to ImageJ: 25 years of image analysis. Nat Methods. 2012 Jul;9(7):671–5.

293. Wang S, Yang S, Lai Z, Ding T, Shen W, Shi L, et al. Effects of culture and transplantation on follicle activation and early follicular growth in neonatal mouse ovaries. Cell Tissue Res. Springer Berlin Heidelberg; 2013 Nov;354(2):609–21.

294. Roness H, Gavish Z, Cohen Y, Meirow D. Ovarian follicle burnout: A universal phenomenon? Cell Cycle. Taylor & Francis; 2014 Oct 29;12(20):3245–6.

295. Woodruff TK, Shea LD. The Role of the Extracellular Matrix in Ovarian Follicle Development. Reproductive Sciences. SAGE Publications; 2007 Dec 1;14(8_suppl):6–10.

296. Kawamura K, Cheng Y, Suzuki N, Deguchi M, Sato Y, Takae S, et al. Hippo signaling disruption and Akt stimulation of ovarian follicles for infertility treatment. Proc Natl Acad Sci USA. National Acad Sciences; 2013 Oct 22;110(43):17474–9.

297. Huang H-L, Hsing H-W, Lai T-C, Chen Y-W, Lee T-R, Chan H-T, et al. Trypsin-induced proteome alteration during cell subculture in mammalian cells. J Biomed Sci. BioMed Central; 2010 May 11;17(1):36.

298. Da Silva-Buttkus P, Jayasooriya GS, Mora JM, Mobberley M, Ryder TA, Baithun M, et al. Effect of cell shape and packing density on granulosa cell proliferation and formation of multiple layers during early follicle development in the ovary. J Cell Sci. The Company of Biologists Ltd; 2008 Dec 1;121(Pt 23):3890–900.

299. Pedersen T, Peters H. Proposal for a classification of oocytes and follicles in the mouse ovary. J Reprod Fertil. 1968 Dec;17(3):555–7.

300. Perloff WH, Schultz J, Farris EJ, Balin H. Some Aspects of the Chemical Nature of Human Ovarian Follicular Fluid. Fertil Steril. Elsevier; 1955 Jan 1;6(1):11–7.

301. Shalgi R, Kraicer P, Rimon A, Pinto M, Soferman N. Proteins of human follicular fluid: the blood-follicle barrier. Fertil Steril. 1973 Jun;24(6):429–34.

302. Berkholtz CB, Shea LD, Woodruff TK. Extracellular matrix functions in follicle maturation. Semin Reprod Med. Copyright © 2006 by Thieme Medical Publishers, Inc., 333 Seventh Avenue, New York, NY 10001, USA; 2006 Sep;24(4):262–9.

303. Monniaux D, Huet-Calderwood C, Bellego F, Fabre S, Monget P, Calderwood D. Integrins in the Ovary. Semin Reprod Med. 2006 Sep;24(4):251–61.

304. Lu P, Takai K, Weaver VM, Werb Z. Extracellular matrix degradation and remodeling in development and disease. Cold Spring Harbor Perspectives in Biology. Cold Spring Harbor Lab; 2011 Dec;3(12):a005058–8.

305. Irving-Rodgers HF, Hummitzsch K, Murdiyarso LS, Bonner WM, Sado Y, Ninomiya Y, et al. Dynamics of extracellular matrix in ovarian follicles and corpora lutea of mice. Cell Tissue Res. Springer-Verlag; 2010 Mar;339(3):613–24.

306. Eppig JJ, Wigglesworth K. Factors affecting the developmental competence of mouse oocytes grown in vitro: oxygen concentration. Mol Reprod Dev. Wiley Subscription Services, Inc., A Wiley Company; 1995 Dec;42(4):447–56.

307. Xia X, Wang T, Yin T, Yan L, Yan J, Lu C, et al. Mesenchymal Stem Cells Facilitate In Vitro Development of Human Preantral Follicle. Reprod Sci. SAGE Publications; 2015 Nov;22(11):1367–76.

308. Merrell AJ, Stanger BZ. Adult cell plasticity in vivo: de-differentiation and transdifferentiation are back in style. Nat Rev Mol Cell Biol. Nature Research; 2016 Jul;17(7):413–25.

309. Campbell L, Trendell J, Spears N. Identification of cells migrating from the thecal layer of ovarian follicles. Cell Tissue Res. Springer-Verlag; 2013 Jul;353(1):189–94.

310. Teng Z, Wang C, Wang Y, Huang K, Xiang X, Niu W, et al. S100A8, An Oocyte-Specific Chemokine, Directs the Migration of Ovarian Somatic Cells During Mouse Primordial Follicle Assembly. J Cell Physiol. 2015 Dec;230(12):2998–3008.

311. Magoffin DA. Ovarian theca cell. The International Journal of Biochemistry & Cell Biology. 2005 Jul;37(7):1344–9.

312. Hummitzsch K, Anderson RA, Wilhelm D, Wu J, Telfer EE, Russell DL, et al. Stem Cells, Progenitor Cells, and Lineage Decisions in the Ovary. Endocrine Reviews. 2015 Feb;36(1):65–91.

313. Orisaka M, Tajima K, Mizutani T, Miyamoto K, Tsang BK, Fukuda S, et al. Granulosa cells promote differentiation of cortical stromal cells into theca cells in the bovine ovary. Biol Reprod. Oxford University Press; 2006 Nov;75(5):734–40.

314. Honda A, Hirose M, Hara K, Matoba S, Inoue K, Miki H, et al. Isolation, characterization, and in vitro and in vivo differentiation of putative thecal stem cells. Proc Natl Acad Sci USA. National Acad Sciences; 2007 Jul 24;104(30):12389–94.

315. Liu C, Peng J, Matzuk MM, Yao HH-C. Lineage specification of ovarian theca cells requires multicellular interactions via oocyte and granulosa cells. Nat Commun. Nature Publishing Group; 2015;6:6934.

316. Stewart RE, Spicer LJ, Hamilton TD, Keefer BE. Effects of insulin-like growth factor I and insulin on proliferation and on basal and luteinizing hormone-induced steroidogenesis of bovine thecal cells: involvement of glucose and receptors for insulin-like growth factor I and luteinizing hormone. J Anim Sci. 1995 Dec;73(12):3719–31.

317. Kwintkiewicz J, Giudice LC. The interplay of insulin-like growth factors, gonadotropins, and endocrine disruptors in ovarian follicular development and function. Semin Reprod Med. © Thieme Medical Publishers; 2009 Jan;27(1):43–51.

318. Adashi EY, Resnick CE, D'Ercole AJ, Svoboda ME, Van Wyk JJ. Insulin-like growth factors as intraovarian regulators of granulosa cell growth and function. Endocrine Reviews. Endocrine Society; 1985;6(3):400–20.

319. Oliver JE, Aitman TJ, Powell JF, Wilson CA, Clayton RN. Insulin-Like Growth Factor I Gene Expression in the Rat Ovary is Confined to the Granulosa Cells of Developing Follicles. Endocrinology. Oxford University

Press; 1989 Jun 1;124(6):2671–9.

320. Yang HY, Cox S-L, Jenkin G, Findlay J, Trounson A, Shaw J. Graft site and gonadotrophin stimulation influences the number and quality of oocytes from murine ovarian tissue grafts. Reproduction. Society for Reproduction and Fertility; 2006 May;131(5):851–9.

321. Snedeker JG, Niederer P, Schmidlin FR, Farshad M, Demetropoulos CK, Lee JB, et al. Strain-rate dependent material properties of the porcine and human kidney capsule. J Biomech. 2005 May;38(5):1011–21.

322. Hebert LA, Stuart KA, Stemper JA. Whole kidney volume/pressure relationships. Kidney Int. 1975 Jan;7(1):45–54.

323. Nishikawa K, Armelin HA, Sato G. Control of ovarian cell growth in culture by serum and pituitary factors. PNAS. National Academy of Sciences; 1975 Feb;72(2):483–7.

324. Johnson LD, Albertini DF, McGinnis LK, Biggers JD. Chromatin organization, meiotic status and meiotic competence acquisition in mouse oocytes from cultured ovarian follicles. J Reprod Fertil. 1995 Jul;104(2):277–84.

325. Rose UM, Hanssen RG, Kloosterboer HJ. Development and characterization of an in vitro ovulation model using mouse ovarian follicles. Biol Reprod. 1999 Aug;61(2):503–11.

326. Durlinger ALL, Gruijters MJG, Kramer P, Karels B, Kumar TR, Matzuk MM, et al. Anti-Müllerian Hormone Attenuates the Effects of FSH on Follicle Development in the Mouse Ovary. Endocrinology. 2001 Nov 1;142(11):4891–9.

327. Morgan S, Campbell L, Allison V, Murray A, Spears N. Culture and co-culture of mouse ovaries and ovarian follicles. J Vis Exp. 2015;(97):e52458–8.

328. Hartshorne GM, Sargent IL, Barlow DH. Growth rates and antrum formation of mouse ovarian follicles in vitro in response to follicle-stimulating hormone, relaxin, cyclic AMP and hypoxanthine. Human Reproduction. 1994 Jun;9(6):1003–12.

329. Mitchell LM, Kennedy CR, Hartshorne GM. Effects of varying gonadotrophin dose and timing on antrum formation and ovulation efficiency of mouse follicles in vitro. Human Reproduction. 2002 May;17(5):1181–8.

330. Boland NI, Humpherson PG, Leese HJ, Gosden RG. Pattern of lactate production and steroidogenesis during growth and maturation of mouse ovarian follicles in vitro. Biol Reprod. 1993 Apr;48(4):798–806.

331. Smitz J, Cortvrindt R, van Steirteghem AC. Normal oxygen atmosphere is essential for the solitary long-term culture of early preantral mouse follicles.

Mol Reprod Dev. Wiley Subscription Services, Inc., A Wiley Company; 1996 Dec 1;45(4):466–75.

332. Torrance C, Telfer E, Gosden RG. Quantitative study of the development of isolated mouse pre-antral follicles in collagen gel culture. J Reprod Fertil. 1989 Sep;87(1):367–74.

333. Grasa P, Ploutarchou P, Williams SA. Oocytes lacking O-glycans alter follicle development and increase fertility by increasing follicle FSH sensitivity, decreasing apoptosis, and modifying GDF9:BMP15 expression. FASEB J. Federation of American Societies for Experimental Biology; 2015 Feb;29(2):525–39.

334. Xu M, Kreeger PK, Shea LD, Woodruff TK. Tissue-engineered follicles produce live, fertile offspring. Tissue Eng. 2006 Oct;12(10):2739–46.

335. Ho W, Tawil B, Dunn JCY, Wu BM. The Behavior of Human Mesenchymal Stem Cells in 3D Fibrin Clots: Dependence on Fibrinogen Concentration and Clot Structure. Tissue Eng. Mary Ann Liebert, Inc. 2 Madison Avenue Larchmont, NY 10538 USA; 2006 Jun;12(6):1587–95.

336. Clark RAF. Fibrin is a many splendored thing. J Invest Dermatol. 2003 Nov;121(5):xxi–xxii.

337. Jackson KS, Inoue K, Davis DA, Hilliard TS, Burdette JE. Three-dimensional ovarian organ culture as a tool to study normal ovarian surface epithelial wound repair. Endocrinology. 2009 Aug;150(8):3921–6.

338. King SM, Quartuccio S, Hilliard TS, Inoue K, Burdette JE. Alginate hydrogels for three-dimensional organ culture of ovaries and oviducts. J Vis Exp. 2011;(52):e2804–4.

339. Hilliard TS, Modi DA, Burdette JE. Gonadotropins activate oncogenic pathways to enhance proliferation in normal mouse ovarian surface epithelium. Int J Mol Sci. Multidisciplinary Digital Publishing Institute; 2013 Feb 28;14(3):4762–82.

340. Higuchi CM, Maeda Y, Horiuchi T, Yamazaki Y. A Simplified Method for Three-Dimensional (3-D) Ovarian Tissue Culture Yielding Oocytes Competent to Produce Full-Term Offspring in Mice. Shen W, editor. PLoS ONE. Public Library of Science; 2015;10(11):e0143114.

341. Swann K, Yu Y. The dynamics of calcium oscillations that activate mammalian eggs. The International Journal of Developmental Biology. UPV/EHU Press; 2008;52(5-6):585–94.

342. Ducibella T, Huneau D, Angelichio E, Xu Z, Schultz RM, Kopf GS, et al. Egg-to-embryo transition is driven by differential responses to Ca(2+) oscillation number. Developmental Biology. 2002 Oct 15;250(2):280–91.

343. Yu Y, Saunders CM, Lai FA, Swann K. Preimplantation development of mouse oocytes activated by different levels of human phospholipase C

zeta. Hum Reprod. 2008 Feb;23(2):365–73.

344. Widner B, Behr R, Dollen Von S, Tang M, Heu T, Sloma A, et al. Hyaluronic acid production in Bacillus subtilis. Appl Environ Microbiol. American Society for Microbiology; 2005 Jul;71(7):3747–52.

345. Donnez J, Dolmans M-M. Ovarian tissue freezing: current status. Curr Opin Obstet Gynecol. 2015 Jun;27(3):222–30.

346. Berkholtz CB, Lai BE, Woodruff TK, Shea LD. Distribution of extracellular matrix proteins type I collagen, type IV collagen, fibronectin, and laminin in mouse folliculogenesis. Histochemistry and Cell Biology. Springer-Verlag; 2006 Jun 7;126(5):583–92.

347. Zhao Y, Luck MR. Gene expression and protein distribution of collagen, fibronectin and laminin in bovine follicles and corpora lutea. J Reprod Fertil. Society for Reproduction and Fertility; 1995 May;104(1):115–23.

348. Rodgers HF, Irvine CM, Van Wezel IL, Lavranos TC, Luck MR, Sado Y, et al. Distribution of the alpha1 to alpha6 chains of type IV collagen in bovine follicles. Biol Reprod. 1998 Dec;59(6):1334–41.

349. McArthur ME, Irving-Rodgers HF, Byers S, Rodgers RJ. Identification and immunolocalization of decorin, versican, perlecan, nidogen, and chondroitin sulfate proteoglycans in bovine small-antral ovarian follicles. Biol Reprod. 2000 Sep;63(3):913–24.

350. Rodgers RJ, Irving-Rodgers HF, Van Wezel IL, Krupa M, Lavranos TC. Dynamics of the membrana granulosa during expansion of the ovarian follicular antrum. Mol Cell Endocrinol. 2001 Jan 22;171(1-2):41–8.

351. Yamada S, Fujiwara H, Honda T, Higuchi T, Nakayama T, Inoue T, et al. Human granulosa cells express integrin alpha2 and collagen type IV: possible involvement of collagen type IV in granulosa cell luteinization. Mol Hum Reprod. 1999 Jul;5(7):607–17.

352. Iwahashi M, Muragaki Y, Ooshima A, Nakano R. Type VI collagen expression during growth of human ovarian follicles. Fertil Steril. Elsevier; 2000 Aug;74(2):343–7.

353. Olsen JV, Ong S-E, Mann M. Trypsin cleaves exclusively C-terminal to arginine and lysine residues. Mol Cell Proteomics. American Society for Biochemistry and Molecular Biology; 2004 Jun;3(6):608–14.

354. Duguay D, Foty RA, Steinberg MS. Cadherin-mediated cell adhesion and tissue segregation: qualitative and quantitative determinants. Developmental Biology. 2003 Jan 15;253(2):309–23.

355. Zhang K, Chen J. The regulation of integrin function by divalent cations. Cell Adh Migr. Taylor & Francis; 2012 Jan;6(1):20–9.

356. Kirkpatrick CJ, Melzner I, Göller T. Comparative effects of trypsin,

collagenase and mechanical harvesting on cell membrane lipids studied in monolayer-cultured endothelial cells and a green monkey kidney cell line. Biochim Biophys Acta. 1985 Jul 30;846(1):120–6.

357. Turco MY, Gardner L, Hughes J, Cindrova-Davies T, Gomez MJ, Farrell L, et al. Long-term, hormone-responsive organoid cultures of human endometrium in a chemically defined medium. Nat Cell Biol. 2017 May;19(5):568–77.

358. Stenn KS, Link R, Moellmann G, Madri J, Kuklinska E. Dispase, a neutral protease from Bacillus polymyxa, is a powerful fibronectinase and type IV collagenase. J Invest Dermatol. 1989 Aug;93(2):287–90.

359. Jennison MW. Bacterial Collagenase. Journal of Bacteriology. American Society for Microbiology (ASM); 1945 Sep;50(3):369–70.

360. Neuman RE, Tytell AA. Action of Proteolytic Enzymes on Collagen. Experimental Biology and Medicine. SAGE PublicationsSage UK: London, England; 1950 Mar 1;73(3):409–12.

361. Matthews BW. Structural basis of the action of thermolysin and related zinc peptidases. Accounts of Chemical Research. American Chemical Society; 2002 May;21(9):333–40.

362. Dolmans M-M, Michaux N, Camboni A, Martinez-Madrid B, Van Langendonckt A, Nottola SA, et al. Evaluation of Liberase, a purified enzyme blend, for the isolation of human primordial and primary ovarian follicles. Hum Reprod. Oxford University Press; 2006 Feb;21(2):413–20.

363. Revel A, Koler M, Simon A, Lewin A, Laufer N, Safran A. Oocyte collection during cryopreservation of the ovarian cortex. Fertil Steril. 2003 May;79(5):1237–9.

364. Gosden RG. Low temperature storage and grafting of human ovarian tissue. Mol Cell Endocrinol. 2000 May 25;163(1-2):125–9.

365. Chinn JA, Horbett TA, Ratner BD. Laboratory preparation of plasticware to support cell culture. Journal of Tissue Culture Methods. 1994 Sep;16(3-4):155–9.

366. Steele JG, Dalton BA, Johnson G, Underwood PA. Adsorption of fibronectin and vitronectin onto Primaria and tissue culture polystyrene and relationship to the mechanism of initial attachment of human vein endothelial cells and BHK-21 fibroblasts. Biomaterials. 1995 Sep;16(14):1057–67.

367. Ruoslahti E. RGD and other recognition sequences for integrins. Annu Rev Cell Dev Biol. Annual Reviews 4139 El Camino Way, P.O. Box 10139, Palo Alto, CA 94303-0139, USA; 1996;12(1):697–715.

368. Ferlay J, Soerjomataram I, Dikshit R, Eser S, Mathers C, Rebelo M, et al. Cancer incidence and mortality worldwide: sources, methods and major

patterns in GLOBOCAN 2012. Int J Cancer. 2015 Mar 1;136(5):E359–86.

369. Ovarian cancer incidence statistics. 2015 May 15. Available from: http://www.cancerresearchuk.org/health-professional/cancer-statistics/statistics-by-cancer-type/ovarian-cancer/incidence

370. Matulonis UA, Sood AK, Fallowfield L, Howitt BE, Sehouli J, Karlan BY. Ovarian cancer. Nat Rev Dis Primers. Nature Publishing Group; 2016 Aug 25;2:16061.

371. Tanaka YO, Tsunoda H, Kitagawa Y, Ueno T, Yoshikawa H, Saida Y. Functioning ovarian tumors: direct and indirect findings at MR imaging. Radiographics. Radiological Society of North America; 2004 Oct;24 Suppl 1(suppl_1):S147–66.

372. Ehya H, Lang WR. Cytology of Granulosa Cell Tumor of the Ovary. American Journal of Clinical Pathology. 1986 Apr 1;85(4):402–5.

373. Vani BR, Geethamala K, Geetha RL, Srinivasa MV. Granulosa cell tumor of ovary: A clinicopathological study of four cases with brief review of literature. J Midlife Health. 2014 Jul;5(3):135–8.

374. Biscotti CV, Hart WR. Juvenile granulosa cell tumors of the ovary. Arch Pathol Lab Med. 1989 Jan;113(1):40–6.

375. Young RH, Dickersin GR, Scully RE. Juvenile granulosa cell tumor of the ovary. A clinicopathological analysis of 125 cases. Am J Surg Pathol. 1984 Aug;8(8):575–96.

376. Sivasankaran S, Itam P, Ayensu-Coker L, Sanchez J, Egler RA, Anderson ML, et al. Juvenile granulosa cell ovarian tumor: a case report and review of literature. J Pediatr Adolesc Gynecol. 2009 Oct;22(5):e114–7.

377. Schumer ST, Cannistra SA. Granulosa cell tumor of the ovary. J Clin Oncol. 2003 Mar 15;21(6):1180–9.

378. Rantala ML. Causes and outcome of infertility in previously unexamined couples. Acta Obstet Gynecol Scand. 1988;67(5):429–32.

379. Meskhi A, Seif MW. Premature ovarian failure. Curr Opin Obstet Gynecol. 2006 Aug;18(4):418–26.

380. Shelling AN. Premature ovarian failure. Reproduction. Society for Reproduction and Fertility; 2010 Nov;140(5):633–41.

381. Shuster LT, Rhodes DJ, Gostout BS, Grossardt BR, Rocca WA. Premature menopause or early menopause: long-term health consequences. Maturitas. Elsevier; 2010 Feb;65(2):161–6.

382. Harris SE, Chand AL, Winship IM, Gersak K, Aittomäki K, Shelling AN. Identification of novel mutations in FOXL2 associated with premature ovarian failure. Mol Hum Reprod. 2002 Aug;8(8):729–33.

383. Aittomäki K, Lucena JL, Pakarinen P, Sistonen P, Tapanainen J, Gromoll J, et al. Mutation in the follicle-stimulating hormone receptor gene causes hereditary hypergonadotropic ovarian failure. Cell. 1995 Sep 22;82(6):959–68.

384. Latronico AC, Anasti J, Arnhold IJP, Rapaport R, Mendonca BB, Bloise W, et al. Brief Report: Testicular and Ovarian Resistance to Luteinizing Hormone Caused by Inactivating Mutations of the Luteinizing Hormone-Receptor Gene. Obstetrical & Gynecological Survey. 1996 Jul 1;51(7):416.

385. Beau I, Touraine P, Meduri G, Gougeon A, Desroches A, Matuchansky C, et al. A novel phenotype related to partial loss of function mutations of the follicle stimulating hormone receptor. J Clin Invest. American Society for Clinical Investigation; 1998 Oct 1;102(7):1352–9.

386. Touraine P, Beau I, Gougeon A, Meduri G, Desroches A, Pichard C, et al. New natural inactivating mutations of the follicle-stimulating hormone receptor: correlations between receptor function and phenotype. Mol Endocrinol. 1999 Nov;13(11):1844–54.

387. Shelling AN. X chromosome defects and premature ovarian failure. Australian and New Zealand Journal of Medicine. Blackwell Publishing Ltd; 2008 Mar 25;30(1):5–7.

388. Brown HM, Russell DL. Blood and lymphatic vasculature in the ovary: development, function and disease. Hum Reprod Update. 2014 Jan;20(1):29–39.

389. Feng Y, Cui P, Lu X, Hsueh B, Möller Billig F, Zarnescu Yanez L, et al. CLARITY reveals dynamics of ovarian follicular architecture and vasculature in three-dimensions. Sci Rep. Nature Publishing Group; 2017 Mar 23;7:44810.

390. Kristensen SG, Rasmussen A, Byskov AG, Andersen CY. Isolation of pre-antral follicles from human ovarian medulla tissue. Hum Reprod. 2011 Jan;26(1):157–66.

391. Delgado-Rosas F, Gaytán M, Morales C, Gómez R, Gaytán F. Superficial ovarian cortex vascularization is inversely related to the follicle reserve in normal cycling ovaries and is increased in polycystic ovary syndrome. Hum Reprod. 2009 May;24(5):1142–51.

392. Macaulay AD, Gilbert I, Scantland S, Fournier E, Ashkar F, Bastien A, et al. Cumulus Cell Transcripts Transit to the Bovine Oocyte in Preparation for Maturation. Biol Reprod. 2016 Jan;94(1):16.

393. Yazdekhasti H, Rajabi Z, Parvari S, Abbasi M. Used protocols for isolation and propagation of ovarian stem cells, different cells with different traits. J Ovarian Res. BioMed Central; 2016 Oct 20;9(1):68.

394. Sitterley G, Karmiol S, Manaster E, Ryan J. Attachment and matrix factors [Internet]. Biofiles (Sigma-Aldrich); 2008. Available from:

http://www.sigmaaldrich.com/content/dam/sigma-aldrich/flashapps/biofiles-movie/pdf/biofiles_issue3.8.pdf

395. Lu C-Y, Chen Y-A, Wu F-C, Ho H-N, Chen H-F. Premature ovarian failure patient-specific induced pluripotent stem (iPS) cells show compromised potential to develop to germ cells and granulosa cells. FASEB J. Federation of American Societies for Experimental Biology; 2017 Apr 1;31(1 Supplement):904.8–904.8.